IDENTIFICATION AND CHARACTERIZATION OF SENESCENCE-ASSOCIATED MICRORNAS IN A MOUSE MODEL OF THE XFE PROGEROID SYNDROME

by

Lolita Sai Nidadavolu

B.A. Chemistry, Johns Hopkins University, 2006

Submitted to the Graduate Faculty of

the School of Medicine in partial fulfillment

of the requirements for the degree of

Doctor of Philosophy

University of Pittsburgh

2013

UNIVERSITY OF PITTSBURGH

SCHOOL OF MEDICINE

This dissertation was presented

by

Lolita Sai Nidadavolu

It was defended on

July 19, 2013

and approved by

Abbe de Vallejo, Ph.D., Associate Professor, Pediatrics and Immunology

Ferruccio Galbiati, Ph.D., Associate Professor, Pharmacology and Chemical Biology

Laura Niedernhofer M.D., Ph.D., Associate Professor, Microbiology and Molecular Genetics

Paul Robbins, Ph.D., Professor, Microbiology and Molecular Genetics

Thesis Advisor: Saleem Khan, Ph.D., Professor, Microbiology and Molecular Genetics

IDENTIFICATION AND CHARACTERIZATION OF SENESCENCE-ASSOCIATED MICRORNAS IN A MOUSE MODEL OF THE XFE PROGEROID SYNDROME

Lolita Sai Nidadavolu, PhD

University of Pittsburgh, 2013

XFE progeroid syndrome, a disease of accelerated aging caused by deficiency in the DNA repair endonuclease XPF-ERCC1, is modeled by *Ercc1* knockout and hypomorphic mice. Tissues and primary cells from these mice senesce prematurely, offering a unique opportunity to identify factors that regulate senescence and aging. We compared microRNA (miRNA) expression in *Ercc1*$^{-/-}$ primary mouse embryonic fibroblasts (MEFs) and wild-type (WT) MEFs in different oxygen growth conditions and at different passages to identify miRNAs that possibly drive cellular senescence. Microarray analysis showed three differentially expressed miRNAs in senescent passage 7 (P7) *Ercc1*$^{-/-}$ MEFs grown at 20% O_2 compared to less senescent *Ercc1*$^{-/-}$ MEFs grown at 3% O_2. Thirty-six differentially expressed miRNAs were identified in *Ercc1*$^{-/-}$ MEFs at P7 compared to early passage (P3) in 3% O_2. Eight of these miRNAs (miR-449a, miR-455*, miR-128, miR-497, miR-543, miR-450b-3p, miR-872 and miR-10b) were similarly downregulated in the liver of progeroid *Ercc1*$^{-/\Delta}$ and old WT mice compared to adult WT mice, a tissue that demonstrates increased senescence with aging. Three miRNAs (miR-449a, miR-455* and miR-128) were also downregulated in *Ercc1*$^{-/\Delta}$ and WT old mice kidneys compared to young WT mice. We also discovered that the miRNA expression regulator Dicer is significantly downregulated in tissues of old mice and late passage cells compared to young controls. Collectively these results support the conclusion that the miRNAs identified may play an

important role in staving off cellular senescence and their altered expression could be indicative of aging.

We also identified IL-6 as a possible target for miR-128, one of the senescence- and DNA damage-associated miRNAs from our microarray analysis of MEFs. IL-6 mRNA levels were reduced significantly when miR-128 was overexpressed and IL-6 mRNA was increased when miR-128 was knocked down by 80%. Furthermore, miR-128 knock-down resulted in increases to the known senescence markers p16 and miR-146a. MiR-128 overexpression resulted in significant IL-6 mRNA reduction, with accompanying reduction in miR-146a.

Based on these studies, we have shown that progeroid models can be a useful method to identify miRNAs that are dysregulated in normal aging processes. We have also identified IL-6 as a possible target for miR-128, a senescence- and DNA-damage associated miRNA that is downregulated in senescent fibroblasts and aged livers and kidney tissues.

TABLE OF CONTENTS

LIST OF TABLES

LIST OF FIGURES

COMMONLY USED ABBREVIATIONS

bp	base pair
DNA	deoxyribonucleic acid
ERCC1	Excision Repair Cross-Complementing 1
GAPDH	Glyceraldehyde-3-Phosphate Dehydrogenase
HGPS	Hutchinson-Guilford Progeria Syndrome
IL-6	interleukin-6
KO	knock out (refers to *Ercc1*$^{-/-}$)
MEF	mouse embryonic fibroblast
mRNA	messenger RNA
miRNA, miR-	microRNA
NF-κB	nuclear factor-κB
nM	nanomolar
P3	passage 3
P7	passage 7
qRT-PCR	quantitative Real-Time Reverse-Transcriptase Polymerase Chain Reaction
RNA	ribonucleic acid
ROS	reactive oxygen species
SASP	senescence-associated secretory phenotype

UTR	untranslated region
WS	Werner Syndrome
WT	wild type
XFE	Xeroderma Pigmentosum F-Excision Repair Cross-Complementing 1
XPF	Xeroderma Pigmentosum F

1.0 INTRODUCTION

1.1 BIOLOGY OF AGING

1.1.1 Impact of aging on society

The percentage of individuals aged 65 years and older is one of the fastest growing segments of the population and is expected to increase by over 180% over the next 40 years [1]. In the United States, individuals 65 years and older are predicted to reach approximately 20% of the total population by the year 2030 [2]. As of 2009, those who survive to age 65 are expected to live for another 19.2 years, on average [3]. Individuals over the age of 65 are more likely to develop many chronic and debilitating diseases such as hypertension, heart disease, arthritis and diabetes, with many individuals suffering from more than one chronic disease [4]. Learning more about the molecular mechanisms that regulate aging and influence longevity is critical to help individuals remain healthy and active longer.

1.1.2 Theories on the biology of aging

At the cellular level, aging is a highly multifactorial process. Accumulation of oxidized proteins, mitochondrial dysfunction and stem cell exhaustion are observed in organismal aging and age-

associated diseases due to both endogenous oxidative species resulting from normal cellular metabolism and exogenous damaging agents [5-8]. One general theory that explains the evolutionary origins of aging is that of antagonistic pleiotropy, which states that genes that are beneficial to young organisms produce deleterious effects when expressed in older individuals. The expression of particular genes provides a growth or reproductive advantage for young organisms but accelerates age-associated pathologies if these genes are expressed later in life. One example of antagonistic pleiotropy is the effect of IGF signaling, which imparts growth benefits to young organisms, but whose upregulation in aged organisms can lead to chronic inflammatory processes associated with aging and shortened lifespan [9]. The evolutionarily conserved mammalian target of rapamycin (mTOR) signaling pathway has beneficial growth and reproductive effects for young organisms; however, mTOR activity drives aging processes once organisms are fully developed, particularly in male mice [10].

The free radical (or mitochondrial) theory of aging, which was advanced in the mid-1950s, describes how endogenously produced reactive oxygen species (ROS), namely superoxide radicals, hydrogen peroxide and hydroxyl radical, can be a source of spontaneous oxidative damage to DNA, proteins and organelles, causing dysfunction [11]. These ROS are endogenously produced by cellular processes such as mitochondrial respiration, peroxisome metabolism, and nitric oxide synthesis [12]. Furthermore, genomic instability in the form of point mutations and deletions in mitochondrial DNA can impair cellular energy production and lead to further production of ROS, creating a “vicious cycle” of oxidative damage and impaired mitochondrial function [13]. Antioxidant enzymes such as superoxide dismutase (SOD), catalase, heme oxygenase and peroxiredoxin all function to scavenge and eliminate ROS to prevent widespread macromolecular damage [14-16]. Engineered mice lacking the gene *SOD1*,

the predominant intracellular SOD isoform, resulted in increased oxidative damage and shortened lifespan by approximately 30% [17]. However, recent studies have complicated the mitochondrial theory of aging. It is now believed that mildly inhibiting mitochondrial respiratory processes can extend lifespan [18, 19]. Also, ROS have demonstrated the ability to act as signaling messenger molecules, when expressed at low levels [20]. These conflicting studies underscore the complex nature of cellular responses to ROS, and how ROS modulation can in fact provide beneficial outcomes to the cell.

1.2 CELLULAR SENESCENCE AND AGING

Cellular senescence, a state of permanent cell cycle arrest, is hypothesized to be both beneficial and detrimental to a cell by suppressing cancer progression but also promoting growth inhibition and aging [21]. Cellular senescence is proposed to be a potent tumor suppression mechanism due to its rapid induction upon oncogene expression and in the presence of persistent DNA damage signaling [22]. Senescent cells typically demonstrate defects in mitochondrial function, lipofuscin accumulation and increased lysosomal beta-galactosidase [23-25]. Chromatin remodeling occurs in senescent cells that appear as senescence-associated heterochromatin foci (SAHF) [26]. DNA segments with chromatin alterations reinforcing senescence (DNA-SCARS) are also present in cells that senesce due to persistent signaling of the DNA damage response [27]. These DNA-SCARS are nuclear foci that contain activated proteins involved in mediating the DNA damage response pathway, namely activated checkpoint kinase 2 (CHK2) and the modified histone γ-H2AX [27]. Studies characterizing aged tissues and cells

have shown high levels of senescent cells [28, 29]. It is theorized that senescence is a key mechanism by which organismal aging is mediated at the cellular level.

The primary purpose of senescence is to prevent the proliferation of cells that are potentially oncogenic. These damaged cells occur in both young and old organisms, however, they are hypothesized to accumulate more in older organisms due in part to decreased clearance of senescent cells and reduced stem cell renewal [30, 31]. There is a tissue-specific increase in many types of DNA mutations with aging, with liver and small intestine demonstrating the highest absolute number of accumulated mutations with aging and brain tissue demonstrating the least amount of accumulated mutations [32, 33]. These mutations range from single point mutations to large genome rearrangements that potentially affect millions of bases and can impair function of tumor suppressor genes or lead to the expression of oncogenes [33].

Cellular senescence can occur via at least four stimuli: telomere shortening, oncogene-expression, DNA damage and epigenomic perturbations. As early as the 1960s, it was observed that human diploid cell lines grown *in vitro* eventually reach a point at which their proliferation is permanently arrested and they undergo mitotic arrest [34]. Subsequent studies showed that this growth arrest occurred due to telomere shortening with each cycle of DNA replication [35]. In addition to telomere-associated senescence, oncogene expression, non-telomere initiated DNA damage signaling, especially DNA double-strand breaks, and epigenetic stresses, such as chromatin modifications, can induce senescence [36-40]. Oncogene-induced senescence is an important pathway in which tumor progression can be inhibited, however this is primarily seen in pre-malignant tumors and not in advanced tumors [41, 42].

The diverse stimuli that can cause cellular senescence converge on two main tumor suppressor pathways, p53 and pRb [43-46]. The p53 tumor suppressor protein plays important

roles in the DNA damage response, cellular senescence, apoptosis, and cell cycle regulation, and is one of the most commonly dysregulated proteins in cancer [47-49]. In the absence of genotoxic stresses or DNA damage response signaling, p53 is bound by the mouse double minute 2 (MDM2) E3 ubiquitin ligase, which leads to the proteasome-mediated degradation of p53 [50, 51]. However, in the presence of persistent DNA damage and other activating stimuli, p53 undergoes a series of phosphorylation events, either directly by the ataxia-telangiectasia mutated (ATM) kinase or indirectly by checkpoint kinase 1/2 (CHK1/2), and is stabilized [52]. These phosphorylation events disrupt the binding site of MDM2 in the p53 transactivation domain leading to reduced p53:MDM2 interactions [53]. P53 consequently accumulates in the cell, assembling into functionally active tetramer complexes and acts as a transcriptional activator, targeting genes that inhibit proliferation and arrest cells at the G1/S checkpoint [54]. An important target of p53 relating to cellular senescence is the CDK-interacting protein 1 (CIP1)/p21, which functions as a universal cyclin-dependent kinase (CDK) inhibitor [55]. P21 is overexpressed in senescent cells, and its levels are generally reduced in cancer cells, resulting in uncontrolled cell division. However, it was recently shown that p21 can function as both a tumor suppressor and oncogene depending upon the cellular micro-environment [56, 57].

The pRb pathway controls the G1 to S checkpoint in the cell cycle. When unphosphorylated or underphosphorylated, Rb is in complex with the E2F1 transcription factor, preventing the transcription of E2F1 target genes essential for the G1/S transition, such as Cyclin E and Cyclin A [58, 59]. Sequestration of E2F1 prevents the transcription of other cell cycle-associated genes through the recruitment of HDACs which act as general repressor complexes [60-63]. Following several phosphorylation events by CDKs, pRb no longer associates with the

E2F family of transcription factors in the cytosol, allowing E2F1 to activate its downstream targets [64].

The protein levels of the p16 tumor suppressor increase in aged tissues and senescent cells, as well as after exposure to DNA damaging agents [29, 65, 66]. P16 is encoded by the inhibitor of cdk4/alternate reading frame (INK4/ARF) locus. There are three tumor suppressor genes at this locus: p16/INK4A, p15/INK4B, and p19/ARF [67]. P16 inhibits CDK4/6, which regulate the G1 to S phase transition in the cell cycle by phosphorylating Rb, which then becomes a substrate for further phosphorylation by CDK2 [68]. P16 is also involved in the enhancement of ROS production which plays a role in triggering the “vicious cycle” of ROS accumulation and mitochondrial dysfunction [69]. Phosphorylated pRb increases p16 levels which in turn inhibits CDK4/6, creating a regulatory feedback loop [70]. Reduced CDK4/6 subsequently reduce pRb phosphorylation, resulting in decreased p16 expression [70]. P16 is commonly used as a biomarker to identify senescent cells in tissues and in cell culture.

Senescent cells also exhibit a unique gene expression profile in response to persistent DNA damage response signaling termed senescence-associated secretory phenotype (SASP), that promotes the release of pro-inflammatory cytokines such as IL-6 and IL-8 [71, 72]. In the absence of genomic DNA damage or epigenomic disruptions, ectopic overexpression of tumor suppressor proteins p16 or p21 does not result in SASP formation [73, 74]. An early response to persistent senescence stimuli is high expression of the cytokine IL-1α, which activates the nuclear factor-κB (NF-κB) signaling pathway [75, 76]. NF-κB transcriptionally activates the inflammatory cytokines IL-6 and IL-8, both of which are primary components of the SASP response. The NF-κB pathway was recently shown to be an important regulator and therapeutic target of aging-associated diseases [77, 78]. Interestingly, the SASP response elicited in

senescence varies depending upon cell type and the process by which senescence was induced. For example, human fibroblasts expressing the BRAF oncogene increase IGFBP7 secretion, while human dermal and prostate fibroblasts experiencing telomere shortening and oxidative stress predominantly secrete cyclooxygenase-2 (COX-2) [79, 80]. It is hypothesized that SASP production in senescent cells promotes maintenance of cellular growth arrest.

The SASP response can also induce hyperproliferative and tumorigenic cell responses in a wide range of cell types [71, 81, 82]. This is likely due to the secretion of a large number of immune-stimulating factors (e.g.: IL-6, IL-8, GRO-α). Senescent vascular smooth muscle cells exhibit a SASP response; however, one of the consequences of senescence for this cell type is the expression of pro-calcification genes [83]. Astrocytes undergoing stress-induced senescence exhibit SAHF, positive SA β-gal staining and upregulation of p16 and p21 [84]. Senescent astrocytes secrete many pro-inflammatory cytokines, and it is hypothesized that this creates a neuroinflammatory environment, which is observed in neurodegenerative diseases such as Alzheimer's Disease, Parkinson's Disease and frontotemporal dementia [82]. It is still unclear what factors influence whether a senescent cell will produce a growth arrest or hyperproliferative microenvironment for adjacent cells.

1.3 DNA REPAIR

1.3.1 DNA Repair Pathways

Nuclear and mitochondrial DNA faces an onslaught of mutagenic agents from exogenous and endogenous sources, including ultraviolet (UV) light, radiation, spontaneous base hydrolysis and reactive oxidative species. These mutagens cause tens of thousands of DNA lesions per cell, per day [85]. The many types of cellular DNA damage necessitate the presence of many DNA repair mechanisms. Key repair pathways include base excision repair (BER), nucleotide excision repair (NER), mismatch repair (MMR), homologous recombination (HR) and non-homologous end joining (NHEJ). NER and BER generally function via “cut and paste” repair mechanisms, MMR acts to correct replication mistakes and HR and NHEJ are both responsible for repairing double-strand DNA breaks.

The connection between DNA repair deficiencies and aging is evident from a variety of progeroid (rapid aging) disorders which have impaired DNA repair proteins, such as the Werner helicase, Lamin-A, and Cockayne Syndrome B proteins. The Werner protein is a RecQ helicase truncated in the progeroid disorder Werner Syndrome (WS). Werner helicase is critical for maintaining chromosomal telomeres and is also implicated in the repair of oxidative base damage [86-88]. WS patients begin to exhibit many classic signs of aging in their mid-30’s, including cataracts, cancer and osteoporosis [89]. Lamin-A mutations are responsible for the Hutchinson-Guilford Progeria Syndrome (HPGS) and result in abnormal nuclei, increased DNA damage and widespread epigenetic changes that are also observed in cells from naturally aged individuals [90-92]. It was recently shown that properly functioning Lamin-A is critical for the

stabilization of DNA repair foci via interactions with the phosphorylated histone variant γ-H2AX [93]. Patients with HGPS demonstrate early signs of aging and over 90% of patients die by around age 13 of complications from severe atherosclerosis and cardiovascular complications [94]. By studying progeroid disorders, key components of DNA repair pathways have been identified and they have revealed the critical effects of dysregulation of genomic repair on aging.

1.3.2 Functions of the ERCC1-XPF complex

Excision repair cross complementing 1-Xeroderma Pigmentosum F (ERCC1-XPF) is a 5'endonuclease that is primarily involved in Nucleotide Excision Repair (NER). NER is the main repair pathway for bulky, helix-distorting lesions such as cyclobutane pyrimidine dimers (CPD) and (6-4) photoproducts, both of which are incorporated into DNA via UV-A and UV-B solar radiation as well as due to endogenous photosensitizers [95-98]. There are two types of NER, global genome (GG-NER) and transcription-coupled (TC-NER) repair [99] (Figure 1). These two pathways have different mechanisms by which DNA damage is detected, but they converge on a common repair pathway following damage recognition. The GG-NER pathway acts as a generalized scanner of genome integrity and repairs any large helix distorting lesions it recognizes, primarily via binding of the Xeroderma Pigmentosum C-Human Rad23 Homolog B (XPC-HR23B) complex at the site of damage [100]. The TC-NER pathway is intimately connected to the transcription machinery and resolves bulky lesions that interfere with the transcription process. TC-NER damage recognition occurs via RNA polymerase II stalling at the site of damage [101, 102]. Despite different methods of substrate recognition, GG-NER and TC-NER converge on a common pathway for endonucleolytic cleavage, excision of damaged DNA

and gap filling [103, 104]. The ERCC1-XPF heterodimer is an integral part of the NER pathway, and acts downstream of the damage recognition step, therefore defects in this complex impair both GG-NER and TC-NER [105, 106].

Figure 1. Nucleotide Excision Repair (NER) Pathway in Eukaryotes [104]

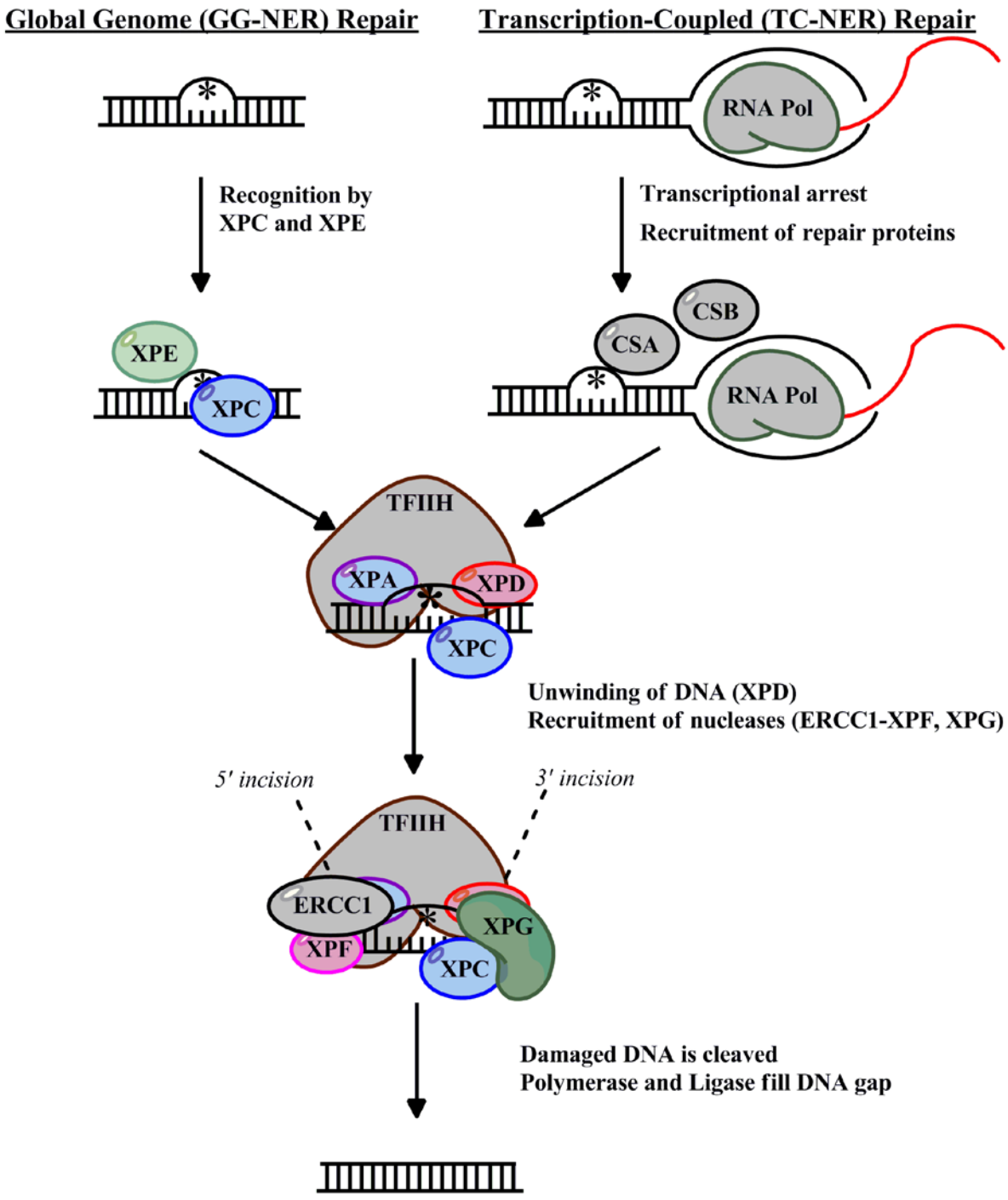

Patients have been identified with defects in both GG-NER and TC-NER pathways, and have strikingly different phenotypes. Xeroderma Pigmentosum (XP) is an autosomal recessive disorder characterized by photosensitivity, increased risk of skin cancer (squamous cell carcinomas and basal cell carcinomas), as well as dry, parchment-like skin (xeroderma) and increased pigmentation in areas that have been exposed to the sun (pigmentosum) [107, 108]. Disease severity is highly heterogeneous depending on which XP family protein is defective, what protein domains are disrupted by a particular mutation and where the protein functions in the GG and TC-NER pathways. Xeroderma Pigmentosum complement group E (XPE), a mild variant of the disease, is caused by a mutation in the DNA damage binding 2 (DDB2), a gene that helps increase the affinity of XPC-HR23B to (6-4) photoproduct substrates in GG-NER [109, 110]. However, Xeroderma Pigmentosum complement group D (XPD), which is a part of the multi-subunit complex Transcription factor II H (TFIIH), is critical to both GG-NER and TC-NER, and therefore patients with a mutation in this gene can present with severe or mild XP, trichothiodystrophy or a combined XP/Cockayne Syndrome (CS) phenotype [111, 112]. The severity of disease in XPD depends upon the site of the mutation and which functional domain in the protein is affected. Patients with impaired TC-NER have mutations in the Cockayne Syndrome A and B proteins (CSA and CSB) and develop mild skin photosensitivity. However, these patients also show signs of premature aging not observed in XP patients, including a wizened appearance, kyphosis, cachexia, deafness and visual impairment as well as cerebral atrophy [113].

In addition to its role in NER, the ERCC1-XPF complex is also involved in other DNA repair processes such as inter-strand cross-link (ICL) repair and double-strand break (DSB) repair [114, 115]. Additionally, both XPF and ERCC1 are involved in promoting transcription of

certain genes in the absence of exogenous genotoxic stress [116]. XPF, in particular, is critical for recruiting the chromatin loop organizing protein CCCTC-binding factor (CTCF), which is involved in regulating gene expression [117]. Also, the XPF-ERCC1 complex co-localizes with Fanconi Anemia group D2 (FANCD2) at fragile sites on mitotic chromosomes and plays a role in anaphase sister chromatid separation [118]. Depletion of Ercc1 resulted in higher incidences of chromosome segregation defects and mitotic failure [118]. These non-NER functions of the ERCC1-XPF heterodimer may explain why the phenotype of humans lacking this protein complex can be so strikingly different and severe when compared to other XP-family disorders.

1.3.3 Ercc1-deficient mouse models

The first human XFE patient was identified in 2006 by Niedernhofer *et al* [119]. The patient achieved all early developmental milestones and demonstrated skin sensitivity, learning disabilities and hearing loss. He presented at age 16 with signs of severe accelerated aging, including liver and kidney dysfunction, anemia, hypertension, ataxia and skin UV sensitivities. A mouse model mimicking this disorder, with the genotype *Ercc1*$^{-/-}$, was developed and found to exhibit similar liver, bone marrow and renal disturbances [105]. The life-span of *Ercc1*$^{-/-}$ mice is 3 to 8 weeks, significantly shorter than the typical 2 to 3 year life-span for normally aged mice, and *Ercc1*$^{-/-}$ mice often die prior to weaning [120]. *Ercc1*$^{-/-}$ MEFs exhibit earlier onset of cellular senescence compared to WT MEFs when cultured in 20% O_2 and typically senesce by passage 7 [105]. Due to the only one month long lifespan of *Ercc1*$^{-/-}$ mice, our studies also included the analysis of *Ercc1*$^{-/\Delta}$ mouse tissues, which have a hypomorphic (Δ) allele of Ercc1, resulting in 10% of normal Ercc1 protein expression [121]. Tissues from *Ercc1*$^{-/\Delta}$ mice are well-

characterized and similar to normally aged mice with regards to intervertebral disk degeneration, peripheral neuropathy and liver aging [122-124]. These prior studies establish the *Ercc1*$^{-/\Delta}$ mouse as a useful model for us to identify microRNAs (miRNAs) and molecular mechanisms that are dysregulated with aging.

1.4 MICRORNAS

1.4.1 Biogenesis and function of microRNAs

MicroRNAs are approximately 22 nucleotide, post-transcriptional gene regulators capable of repression of translation or degradation of their messenger RNA (mRNA) targets. MiRNA genes are generally transcribed by RNA Polymerase (Pol) II to generate primary-miRNA (pri-miRNA), which is then processed by Drosha, an RNase III enzyme that generates the hairpin precursor miRNA (pre-miRNA) [125, 126]. Following export to the cytoplasm, the RNase III enzyme Dicer further processes the hairpin structure, producing a 22 nucleotide miRNA duplex [127, 128]. The mature single stranded miRNA from the duplex is incorporated into the RNA-induced silencing complex (RISC) containing an Argonaute protein [129-132]. The RISC complex carries the mature miRNA to its target mRNA [133].

MiRNAs generally bind to their target mRNAs at their 3' untranslated regions (3' UTRs), via complementary base-pairing through the miRNA seed sequence (nucleotides 2-8 at the 5' end of the miRNA) [134]. The degree of complementarity between the seed sequence and other regions of the miRNA:mRNA duplex determines if the mRNA is translationally repressed or

targeted for degradation [135, 136]. The net outcome of miRNA binding to mRNA by either mechanism is reduced levels of the protein encoded by the target gene.

Figure 2: MicroRNA Processing Pathway[137]

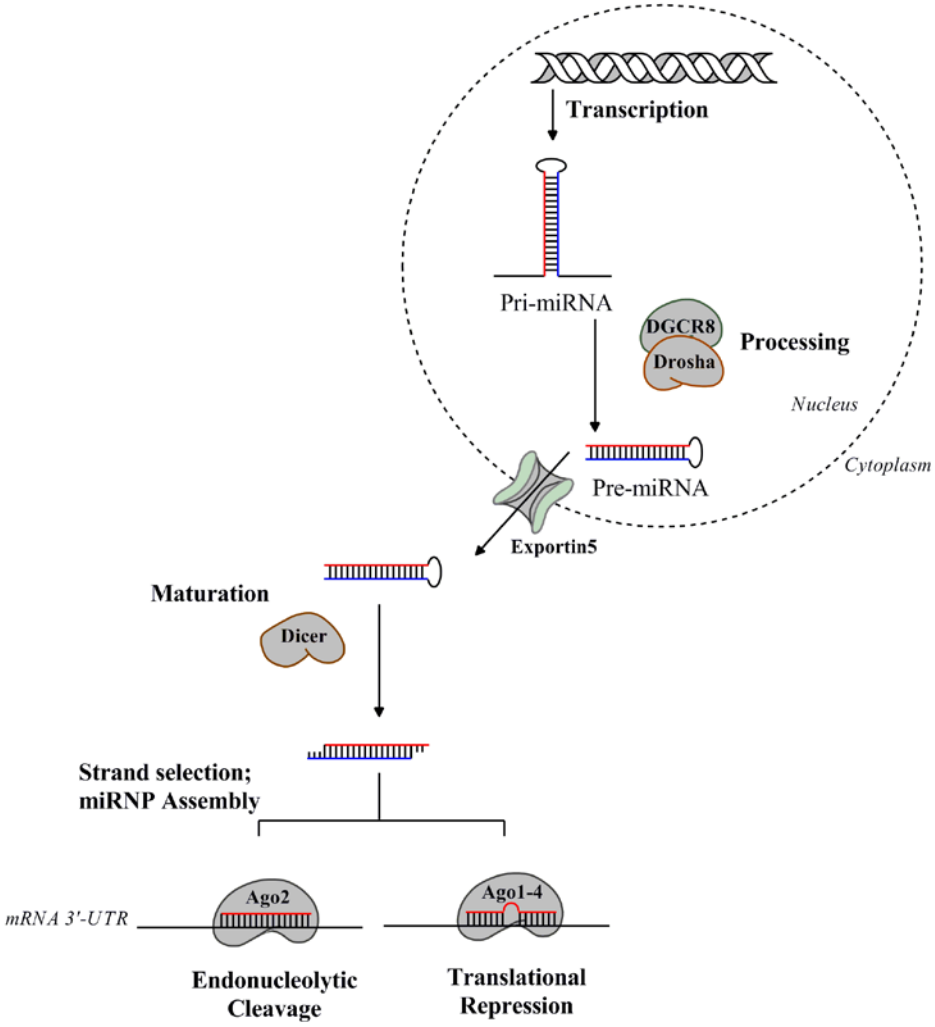

1.4.2 MicroRNAs and DNA repair

MiRNAs can regulate DNA damage responses (DDR) in several ways. MiR-155 directly targets two proteins critical to mismatch repair (MMR), mutL homolog 1 (MLH1) and mutS homolog 2 (MSH2) [138]. This reduction in MLH2 and MSH2 levels increases the cellular mutation rate, increasing cancer incidence [138]. MiR-182-5p is upregulated in breast cancer and targets breast cancer 1 (BRCA1), checkpoint kinase 2 (CHEK2) and tumor protein p53 binding protein 1 (TP53BP1), all of which are essential to the HR pathway [139, 140].

MiRNAs can also regulate DDR by targeting critical cell cycle checkpoint proteins such as cell division cycle 25A (CDC25A), which is targeted by miR-16 [141]. MiR-16 is rapidly upregulated after UV irradiation and has been implicated in the rapid reduction of CDC25A protein which occurs in the minutes following UV-induced damage [142]. There are three levels of regulation of CDC25A following DNA repair pathway activation: (i) Immediate protein degradation by ATM and Rad 3-related (ATR)-dependent phosphorylation of CDC25A, (ii) prevention of CDC25A protein translation by miR-16 binding to CDC25A mRNA and (iii) long-term transcriptional suppression of the *CDC25A* gene via p53 pathway signaling [141]. The role for other miRNA regulators of cell cycle control in the presence of *de novo* DNA damage may be similar to that of miR-16; miRNA modulation of protein levels is a faster process than transcriptional regulation, which in the case of CDC25A occurs approximately 9 hours following UV treatment in a p53 and p21dependent manner [143].

DDR components can also directly regulate miRNA production. KH-type splicing regulatory protein (KSRP) is associated with the miRNA processing proteins Drosha and Dicer, and acts to enhance the maturation of a subset of miRNAs involved in cell proliferation by

directly binding to precursor pri-miRNAs [144]. ATM phosphorylation is critical in the activation of KSRP as a regulator of miRNA maturation, and KSRP-pri-miRNA interactions are enhanced in the presence of DNA damage, which globally increases miRNA biogenesis [144]. BRCA1 associates with Drosha and enhances the processing of BRCA1 associated miRNAs [145]. BRCA1 also interacts with histone deacetylase 2 (HDAC2) to suppress the expression of the oncogenic microRNA miR-155 [146].

MicroRNAs can also be involved in feedback loops that modulate DDR pathways. The tumor suppressor p53 activates the expression of several tumor suppressive microRNAs: miR-34a/b/c, miR-145, miR-107, miR-192 and miR-215 [147-149]. MiR-34a also acts to enhance p53 activity by binding to the 3'-UTR of the deacetylase sirtuin 1 (SIRT1), which targets and inactivates p53 [150, 151]. Over-expression of miR-34a induces p53-mediated apoptosis and senescence from this positive feedback loop [152, 153].

1.4.3 MicroRNAs and cellular senescence

Cellular senescence is an irreversible, actively maintained cell fate, and consequently regulation of this process occurs at several levels in addition to transcriptional regulation, including regulation by small RNAs and protein post-translational modifications [154, 155]. MicroRNAs and other non-coding small RNAs play an important role in fine-tuning cellular responses to stress, tipping the balance between transient versus permanent cell cycle arrest. Recently, the role that microRNAs play in regulating and mediating cellular senescence has begun to be elucidated (Table 1). However, confounding factors in finding roles for miRNAs in senescence are the wide diversity of possible miRNA targets based on 3'-UTR predicted binding sites and the differential

expression of miRNAs in different tissues and cell types. There is a significant amount of overlap between miRNAs identified as regulating DDR and those that regulate cellular senescence and aging pathways. One example of the interplay between DDR and senescence signaling pathways is with miR-34a, which in addition to targeting the p53 regulator SIRT1 also inhibits expression of the Myc proto-oncogene in fibroblasts that are induced to senesce via B-RAF oncogene expression [156].

The microRNA processing pathway also plays a role in regulating cellular senescence. Dicer conditional knock-down in primary mouse embryonic fibroblasts (MEFs) resulted in activation of p53-mediated cellular senescence pathways [157]. The pro-senescent effect of Dicer knock-down was completely abrogated in cells with p53 deletions [157]. In these Dicer-ablated MEFs, miRNA processing was halted at the pre-miRNA step, resulting in accumulation of hairpin-loop structures in the cytoplasm. Another study knocked-down the auxiliary processing protein Di Georges critical region 8 (DGCR8), which works in concert with the Drosha ribonuclease to form a pre-miRNA, and showed subsequent growth arrest in human primary fibroblasts and MEFs [158]. Fibroblasts with reduced DGCR8 expression had reduced BrdU incorporation, expressed SAHF and had increased SA β-gal staining, in part due to p21 upregulation and the absence of several miRNAs that function to regulate the cell cycle [158].

MiR-146a/b was identified as being upregulated in senescent cells, and plays a role in modulating the senescence associated secretory phenotype (SASP) [75]. Previous work has shown a negative feedback loop in which NF-κB induces expression of miR-146, and increased miR-146 subsequently leads to reduced NF-κB activity via downregulation of the IL-1 receptor associated kinase 1 (IRAK1) [159, 160]. The SASP response is therefore able to be reduced via miR-146a/b upregulation. It is likely that this regulatory mechanism evolved because of the

negative consequences that could occur if a robust SASP response were to go unchecked. Long-term upregulation of inflammatory cytokines can create a pro-tumorigenic environment, as several types of cancer stem cells were shown to be induced by IL-6 [161-163].

The oncogenic miR-21 was shown to be upregulated in replicative senescence as well as in oxidative stress-induced senescence in human umbilical vein endothelial cells (HUVEC) [164]. MiR-21 targets two genes that regulate cell cycle arrest, CDC25A which regulates the activity of CDK2, and nuclear factor 1 B-type (NF1B) which represses p21 transcription [164, 165]. In eosinophil progenitor cells and cardiomyocytes, downregulation of miR-21 results in decreased cell proliferation; therefore the observation that miR-21 overexpression has anti-proliferative effects in HUVEC, while having pro-proliferative effects in other tissues reiterates that miRNAs expressed in different cell types can have different effects, due in part to transcriptome variability [166, 167]. It is especially interesting to note that cellular expression of oncogenic Ras leads to increased miR-21 expression, and reduced expression of CDC25A and NF1B by miR-21 are possible mechanisms by which Ras can lead to oncogene-induced senescence in HUVEC [168]. Other miRNAs that play a role in oncogene-induced senescence are listed in Table 2.

MiRNAs identified as modulating senescence in previous studies (Table 1 and 2) have a large number of targets that are modulators of p53 signaling and cell cycle regulation, notably SIRT1, p21, CDK6 and E2F family proteins. One common miRNA target is the high mobility group A2 (HMGA2) protein. HMGA2 protein levels were reduced in human umbilical cord blood stem cells and endothelial cells undergoing replicative senescence, and was associated with the upregulation of miR-10b*, miR-21, miR-23a, miR-26 and miR-30, all which have binding sites in the HMGA2 3’-UTR [169, 170]. Another target of the above miRNAs is the

RNA-binding protein Human antigen R (HuR) which binds to AU-rich elements in the 3'-UTR regions of mRNA [171]. HuR can modulate miRNA interactions with their target mRNA 3'-UTRs by displacing microRNA-induced silencing complexes (miRISC) from their binding sites [172, 173]. Downregulation of HuR is observed in replicative senescence and is mediated in part by miR-519 upregulation [174, 175].

Most studies to date have investigated miRNA dysregulation due to replicative (telomere-induced) senescence, stress-induced senescence (treating with exogenous DNA damaging agents and epigenetic modifiers) or oncogene-induced senescence (over-expressing Ras). Progeroid mouse models have recently been used to identify microRNA dysregulation in aging and cellular senescence, particularly Hutchinson Guildford Progeria Syndrome (HGPS) and Werner Syndrome (WS) [176, 177]. However, despite some phenotypic similarities to natural aging, these two models demonstrate a major disadvantage when compared to *Ercc1*-deificient mice because they do not examine the effect of endogenous DNA damage on aging. The main cellular perturbations in these other progeroid diseases, nuclear lamin dysfunction in HGPS and premature telomere dysfunction in WS are not commonly observed in the human population, and because of this, the conclusions that can be made regarding microRNA dysregulation in HGPS and WS will have to be considered within the context of that particular progeroid model. However, microRNA dysregulation in the *Ercc1*-deficient mouse model are more generalizable to normal mouse aging, due to the ubiquity with which these animals are exposed to endogenous DNA damage.

Currently, little is known about microRNA regulation of cellular senescence induced by endogenous, non-telomeric DNA damage. This study seeks to address this gap in knowledge.

Table 1: MicroRNA regulators of replicative senescence and DNA damage-induced senescence

microRNA	Gene Target(s)	Regulation in Senescence	Cell Type	Reference
Let-7	HMGA2, EZH2, Rb1, E2F	Up	Fibroblast, Mesenchymal Stem Cell	[178, 179]
miR-9	SIRT1	Up	Fibroblast, Endothelial	[81, 180]
miR-10a	KLF4	Up	Mesenchymal Stem Cells	[181]
miR-10a*	HMGA2	Up	Endothelial	[170]
miR-22	CDK6, SIRT1, Sp1, OGN	Up	Fibroblast	[182, 183]
miR-23a	HMGA2	Up	Cord blood-derived stem cells	[169]
miR-26	HMGA2	Up	Cord blood-derived stem cells	[169]
miR-28	ASF/SF2	Up	Fibroblast	[184]
miR-29a/b/c	COL4α1 – α6, B-MYB	Up	Lung, Liver, Kidney, Heart, HeLa, Mesenchymal Stem cells	[185, 186]
miR-30	B-Myb	Up	HeLa	[186]
miR-34a	SIRT1, MYC, TXNRD2	Up	Endothelial, Fibroblast, Mesangial	[150, 156, 187]
miR-101	EZH2	Up	Fibroblast	[188]
miR-106	P21, RB1	Down	Aged normal tissues and tumor tissues	[189, 190]
miR-107	HIF1B, CDK6, NOTCH2	Up	Colon Cancer, Glioma	[148]
miR-126	VCAM-1	Down	Endothelial	[191]
miR-146a/b	IRAK1, TRAF6	Up	Fibroblast, Human trabecular meshwork	[75, 192]
miR-152	ITGA5	Up	Fibroblast	[193]
miR-155	SPI1, DC-SIGN, AID, IRF8, MYB	Up	Monocyte, Fibroblast	[194-197]
miR-181a	COL16A1	Up	Fibroblast	[193]
miR-181a	DUSP6	Down	T cells	[198]

miR-191	SATB1, CDK6	Up	Keratinocyte	[199]
miR-200c	ZEB1	Up	Endothelial	[200]
miR-203	E2F3, CAV1	Up	Melanoma, Breast tissue	[201]
miR-205	E2F1, E2F5	Up	Melanoma	[202]
miR-217	SIRT1	Up	Endothelial	[203]
miR-221	eNOS	Up	Endothelial	[191]
miR-222	eNOS	Up	Endothelial	[191]
miR-290	LRF	Up	Fibroblast	[204]
miR-299-3p	IGF1	Up	Endothelial	[205]
miR-335	SOD2	Up	Mesangial	[187]
miR-375	LDHB, SP1	Up	Myeloid leukemia	[206]
miR-486-5p	SIRT1	Up	Mesenchymal Stem Cells	[207]
miR-494	IGF2BP1	Up	Lung Cancer	[208]
miR-505	ASF/SF2	Up	Fibroblast	[184]
miR-519	HuR	Up	Fibroblast, Ovary, Kidney, Lung, HeLa	[175]

Table 2: MicroRNA regulators of oncogene-induced senescence

miR-17-92 cluster	P21	Down	Aged normal tissues	[189]
miR-20a	LRF, P21	Up	Fibroblast	[189, 209]
miR-21	CDC25A, HMGA2, NF1B, PDCD4	Up	Endothelial	[164, 170, 210]
miR-29c	SIRT1, CDK6	Up	Glioma, Hepatocellular Carcinoma	[211, 212]

1.5 PROJECT HYPOTHESIS

We hypothesize that miRNAs are important in modulating many of the cellular changes that occur during aging and cellular senescence, and propose to use the XFE Progeroid Syndrome as a model system to identify miRNAs that are involved in regulating this process. Using cells and tissues from *Ercc1*$^{-/-}$ and *Ercc1*$^{-/\Delta}$ mice will allow us to identify miRNAs dysregulated primarily by endogenous DNA damage. We will also focus on miRNAs that are commonly dysregulated in tissues from both the progeroid as well as normally aged mice. Once we have identified senescence-associated miRNAs, we plan to identify novel gene targets for these miRNAs that are relevant to the regulation of cellular senescence.

2.0 DYSREGULATION OF MICRORNAS IN THE *ERCC1* MOUSE MODEL OF PROGERIA

Work described in this section was published in Aging (Aging (Albany NY). 2013 Jun;5(6):460-73.) with authors Lolita S. Nidadavolu, Laura J. Niedernhofer and Saleem A. Khan.

2.1 INTRODUCTION

MicroRNAs (miRNAs) are ~22 nucleotide long, single-stranded, non-coding RNAs that regulate gene expression. They generally bind the 3' untranslated regions (UTRs) of target mRNAs with varying affinity, resulting in mRNA degradation or inhibition of protein translation [1]. The biogenesis of miRNAs is well-characterized, although the mechanisms by which they participate in post-transcriptional silencing are still being elucidated [2, 3]. A wide range of disease processes including cancer are regulated by miRNAs [4].

MicroRNAs are implicated in the regulation of cellular senescence and aging. Cellular senescence, a state of permanent cell cycle arrest, is hypothesized to be a double-edged sword by suppressing cancer progression while promoting growth inhibition and aging-related tissue degeneration [5]. Cellular senescence can result from events such as telomere shortening, activation of DNA damage response (DDR), epigenetic stresses, or expression of oncogenes such as Ras [6-9]. DDR signaling in senescent cells can also take place with little to no DNA damage, termed the "pseudo-DNA damage response" [10]. This phenomenon occurs in cells ectopically expressing p16 and p21 as well as in cells treated with epigenetic modifiers, such as sodium butyrate, an HDAC inhibitor [10, 11]. Senescent cells exhibit a unique gene expression profile, termed senescence-associated secretory phenotype (SASP), and promote the release of pro-inflammatory markers, including IL-6 [12]. The P16INK4A (p16) tumor suppressor is significantly upregulated in senescent cells [13]. A recent paper describing the selective

apoptosis of p16-expressing cells in a progeroid mouse (BubR1) directly connects accumulation of senescent cells and age-associated phenotypes in mice [14].

Senescent fibroblasts displaying high SASP express miR-146a/b, which attenuates SASP activity in a negative-feedback loop [15]. MiR-22, miR-519, miR-152 and miR-181a, among others, were recently identified as inducers of cellular senescence [16-18]. Knocking down Dicer, a key component in the miRNA processing pathway, causes inhibition of miRNA biogenesis and results in cellular senescence via activation of p53 signaling [19]. Also, MEF immortalization results in the downregulation of certain tumor suppressor miRNAs: miR-21, miR-28 and miR-34a [20]. These data suggest that miRNAs are critical for regulating senescence.

The insulin-like growth factor (IGF) signaling pathway is involved in regulating lifespan and mouse mutants with reduced IGF signaling have lifespans 40-70% greater than those of wild-type (WT) mice [21-23]. Several studies examining miRNA dysregulation in aging have utilized naturally aged or long-lived animals. MicroRNA profiling studies examined liver and brain tissues of normally aged mice as well as liver from long-lived Ames Dwarf mouse [24-27]. Additional studies have identified that the neuroprotective effects observed in calorie restriction in mice is due, in part, to downregulation of miRNAs targeting the pro-survival gene Bcl-2 [28]. Human centenarian studies have also demonstrated miRNA expression differences between blood samples from long-lived humans and young controls [29, 30]. MicroRNAs have also been identified as useful biomarkers for early, non-invasive detection of mild cognitive impairment [31]. However, few studies link both senescence and aging with changes in miRNA expression.

To address this gap in knowledge, we measured miRNA expression in a murine model of a progeroid syndrome in tissues where senescence is established, as well as tissues of naturally

aged mice and senescent primary mouse embryonic fibroblasts. The XFE progeroid syndrome is a disease of accelerated aging caused by a deficiency in the XPF-ERCC1 DNA repair endonuclease. Murine models of XFE progeroid syndrome (*Ercc1*$^{-/-}$ knock-out and *Ercc1*$^{-/\Delta}$ hypomorphic mice) are well-characterized models that mimic the histopathology of normal aging [119, 124, 213-215]. XPF-ERCC1 is essential for nucleotide excision repair (NER) of helix-distorting monoadducts, repair of DNA interstrand crosslinks, as well as repair of some double-strand breaks [114, 216, 217]. *Ercc1*$^{-/\Delta}$ mice accumulate oxidative DNA damage more rapidly than WT mice, and this is presumed to drive their accelerated aging [218]. Liver transcriptome analysis of *Ercc1*$^{-/-}$ and *Ercc1*$^{-/\Delta}$ mice revealed gene expression profiles similar to those of livers from aged WT mice, including a decrease in the IGF-1/somatotrophic axis and carbohydrate metabolism [119]. Additionally, *Ercc1*$^{-/\Delta}$ mice also demonstrate increased p16 expression, cellular senescence, and nuclear abnormalities that are similar to those observed in WT old mice [124].

Primary mouse embryonic fibroblasts (MEFs) undergo stress-related senescence due to growth conditions, in particular the supra-physiological concentrations of oxygen in standard tissue culture conditions [219]. When MEFs are grown in 3% O_2 conditions, they demonstrate delayed onset of cellular senescence and behave similarly to human fibroblasts expressing telomerase [219]. MEFs grown in 20% O_2 have three-fold more DNA damage than human fibroblasts grown at 20% O_2, and have more chromosomal breaks than MEFs grown in 3% O_2, further underscoring the exquisite sensitivity of MEFs to oxidative damage [219]. *Ercc1*$^{-/-}$ MEFs, which are deficient in DNA repair, quickly accumulate global DNA damage and demonstrate cellular senescence phenotypes at earlier passages compared to WT MEFs [105, 119]. Table 3 demonstrates a characterization of several senescence endpoints in WT and *Ercc1*$^{-/-}$ MEFs grown

to 20% and 3% O_2 at increasing passage (Passages 3, 5 and 7) [Gregg and Niedernhofer, personal correspondence].There is a clear increase in SA β-gal and γ-H2AX foci, and a decrease in cell proliferation with increased passage, particularly in *Ercc1*$^{-/-}$ MEFs grown in 20% O_2 conditions (Table 3).

Table 3: Summary of senescence endpoints in WT and *Ercc1*$^{-/-}$ MEFs.

WT and *Ercc1*$^{-/-}$ MEFs were grown in both 20% and 3% O_2 conditions to passages 3, 5 or 7. Several different senescence endpoints, cell proliferation, senescence-associated β-galactosidase and γ-H2AX foci, were measured and compared to WT MEFs grown in 3% O_2. Up and down arrows indicate relative expression of the particular endpoint relative to WT MEFs grown in 3% O_2 at the same passage. SA β-gal, Senescence-associated β-galactosidase. NC, no change. [Gregg and Niedernhofer, personal correspondence]

	WT MEF			***Ercc1*$^{-/-}$ MEF**					
Passage	**3**	**5**	**7**	**3**	**5**	**7**	**3**	**5**	**7**
Oxygen %	**20**	**20**	**20**	**20**	**20**	**20**	**3**	**3**	**3**
Proliferation	**NC**	**NC**	↓	**NC**	↓	↓	**NC**	**NC**	↓
SA β-gal	**NC**	**NC**	↑	**NC**	**NC**	**NC**	**NC**	**NC**	**NC**
γ-H2AX	**NC**	↑	**NC**	↑	↑	**NC**	↑	↑	**NC**

An additional benefit of using progeroid mouse models to identify dysregulated miRNAs in tissues is that studies can be performed in a relatively short period of time compared to studies using normal or long-lived animal models. A previously published study demonstrated the usefulness of progeroid models, in particular the Zmpste24-null mouse modeling Hutchinson-Guilford Progeria Syndrome, in identifying miRNAs regulating organismal aging. This study showed that the miR-29 family is linked to the cellular DNA damage response and when upregulated in a p53-dependent manner, miR-29b reduces cell proliferation and increases cellular senescence [176]. Mir-29 acts as a tumor-suppressive, pro-aging molecule via chronic activation of p53 signaling [176].

We wished to identify miRNAs associated with senescence driven by DNA damage and oxidative stress by analyzing changes in miRNA expression in *Ercc1*$^{-/-}$ MEFs compared to the WT MEFs cultured to late passage in both high and low oxygen conditions. A subset of differentially expressed miRNAs was found to be dysregulated in *Ercc1*$^{-/-}$ MEFs driven to senescence compared to non-senescent *Ercc1*$^{-/-}$ MEFs. Additionally, we demonstrate that several miRNAs differentially expressed in the *Ercc1*$^{-/-}$ MEFs (miR-449a, miR-455*, miR-128, miR-497, miR-543, miR-450b-3p, miR-872 and miR-10b) were also dysregulated in liver tissues of both progeroid *Ercc1*$^{-/\Delta}$ and old WT mice compared to young WT mice. We show that three of the above miRNAs (miR-449a, miR-455* and miR-128) were downregulated in kidney tissues from *Ercc1*$^{-/\Delta}$ progeroid and WT old mice compared to the young mice. Finally, the regulator of miRNA biogenesis, Dicer, was significantly downregulated in late passage MEFs compared to early passage and in livers of old WT mice compared to young mice. The identified miRNAs in this study may play a critical role in staving off cellular senescence and aging.

2.2 MATERIALS AND METHODS

2.2.1 Animal Care and Experimentation

All experiments involving mouse tissues and cells were approved by the University of Pittsburgh Institutional Animal Care and Use Committee and were in accordance with NIH guidelines for humane care of animals. *Ercc1*$^{-/-}$ and *Ercc1*$^{-/\Delta}$ mice were bred and genotyped as previously described [217]. All mice used for tissue miRNA qRT-PCR analysis were in a f1 mixed genetic background (FVB/n:C57Bl/6). Twenty-week old progeroid *Ercc1*$^{-/\Delta}$ mice along with age-matched WT littermates with aged (30 month) WT mice were euthanized by CO_2 inhalation and tissues were excised and flash-frozen in liquid nitrogen. Three mice of each genotype were used for subsequent qRT-PCR analysis. The livers and kidneys were homogenized with a hand-held homogenizer (Omni International, Kennesaw, GA, USA) and RNA was extracted using the Ultraspec RNA Isolation System (Biotecx, Houston, TX, USA). Following isolation, RNA quantity was measured using a Nanodrop (Thermo Fisher Scientific Inc., Waltham, MA, USA). RNA quality was assessed by formaldehyde-agarose gel electrophoresis.

2.2.2 Primary Mouse Embryonic Fibroblasts

The following primary cells were used: wild-type (WT) isogenic mouse embryonic fibroblasts (MEFs) and *Ercc1*$^{-/-}$ (KO) MEFs derived from 13.5-day embryos with a 50:50 C57Bl/6:FVB/n background. Cells were serially passaged at either 3% or 20% O2 to passage 3 or passage 7,

pelleted and total RNA extracted using the Ultraspec RNA Isolation System. Two independent cell lines were used for microarray and qRT-PCR analysis.

2.2.3 MicroRNA Microarray

MicroRNA microarray studies were performed using 100 nanograms of total RNA obtained from WT and *Ercc1*$^{-/-}$ MEFs grown to P3 and P7 in 3% or 20% O2. Two independent cell lines were used for each sample and both cell lines were analyzed via microarray. We used the Agilent mouse miRNA microarrays (V2) (Agilent Technologies, Santa Clara, CA, USA) according to the manufacturer's instructions. Each microarray contains sixteen to twenty oligonucleotide probes for each of the 627 mouse miRNAs and 39 mouse viral miRNAs based on the Sanger database version 12. The array contains 281 positive controls consisting of high-signal endogenous mouse-specific probes, and 434 negative controls consisting of random sequences that have low signal and poor hybridization to mouse RNA. RNA was isolated from MEFs using the Ultraspec RNA Isolation System, dephosphorylated with calf intestinal alkaline phosphatase, and then denatured with dimethyl sulfoxide. The 3' ends were then ligated to a Cyanine3-pCp molecule using T4 RNA ligase. Labeled RNA was purified using a MicroBio-spin 6 column containing Bio-Gel P-6 in Tris buffer (Bio-Rad Laboratories, Inc. Hercules, CA, USA). The labeled RNA samples were hybridized to Agilent microarray slides at 55˚C for 20 hours. Following hybridization, the slides were washed with Agilent-supplied Gene Expression Wash Buffers 1 and 2. Slides were immediately scanned with an Agilent Microarray Scanner.

MicroRNA microarray studies were performed using 100 nanograms of total RNA obtained from WT and *Ercc1*$^{-/-}$ MEFs grown to P3 and P7 in 3% or 20% O_2. Two independent cell lines were

used for each sample and both cell lines were analyzed via microarray. We used the Agilent mouse miRNA microarrays (V2) (Agilent Technologies, Santa Clara, CA, USA) according to the manufacturer's instructions. Each microarray contains sixteen to twenty oligonucleotide probes for each of the 627 mouse miRNAs and 39 mouse viral miRNAs based on the Sanger database version 12. The array contains 281 positive controls consisting of high-signal endogenous mouse-specific probes, and 434 negative controls consisting of random sequences that have low signal and poor hybridization to mouse RNA. RNA was isolated from MEFs using the Ultraspec RNA Isolation System, dephosphorylated with calf intestinal alkaline phosphatase, and then denatured with dimethyl sulfoxide. The 3' ends were then ligated to a Cyanine3-pCp molecule using T4 RNA ligase. Labeled RNA was purified using a MicroBio-spin 6 column containing Bio-Gel P-6 in Tris buffer (Bio-Rad Laboratories, Inc. Hercules, CA, USA). The labeled RNA samples were hybridized to Agilent microarray slides at 55˚C for 20 hours. Following hybridization, the slides were washed with Agilent-supplied Gene Expression Wash Buffers 1 and 2. Slides were immediately scanned with an Agilent Microarray Scanner.

2.2.4 Microarray Statistical Analysis

After scanning, images were processed using Agilent's Feature Extraction Software, version 9.5.3. Extracted data were exported into Agilent's GeneSpring GX version 10 and microarray data was $\log_2$ transformed and normalized to the mean of each array. An unpaired t-test with unequal variance was used to identify differentially expressed miRNAs ($P< 0.05$). We selected microRNAs with 2-fold or greater changes for further study. Microarray experiments conform to Minimum Information About a Microarray Experiment (MAIME) guidelines and a full data set

has been submitted to the National Center for Biotechnology Information (NCBI) Gene Expression Omnibus database (GEO).

2.2.5 Real-Time Quantitative Reverse-Transcriptase Polymerase Chain Reaction (qRT-PCR) Analysis

QRT-PCR analysis was performed on total RNA prepared by Ultraspec RNA isolation by using a two-step individual Mature Taqman® MicroRNA Assays kit (Applied Biosystems, Foster City, CA, USA) and the Real-Time Thermocycler iQ5 (Bio-Rad, Hercules, CA, USA). All qRT-PCR assays were performed according to manufacturer's instructions and miRNA expression levels were normalized to snoRNA135. For all experiments, two independent cell lines were used and all assays were performed in triplicate. Relative expression was calculated using the $2^{-\Delta\Delta CT}$ method [220]. Welch's unpaired *t* test with 95% confidence intervals was performed for statistical analysis of all qRT-PCR experiments using Prism software (GraphPad Software, Inc., La Jolla, CA, USA).

Dicer expression in primary MEFs and mouse livers was quantified via qRT-PCR using the iScript One-Step RT-PCR Kit with SYBR Green (BioRad) in accordance with the manufacturer's instructions. Dicer mRNA was amplified using the forward primer sequence 5'-GGAAGCAGCCAACAAAAGAG- 3' and the reverse primer 5'-TGAGGGTTTTCTCTGCGTC T-3', amplifying a 145-bp region. The annealing temperature for Dicer qRT-PCR reactions was 50°C. Dicer mRNA levels were normalized to the glyceraldehyde-3-phosphate dehydrogenase (GAPDH) gene, using the forward primer 5'-AACTTTGGCATT GTGGAAGG-3' and the reverse primer 5'-GGATGCAGGGATGATGTTCT-3', amplifying a 132-bp region. DNase I-

treated total RNA (1 µg) was used for each reaction, and all the reactions were performed in triplicate. Relative Dicer mRNA expression was calculated using $2^{-\Delta\Delta CT}$ values [220]. Welch's unpaired *t* test with 95% confidence intervals was performed for statistical analysis of MEF microRNA qRT-PCR experiments. A one-way ANOVA with a Tuckey's multiple comparison test was used for statistical analysis of Dicer mRNA qRT-PCRs in MEFs. A one-way ANOVA with a Dunnett's multiple comparison test was performed on all microRNA qRT-PCRs of liver and kidney tissues. All statistical analyses were performed using Prism software (GraphPad Software, Inc., La Jolla, CA, USA).

2.3 RESULTS

2.3.1 Identification of senescence- and DNA damage-associated miRNAs in *Ercc1*$^{-/-}$ MEFs

We performed miRNA microarray analysis using RNA isolated from early (passage 3) and late passage (passage 7) WT and *Ercc1*$^{-/-}$ MEFs to identify miRNAs that may contribute to cellular senescence. *Ercc1*$^{-/-}$ MEFs grow slower than WT MEFs at 20% O_2 and senesce prematurely by passage 7 [78, 119]. Several markers of cellular senescence, such as reduced proliferation, increased senescence-associated β-galactosidase staining, increased γ-H2AX foci, appear at earlier passage time points in *Ercc1*$^{-/-}$ MEFs grown in 20% O_2 compared to *Ercc1*$^{-/-}$ MEFs grown in 3% O_2 and WT MEFs grown in 20% O_2 (Table 3). Growing MEFs at 3% O_2 delays the onset of senescence due in part to decreased oxidative stress [219]. We compared the miRNA expression profiles of *Ercc1*$^{-/-}$ and WT MEFs grown in low (3%) and high (20%) oxygen to

passage 3 (P3) and passage 7 (P7) using mouse microRNA microarrays to discover miRNAs that correlate with senescence. We utilized Agilent mouse miRNA microarrays (V2), which probed for 627 total murine miRNAs. All microRNAs included in the microarray are listed in Appendix A. The microarray design allows for low sample input (100 ng of total RNA) and has a low detection limit, with the ability to detect miRNAs in the 1 x 10^{-9} nanomole range. However, a limitation of this screen is that we only identified miRNAs that were available in the Sanger miRBase, version 12.0. This database and the updated version of this microarray have since been updated to include over 620 additional microRNAs. Therefore, the analysis that we performed using the Agilent mouse miRNA microarrays V2 does not include all currently known murine microRNAs.

We focused on miRNAs that were significantly dysregulated, which was defined as ≥2-fold change in expression and $p \leq .05$. A comparison of the miRNA profiles of P3 (early passage) *Ercc1*$^{-/-}$ and congenic WT MEFs grown along with further qRT-PCR validation showed minimal differences between the two samples regardless of oxygen tension (data not shown). This was not unexpected since the growth properties of *Ercc1*$^{-/-}$ MEFs are not appreciably different from the WT MEFs at this early passage. We next compared the miRNA expression profiles of P7 *Ercc1*$^{-/-}$ and WT MEFs of cells grown in either 20% O_2 or 3% O_2 to examine inherent changes in miRNA expression due to genotype. Comparison of P7 *Ercc1*$^{-/-}$ and WT MEFs grown in 20% O_2 identified one significantly upregulated miRNA, miR-467a, which was over-expressed 2.19 fold in P7 *Ercc1*$^{-/-}$ MEFs compared to WT cells. MiR-467a may be upregulated as a result of a defect in DNA repair capacity. Additionally, we identified six downregulated miRNAs (miR-301a, miR-326, miR-455*, miR-497, miR-543 and miR-872) in late-passage P7 *Ercc1*$^{-/-}$ MEFs compared to the WT MEFs grown in 3% O_2 (Table 4), all of which are possibly microRNAs

dysregulated due to DNA damage accumulation. QRT-PCR analysis confirmed downregulation of these six miRNAs in *Ercc1*$^{-/-}$ compared to WT MEFs, although there were differences in the fold-change downregulation based on the two approaches (Figure 3).

Table 4: MiRNAs differentially expressed in *Ercc1*$^{-/-}$ MEFs compared to WT MEFs grown at 3% O_2.

DNA repair-deficient *Ercc1*$^{-/-}$ primary MEFs were grown at 3% O_2 to prevent cellular senescence. Congenic WT cells isolated from a littermate embryo were handled in parallel as a control. At passage 7, total RNA was isolated and miRNA expression measured by microarray. Significant changes were defined as ≥2-fold and $p < .05$ as determined by Welch's unpaired t test.

MicroRNA	Fold-change	*p*-value
mmu-miR-301a	-2.24	0.007
mmu-miR-543	-2.60	0.023
mmu-miR-326	-3.05	0.029
mmu-miR-455*	-3.23	0.020
mmu-miR-872	-6.72	0.044
mmu-miR-497	-6.87	0.002

Figure 3: QRT-PCR confirmation of downregulation of six miRNAs identified from the microarray experiments in *Ercc1*$^{-/-}$ MEFs, compared to WT MEFs.

MiRNA microarray data (Table 4) was validated by qRT-PCR analysis of *Ercc1*$^{-/-}$ MEFs at P7 compared to WT MEFs at P7, grown to 3% O_2. WT MEFs at P7 were assigned a value of -1. Six miRNAs identified in the microarray were confirmed to be downregulated by qRT-PCR. MiR-455* refers to the less abundant miRNA product derived from the miR-455 stem-loop precursor. *P*-values were calculated using Welch's t-tests and are indicated by * ($p<$ .001) and ** ($p<$ .0001).

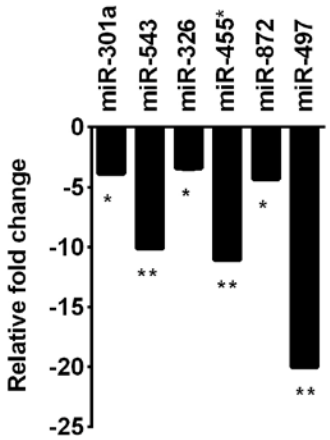

Three miRNAs (miR-450B-3p, miR-33 and miR-323-3p) were significantly upregulated in P7 *Ercc1*$^{-/-}$ MEFs grown at 20% O_2 compared to those grown at 3% O_2 (Table 5), which examined isogenic senescent vs. non-senescent cells in the presence of high and low oxygen conditions. We next compared miRNA expression in P7 vs. P3 *Ercc1*$^{-/-}$ MEFs grown in 3% (Table 6) or 20% O_2 (Table 7), which identified miRNAs dysregulated in *Ercc1*$^{-/-}$ MEFs with sequential passaging of cells under different oxidative stress conditions. Fourteen miRNAs were significantly upregulated and 22 downregulated in P7 *Ercc1*$^{-/-}$ MEFs compared to P3 *Ercc1*$^{-/-}$ MEFs grown at 3% O_2 (Table 6). One miRNA, miR-24-2*, was upregulated and three miRNAs, miR-204, miR-218, miR-455* were downregulated in P7 *Ercc1*$^{-/-}$ MEFs grown in 20% O_2

compared to P3 *Ercc1*$^{-/-}$ MEFs (Table 7). MiR-455* was downregulated in late passage cells compared to early passage in both analyses. Finally, we compared miRNA expression profiles of the most senescent cells in our analysis, P7 *Ercc1*$^{-/-}$ MEFs grown at 20% O_2, to the least senescent cells in our analysis, P3 WT MEFs grown at 3% O_2. This revealed significant upregulation of one miRNA, miR-129-5p, which was increased 603-fold in *Ercc1*$^{-/-}$ MEFs.

Table 5: MiRNAs differentially expressed in *Ercc1*$^{-/-}$ MEFs grown at 20% vs. 3% O_2.

DNA repair-deficient *Ercc1*$^{-/-}$ primary MEFs were grown at 20% O_2 to induce cellular senescence. A parallel culture of the same cells was grown at 3% O_2 to prevent senescence. At passage 7, total RNA was isolated and miRNA expression measured by hybridization-based microarray. Shown is the fold difference in expression for 20% versus 3% O_2. Significant changes were defined as ≥2-fold and p <.05 as calculated via Welch's unpaired t test.

MicroRNA	Fold-change	*p*-value
mmu-miR-323-3p	2.14	0.003
mmu-miR-33	2.10	0.001
mmu-miR-450b-3p	2.06	0.015

Table 6: MiRNAs differentially expressed in late vs. early passage *Ercc1*$^{-/-}$ MEFs grown in 3% O_2.

DNA repair-deficient *Ercc1*$^{-/-}$ primary MEFs were grown at 3% O_2. At passage 3 and 7, total RNA was isolated and miRNA expression measured by hybridization-based microarray. Shown is the fold difference in expression in P7 versus P3 cells. Significant changes were defined as ≥2-fold and p <.05 as determined by Welch's unpaired t test.

MicroRNA	Fold-change	*p*-value	MicroRNA	Fold-change	*p*-value
mmu-miR-671-5p	14.3	0.025	mmu-miR-29b*	-2.15	0.003
mmu-miR-1892	12.7	0.041	mmu-miR-449a	-2.24	0.043
mmu-miR-483	12.6	0.020	mmu-miR-455*	-2.77	0.004
mmu-miR-1894-3p	8.46	0.050	mmu-miR-340-3p	-2.96	0.036
mmu-miR-1895	7.28	0.039	mmu-miR-362-5p	-3.56	0.038
mmu-miR-680	6.54	0.023	mmu-miR-675-3p	-3.94	0.041
mmu-miR-721	6.43	0.029	mmu-miR-466a-3p	-3.95	0.037
mmu-miR-129-5p	5.06	0.046	mmu-miR-128	-4.41	0.047
mmu-miR-1906	3.82	0.006	mmu-miR-497	-5.16	0.048
mmu-miR-222	3.73	0.034	mmu-miR-362-3p	-5.23	0.012
mmu-miR-320	3.62	0.010	mmu-miR-192	-5.61	0.004
mmu-miR-290-5p	3.41	0.002	mmu-miR-496	-5.79	0.044
mmu-miR-22	3.27	0.023	mmu-miR-543	-6.81	0.023
mmu-miR-877	2.86	0.039	mmu-miR-30e*	-8.15	0.016
			mmu-miR-382*	-10.1	0.029
			mmu-miR-337-3p	-11.3	0.049
			mmu-miR-450b-3p	-12.4	0.014
			mmu-miR-872	-14.7	0.021
			mmu-miR-369-5p	-15.1	0.024
			mmu-miR-380-3p	-15.7	0.048
			mmu-miR-154*	-31.6	0.019
			mmu-miR-10b	-32.5	0.041

Table 7: MiRNAs differentially expressed in late vs. early passage *Ercc1*$^{-/-}$ MEFs grown in 20% O_2.

DNA repair-deficient *Ercc1*$^{-/-}$ primary MEFs were grown at 20% O_2. At passage 3 and 7, total RNA was isolated and miRNA expression measured by hybridization-based microarray. Shown is the fold difference in expression in P7 versus P3 cells. Significant changes were defined as ≥2-fold and p <.05 as calculated via Welch's unpaired t test.

MicroRNA	Fold-change	*p*-value
miR-24-2*	3.14	0.028
miR-455*	-3.98	0.036
miR-218	-10.3	0.032
miR-204	-13.1	0.022

For further studies, we selected seven upregulated and ten downregulated miRNAs that were altered in our microarray comparison from Table 6 for validation by qRT-PCR analysis. The microRNAs we selected were those that appeared in several comparisons, indicating that these microRNAs are possibly senescence- or DNA damage-associated. This subset of 17 miRNAs was selected because they are known to have human homologs based on the miRBase database [221-224]. Of the seven upregulated miRNAs, three (miR-680, miR-320 and miR-22) were confirmed to be upregulated by qRT-PCR analysis (Figure 4A). The other miRNAs showed either no significant change or were found to be downregulated as determined by qRT-PCR analysis. Ten downregulated miRNAs were confirmed to be downregulated by qRT-PCR analysis (Figure 4B). MiR-455*, miR-497 and miR-543 were significantly downregulated in Table 4, which compared late passage DNA repair deficient to DNA repair proficient MEFs, and Table 6, comparing DNA repair deficient MEFs at early versus late passage, showing the

effect of sequential passaging on miRNA expression. This suggests that miR-455*, miR-497 and miR-543 may be dysregulated as a result of deficient DNA repair and/or sequential passaging.

Figure 4: QRT-PCR validation of miRNAs identified from the microarray analysis of late passage *Ercc1*$^{-/-}$ MEFs normalized to early passage *Ercc1*$^{-/-}$ MEFs.

(A) Three miRNAs (miR-680, mir-320 and miR-22) identified as being upregulated in late *Ercc1*$^{-/-}$ MEFs compared to early passage via microarray (Table 6) were confirmed to be upregulated by qRT-PCR. QRT-PCR expression values are relative to *Ercc1*$^{-/-}$ passage 3 samples, which were normalized to a value of either 1 or -1. **(B)** Ten downregulated miRNAs in P7 *Ercc1*$^{-/-}$ MEFs from the microarray analysis (Table 6) were confirmed to be downregulated by qRT-PCR. MiR-455* refers to the less abundant miRNA product derived from the miR-455 stem-loop precursor. Expression values are relative to *Ercc1*$^{-/-}$ passage 3 samples, which were normalized to a value of -1. *P*-values for qRT-PCR data were calculated using Welch's t-tests and are indicated by * ($p < .05$), ** ($p < .01$) and # ($p < .0001$).

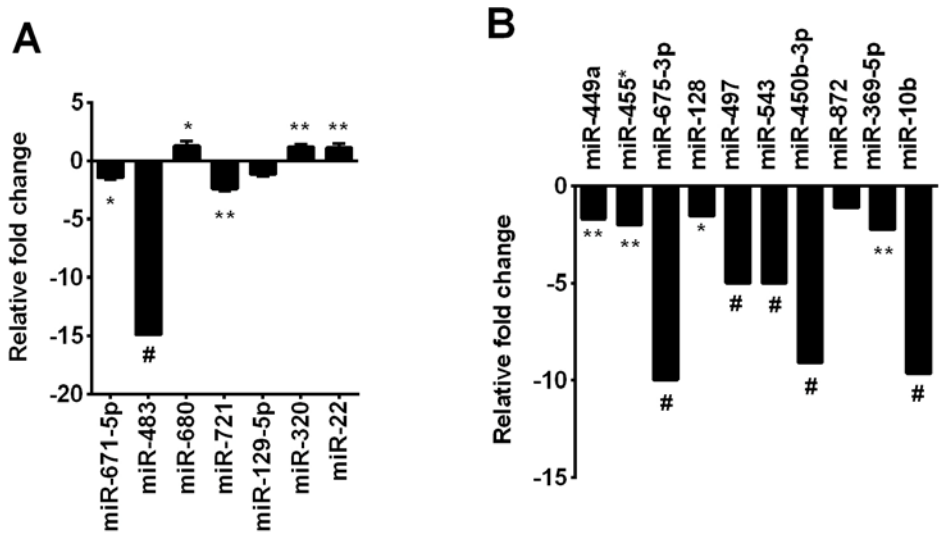

We also confirmed that miR-467a was overexpressed in P7 *Ercc1*$^{-/-}$ versus WT MEFs grown in 20% O_2 using qRT-PCR (Figure 5A) and observed that it was also overexpressed in P7 versus P3 *Ercc1*$^{-/-}$ MEFs grown in 20% O_2, despite not appearing upregulated in the microarray data (Figure 5B). Additionally, because miR-129-5p was the only miRNA dysregulated in the comparison of our most senescent to least senescent cells, we examined expression of this miRNA via qRT-PCR and confirmed that it is over-expressed in P7 *Ercc1*$^{-/-}$ MEFs in 20% O_2 compared to P3 WT MEFs in 3% O_2 (Figure 6).

Figure 5: QRT-PCR expression of miR-467a in Passage 3 *Ercc1*$^{-/-}$ MEFs, Passage 7 WT MEFs and Passage 7 *Ercc1*$^{-/-}$ MEFs grown in 20% O_2.

(A) MiR-467a is upregulated in *Ercc1*$^{-/-}$ MEFs (KO) grown to Passage 7 (P7) in 20% O_2 compared to WT P7 MEFs grown to 20% O_2. QRT-PCR expression values are relative to WT P7 samples, which were normalized to a value of 1. **(B)** MiR-467a is upregulated in *Ercc1*$^{-/-}$ MEFs (KO) grown to Passage 7 (P7) in 20% O_2 compared to *Ercc1*$^{-/-}$ MEFs (KO) grown to Passage 3 in 20% O_2. Expression values are relative to *Ercc1*$^{-/-}$ passage 3 samples, which were normalized to a value of 1. All experiments were performed in triplicate and the standard deviation is plotted as error bars.

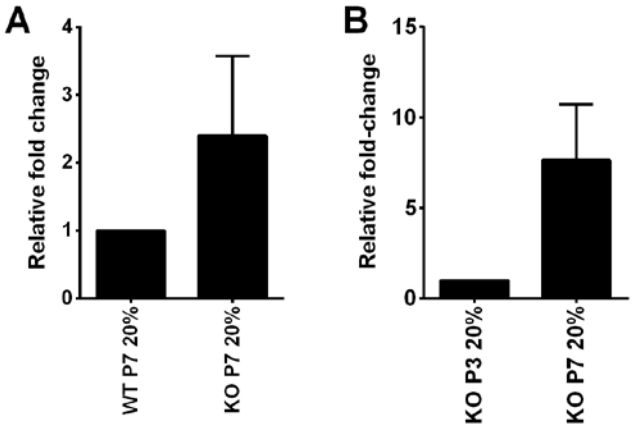

Figure 6: QRT-PCR expression of miR-129-5p in Passage 3 WT MEFs grown in 3% O_2 and Passage 7 *Ercc1*$^{-/-}$ MEFs grown in 20% O_2.

MiR-129-5p is upregulated in late passage senescent *Ercc1*$^{-/-}$ MEFs (KO P7) grown in 20% O_2 compared to WT Passage 3 (P3) MEFs grown in 3% O_2,which are the least senescent cells that we examined in our microarray experiments. QRT-PCR expression values are relative to WT passage 3 MEFs, which were normalized to a value of 1. All experiments were performed in triplicate and the standard deviation is plotted as error bars. *P*-values for qRT-PCR data were calculated using Welch's t-tests and are indicated by * ($p < .05$).

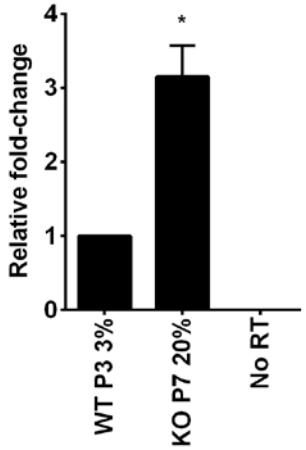

As the majority of miRNAs identified as dysregulated in ERCC1-depleted cells and tissue or old WT mice were downregulated rather than upregulated, we also measured expression of Dicer, which is required for miRNA biogenesis (Figure 7A). Dicer mRNA was reduced significantly in late passage *Ercc1*$^{-/-}$ MEFs, regardless of oxygen percentage (Figure 7A). This strongly suggests that downregulation of Dicer may also be in response to the accumulation of unrepaired DNA damage. Notably, levels of Dicer mRNA were also significantly reduced in old WT mouse liver compared to tissue from young mice and in late passage MEFs compared to early passage (Figure 7B). However, not all microRNAs identified from our microarray were downregulated. We identified a representative microRNA from our initial microarray that was not significantly changed in expression in non-senescent versus senescent cells, miR-31* (Figure

8). MiR-31* demonstrated 1.20-fold upregulation in the array, when comparing late passage *Ercc1*$^{-/-}$ MEFs compared to WT MEFs, all grown in 20% O_2. This was below our fold-change cut-off of 2, and therefore we determined that the dysregulation of miR-31* was not significant. When confirming this finding by qRT-PCR, miR-31* is shown to be expressed at approximately the same level in WT and *Ercc1*$^{-/-}$ MEFs at late passage, grown in 20% O_2 (Figure 8). Therefore downregulation of numerous miRNAs with senescence and aging may arise as a consequence of reduced global miRNA biosynthesis due to reduced Dicer expression. However, as is seen in the case of miR-31*, this downregulation is not universal, and some miRNAs do not demonstrate any dysregulation in senescent cells.

Figure 7: QRT-PCR of Dicer mRNA in primary MEFs and in liver tissues shows reduced expression in senescence and aging.

(A) Dicer mRNA is downregulated in Passage 7 *Ercc1*$^{-/-}$ (P7 KO) MEFs grown in both 20% O_2 and 3% O_2. QRT-PCR expression values are relative to WT Passage 3 (P3 WT) samples, which were normalized to a value of 1. **(B)** QRT-PCR analysis was performed on livers of WT young (20 weeks), progeroid *Ercc1*$^{-/\Delta}$ mice (20 weeks), and WT old mice (30 months) to examine Dicer mRNA expression. Dicer mRNA is downregulated significantly in WT Old mouse livers compared to WT Young and *Ercc1*$^{-/\Delta}$ livers. The mean of three independent mouse livers for each condition is graphed as fold-change expression relative to WT young livers, which were normalized to a value of -1. All experiments were performed in triplicate and the standard deviation is plotted as error bars. *P*-values for MEF qRT-PCRs (A) were calculated using one-way ANOVA with post hoc Tuckey's multiple comparison tests. *P*-values for liver tissues (B) were calculated using one-way ANOVA with a post hoc Dunnett's multiple comparison test, with WT young as the control sample: ** ($p < .01$), *** ($p < .001$) and # ($p < .0001$).

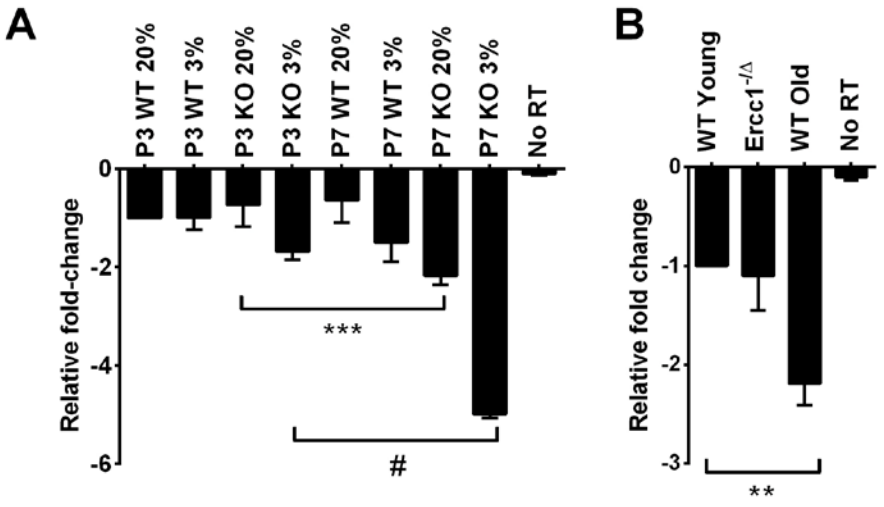

Figure 8: MiR-31* shows no change in expression in senescent *Ercc1*$^{-/-}$ MEFs compared to non-senescent WT MEFs.

MiR-31* demonstrates no change in late passage senescent *Ercc1*$^{-/-}$ MEFs (KO P7) grown in 20% O_2 compared to late passage WT MEFs (WT P7) grown in 20% O_2,which are less senescent due to less accumulated DNA damage. QRT-PCR expression values are relative to WT passage 7 MEFs, which were normalized to a value of 1. Microarray expression value for this comparison is listed in the graph to the far right. All qRT-PCR experiments were performed in triplicate and the standard deviation is plotted as error bars.

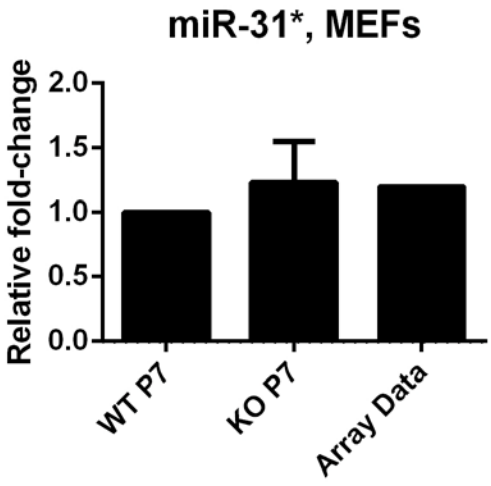

2.3.2 Senescence-associated miRNAs identified in *Ercc1*$^{-/-}$ MEFs are downregulated in livers of progeroid mice

The liver undergoes many significant changes during the normal aging process. Liver size reduces in general, there are decreases in hepatic blood flow and liver regeneration after partial hepatectomy is impaired [225-227]. Hepatocyte nuclei become enlarged and develop polyploidy and hepatocyte cytoplasm accumulates lipid droplets [228, 229]. The liver of 20 week-old progeroid *Ercc1*$^{-/\Delta}$ mice and 26 month-old WT mice show signs of profound cellular senescence and demonstrate increases in lipofuscin and lipid hydroperoxide as well as similar genome-wide transcriptional changes [124]. Using liver tissues from *Ercc1*$^{-/\Delta}$ and WT old mice offers a unique opportunity to determine if the miRNA identified to correlate with senescence in vitro might play a role in senescence and aging in vivo. We analyzed the levels of 13 miRNAs confirmed to be dysregulated in P7 *Ercc1*$^{-/-}$ MEFs compared to P3 *Ercc1*$^{-/-}$ MEFs (miR-680, miR-320, miR-22, miR-449a, miR-455*, miR-675-3p, miR-128, miR-497, miR-543, miR-450b-3p, miR-872, miR-369-5p and miR-10b) in RNA samples prepared from the livers of WT young (20 weeks), the progeroid *Ercc1*$^{-/\Delta}$ mice, and WT old mice (30 months). Several of the microRNAs we selected were also dysregulated in late passage *Ercc1*$^{-/-}$ MEFs compared to late passage WT MEFs (Table 4). Of the ten miRNAs downregulated in *Ercc1*$^{-/-}$ MEFs, eight (miR-449a, miR-455*, miR-128, miR-497, miR-543, miR-450b-3p, miR-872 and miR-10b) were also downregulated in both the progeroid and old WT mouse livers compared to the WT young (20 week) control mouse livers (Figure 9). The two remaining miRNAs downregulated in *Ercc1*$^{-/-}$ MEFs, miR-369-5p and miR-675-3p, showed no expression changes in *Ercc1*$^{-/\Delta}$ mouse livers (data not shown). Three

miRNAs (miR-680, miR-320, and miR-22) which were upregulated in P7 compared to P3 *Ercc1*$^{-/-}$ MEFs (Table 6) as measured by microarray did not show upregulation in livers from progeroid and WT old mice compared to young WT controls as measured by qRT-PCR (data not shown).

Figure 9: QRT-PCR quantification of miRNA identified as down-regulated in the liver of old WT mice and progeroid *Ercc1*$^{-/\Delta}$ mice compared to adult WT mice.

QRT-PCR analysis was performed on livers of WT young (20 weeks), *Ercc1*$^{-/\Delta}$ (20 weeks), and WT old mice (30 months). **(A)** MiR-449a. **(B)** MiR-455*. **(C)** MiR-128. **(D)** MiR-497. **(E)** MiR-543. **(F)** MiR-450b-3p. **(G)** MiR-872. **(H)** MiR-10b. All eight miRNAs were downregulated in *Ercc1*$^{-/\Delta}$ progeroid mice and WT old mice compared to WT young mice. No RT, no reverse transcriptase added. Three mouse livers are in each condition. The mean of three experimental replicates for each sample is graphed as relative to WT young samples, which were normalized to a value of -1. The standard deviation is plotted as error bars. *P*-values were calculated using one-way ANOVA with Dunnett's post hoc test, with WT young as the control sample: * ($p < .05$), ** ($p < .01$), *** ($p < .001$) and # ($p < .0001$).

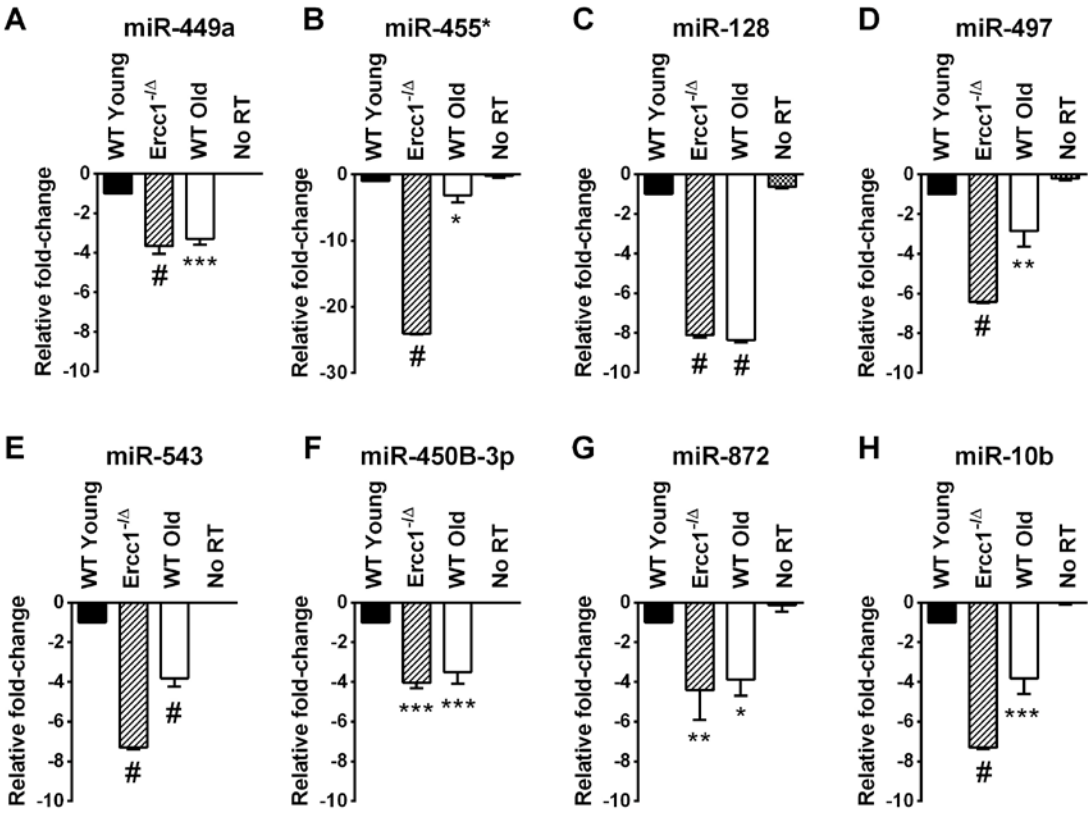

2.3.3 Three senescent-associated miRNAs identified in *Ercc1*$^{-/-}$ MEFs are also downregulated in progeroid mice kidneys

In addition to severe liver abnormalities, ERCC1-deficient mice also develop significant renal dysfunction, as demonstrated by increased proteinuria and creatinine levels [119]. Renal histopathology is evident, including dilated renal tubules, nuclear abnormalities and fibrosis [213]. We examined RNA prepared from kidneys of young (20 weeks) *Ercc1*$^{-/\Delta}$ and WT mice, and old (30 months) WT mice to determine whether any of the aging-associated miRNAs we identified in this study were similarly dysregulated in the kidney tissue. Of the 8 downregulated miRNAs in *Ercc1*$^{-/\Delta}$ and WT old mouse liver compared to WT young mouse liver (Figure 9), three miRNAs (miR-449a, miR-455*, miR-128) were also downregulated in the kidneys of progeroid mice compared to WT young mice (Figure 10). Interestingly, these three miRNAs were also downregulated in the kidneys of old WT mice compared to the young WT mice (Figure 9), further strengthening the conclusion that these miRNAs may be aging-associated.

Figure 10: QRT-PCR quantification of miRNA identified as down-regulated in the kidney of old WT and progeroid *Ercc1*$^{-/\Delta}$ mice compared to adult WT kidney.

QRT-PCR analysis was performed on kidneys of WT young (20 weeks), *Ercc1*$^{-/\Delta}$ (20 weeks), and WT old mice (30 months). **(A)** MiR-449a. **(B)** MiR-455*. **(C)** MiR-128. All three miRNAs identified in the microarray were significantly downregulated in kidney tissue of *Ercc1*$^{-/\Delta}$ progeroid mice and old mice compared to WT young mice. No RT, no reverse transcriptase added. Three mouse kidneys are in each condition. The mean of three experimental replicates for each sample is graphed as relative to WT young samples, which were normalized to a value of -1. The standard deviation is plotted as error bars. *P*-values were calculated using one-way ANOVA with Dunnett's post hoc test, with WT young as the control sample: *** ($p < .001$) and # ($p < .0001$).

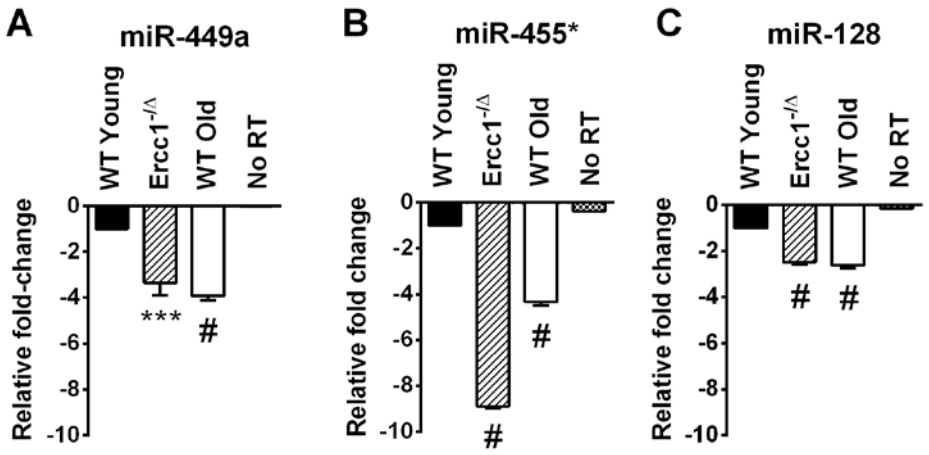

2.4 DISCUSSION

This study is the first characterization of miRNA profiles in the mouse model of the XFE Progeroid Syndrome, enabling identification of miRNAs that are dysregulated as a consequence of cellular senescence and aging driven by endogenous DNA damage. We also compared the expression of differentially expressed miRNAs in liver and kidney tissues of *Ercc1*$^{-/\Delta}$ and WT old mice to those of young WT controls and found similarities between the progeroid and old mice. *Ercc1*$^{-/\Delta}$ mice have been established as a useful model for studying diseases of aging such as peripheral neuropathy, osteoporosis, intervertebral disk degeneration, and sarcopenia [122, 123, 230]. These previous studies showed that the rapid aging of *Ercc1*$^{-/\Delta}$ mice is very similar to that of normally aged mice. The mice used in this study are genetically identical with the exception of the *Ercc1* mutation and are all in an f1 background (50:50 mix of C57Bl/6 and FVB).

Here we show that several downregulated miRNAs in the ERCC1-deficient mouse model of progeria are also downregulated during normal murine aging. Both the liver and kidney of progeroid ERCC1-deficient mice and old WT mice show aging-related functional and degenerative changes as well as profound cellular senescence [124, 231]. Eight miRNAs (miR-449a, miR-455*, miR-128, miR-497, miR-543, miR-450b-3p, miR-872 and miR-10b) are significantly downregulated in the livers of progeroid *Ercc1*$^{-/\Delta}$ and naturally aged mice compared to young adult mice (Figure 9). Three of these miRNAs (miR-128, miR-449a and miR-455*) were also downregulated in the kidneys of progeroid and WT old mouse compared to the young

WT mouse kidneys (Figure 10). These data strongly support the conclusion that these miRNAs are dysregulated due to accelerated and natural aging. The combination of in vitro and in vivo data strongly point to the conclusion that these miRNAs play a role in driving cellular senescence and aging, or are powerful biomarkers of these physiological changes.

Previously confirmed gene targets of the miRNAs identified in this study that are linked to cellular senescence and aging (miR-449a, miR-455*, miR-128, miR-497, miR-543, miR-450b-3p, miR-872 and miR-10b) are listed in Table 8. Several of the 43 gene targets such as Sirt1, Bcl2, Sod1, and Myc are involved in cell cycle control and cellular stress responses. Genes associated with cellular senescence as well as p53 downstream targets (Ccnd1, Cdk6) are also target genes. This list of potential miRNA targets is consistent with a possible role of these miRNAs in cellular senescence and aging.

Table 8: Experimentally validated target genes for miRNAs identified in this study.

3'-UTR homology between human and mouse gene orthologs was determined using Targetscan 6.2 [232].

miRNA	Target gene(s)	References
miR-10b	Bcl2l11, Hoxd10, Tfap2c	[233]
miR-128	Abcc5, Bax, Bmi1, E2F3a, E2f5, Hoxa10, Ntrk3, Reln, Ret, Rps6kb1	[234-238]
miR-449a	Bcl2, Ccnd1, Ccne2, Cdc25a, Cdk6, Dll1, E2f2, E2f3, E2f5, Gmnn, Hdac1, Hnf4a, Lef1, Met, Myc, Mycn, Notch1, Sirt1	[239]
miR-450b-3p	No confirmed mRNA targets	
miR-455*	No confirmed mRNA targets	
miR-497	Bcl2, Bcl2l2, Ccnd1, Ccnd2, Igf1r, Map2k1, Raf1	[240-242]
miR-543	Twist1	[243]
miR-872	Sod1	[244]

Three miRNAs (miR-128, miR-449a and miR-455*) are downregulated in late passage MEFs as well as liver and kidney tissues of both progeroid *Ercc1*$^{-/\Delta}$ and WT old mice. MiR-128 is known to promote cell survival [245]. MiR-449a targets critical cell cycle regulatory proteins

such as Cyclin D1 [246, 247]. Interestingly, it was shown that high Cyclin D1 expression is observed in senescent cells exhibiting a “pseudo-DNA damage response” and that Cyclin D1 is overexpressed in fibroblasts undergoing replicative senescence [248, 249]. These observations are in line with our results that miR-449a is downregulated in senescent cells. The transcription factor, Hnf4a, is a target of miR-449a in liver cells [250]. Hnf4a is essential to liver development and maintenance, and when suppressed, it can cause epigenetic changes that lead to increased incidence of hepatocellular cancer [251]. Reduced expression of miR-449 in aging liver would increase Hnf4a expression, possibly preventing hepatocyte transformation.

MiR-10b, which we detected as significantly downregulated in senescent MEFs and aged liver, is upregulated in breast cancer and gliomas and its expression closely correlates with tumor cell metastatic potential [233]. It is possible that dysregulation of one or more of the above miRNAs may result in reduced cell growth and increased cellular senescence through their regulation of target genes. Less is known about the cellular targets and function of miR-450b-3p, miR-455*, miR-543 and miR-872 (all downregulated in our studies).

Since the majority of differentially expressed miRNA identified in this study were downregulated in senescence and aging, we examined Dicer expression and found it to be downregulated in senescent MEFs (Figure 7A). Dicer protein and mRNA transcript were significantly downregulated in normally aged mice white adipose tissues and elderly human preadipocytes [252]. A recent study examining early passage versus senescent human umbilical vein endothelial cells demonstrated that senescent cells had about 2-fold downregulation in Dicer expression, further implicating a role for Dicer downregulation in senescence and aging [164].

The *Zmpste24*$^{-/-}$ mouse model of Hutchinson-Gilford progeria demonstrates miR-29b is upregulated in liver and muscle of both progeroid and normally aged mice [176]. MiR-29b is a

positive regulator of the p53-mediated DNA damage response. The paper by Ugalde et al. was the first to use a progeroid mouse models in identifying miRNAs that regulate DNA repair processes and senescence. Another study used the mouse and *Caenorhabditis elegans* models of the progeroid disease Werner Syndrome to identify miR-124 modulator of reactive oxygen species and ATP production [177]. Our study further underscores the utility of rapid aging mouse models to study miRNA dysregulation in aging and cellular senescence. We have used a progeroid model of endogenous DNA damage accumulation to identify miRNA dysregulation common to both the Ercc1-deficient mouse model of progeria and normal mouse aging in liver and kidney tissues.

In summary, we identified several miRNAs that are similarly dysregulated in senescent primary MEFs and senescent tissues of progeroid and naturally aged mice (miR-449a, miR-455*, miR-128, miR-497, miR-543, miR-450b-3p, miR-872 and miR-10b). We have shown that Dicer expression is downregulated in senescence induced by genotoxic stress, and that the miRNA downregulation that we observe in this study could be a consequence of global miRNA downregulation. These miRNA are promising as biomarkers of aging and factors that may be critical for preventing cell senescence and aging-related degenerative changes in response to genotoxic stress.

3.0 MICRORNA-128A MODULATES IL-6, A COMPONENT OF THE SENESCENCE-ASSOCIATED SECRETORY PHENOTYPE

3.1 INTRODUCTION

Frailty, a geriatric syndrome characterized by decreased physiologic reserve and resistance to stress, exhibits increased inflammatory markers, particularly pro-inflammatory cytokines such as interleukin-6 (IL-6) [253, 254]. Function of the immune system declines with increasing age and it has diminished capacity to fight infections, mount new immune responses, prevent the creation of auto-antibodies, and to perform immune surveillance for cancer cells [255-258]. Rat neutrophil functionality decreases with age and results in reduced ability to produce superoxide bursts, which is critical for intracellular killing of ingested microorganisms [259]. Dendritic cells (DCs) from healthy older adults demonstrate elevated basal levels of cytokine production compared to DCs from young adults [260]. Aged DCs also demonstrate reduced function of toll-like receptor (TLR) family proteins, and have diminished responses to immunization with the influenza vaccine [260]. Aged murine macrophages produce significantly less nitric oxide compared to young mouse macrophages [261]. Following thymic involution, older individuals experience decreased T cell production and significantly reduced T cell receptor diversity compared to healthy young controls [262]. With age, T cells progressively lose CD28, a critical co-stimulatory marker required for T cell activation [263]. Aged human B cells have reduced antibody diversity and demonstrate higher incidence of auto-antibody production [264]. Collectively, this age-associated dysregulation of both innate and adaptive immune processes is termed “immune senescence.” Immune senescence leaves elderly individuals exquisitely sensitive to infections, either via re-emergence of latent infections or infection with opportunistic pathogens.

The gradual development of age-related immune system imbalance can lead to chronic inflammation, or inflammaging,. Inflammatory mediators prevent infection in young organisms however, aging associated dysregulation of immune cells pre-disposes the older organism to diseases caused by chronic low-grade inflammation [265]. Inflammaging is a major contributor to the pathogenesis of Alzheimer's disease and cardiovascular disease, both of which have an increase in incidence with age [266, 267]. The expression of Interleukin-10 (IL-10), an anti-inflammatory cytokine, is reduced with age, further exacerbating the chronic low-grade inflammation of aging [268]. Several driving factors of inflammaging have been proposed, including age-associated increases in adipocytes, decreased sex steroid production and persistent herpes virus infections [269, 270]. Interestingly, IL-6 was not observed to be increased with aging in centenarians and in families with longevity [271, 272]. Approximately 20% of the participants in the Cardiovascular Healthy All Star Study, with median age of 86 years, demonstrated doubling of serum IL-6 over the study period and these participants had a higher risk of cognitive or physical impairment and mortality [273].

IL-6 demonstrates increased expression in older adults as well as in late-life diseases such as atherosclerosis and osteoporosis [274, 275]. IL-6 production is increased in B cells of patients with Multiple Sclerosis compared to healthy controls and depletion of IL-6 over-producing B cells leads to reduced disease severity in a mouse model of autoimmune encephalitis [276]. Many functions have been attributed to IL-6 depending on the cellular context and IL-6 is produced by many cell types, including adipocytes, monocytes, fibroblasts, hepatocytes and endothelial cells [277-281]. Approximately one-fourth of circulating IL-6 is produced by adipocytes, and increased circulating IL-6 can induce insulin resistance and stimulate hepatocytes to increase production of acute phase proteins such as C-reactive protein and

fibrinogen [277, 282-284]. IL-6 also acts as a growth factor for tumor cells, particularly renal cell carcinoma and multiple myeloma [285, 286]. Total cellular IL-6 in non-activated cells is usually in the range of pg/ml and in activated cells it increases approximately 1,000-fold to the ng/ml range [287].

In the context of cellular senescence, IL-6 functions as a key mediator of the senescence-associated secretory phenotype, acting in a paracrine manner on the microenvironment [288]. IL-6 expression increases in response to nuclear factor-kappa B (NF-κB) activation that occurs from activation of DNA repair pathways or oncogene-induced senescence [72, 289, 290]. NF-κB is a transcription factor that responds to a variety of environmental changes and was first characterized as an activator of inflammatory genes [291, 292]. In addition to its role in pro-inflammatory pathways, NF-κB is also involved in regulating embryonic development, apoptosis and proliferation [293-295]. In mammals, NF-κB consists of five different members that form homodimers or heterodimers: RelA/p65, RelB, c-Rel, p105/p50 and p100/p52 [296]. When inactive, NF-κB is bound to cytosolic inhibitory (IκB) proteins. Following activation, IκB proteins are phosphorylated by IκB-specific kinases (IKKα and IKKβ) and degraded in the proteasome, resulting in NF-κB translocation to the nucleus [297-299]. Once in the nucleus, NF-κB binds to specific DNA sequences in the promoter regions of pro-inflammatory genes such as IL-6, C-reactive protein and cyclo-oxygenase-2 [300-302]. Activation of NF-κB can be induced by upstream pro-inflammatory signals, such as bacterial lipopolysaccharide, IL-1, tumor necrosis factor alpha (TNF-α), or genotoxic stress [303-306].

NF-κB is a transcription factor that contributes to many of the changes observed in inflammaging. Young keratinocytes undergo premature senescence when NF-κB is overexpressed [307]. This NF-κB induced premature senescence was found to be mediated by

manganese superoxide dismutase, which led to increased cellular H_2O_2 and reactive oxygen species generation [307]. Tissue atrophy, which increases in aging organisms, is mediated by increased NF-kB signaling [308, 309].

NF-kB is also upregulated in response to DNA damage signaling, via ATM phosphorylation of NEMO, a regulator of IKK [310-312]. Other genotoxic stresses, such as oxidative stress and ultraviolet light damage can activate NF-kB signaling [313, 314]. Furthermore, NF-kB signaling mediates the effects of the senescence-associated secretory phenotype [315]. Increased nuclear localization of the p52 and p65 proteins was observed in aged rat livers, with changes in inhibitory IkB complexes or IKK activation, further implying that there is an age-associated increase in NF-kB gene targets [316]. A meta-analysis of several studies examining gene expression changes in aging mice, rats and humans showed that inflammation and immune response genes were highly overexpressed [317]. Genes associated with longevity, such as Sirtuin 1 (SIRT1), Sirtuin 6 (SIRT6) and the Foxo3a transcription factor, are able to suppress overactive NF-kB signaling [318-320]. Collectively, these data suggest that NF-kB signaling and its pro-inflammatory downstream targets are overexpressed in aging tissues.

A recent paper examined NF-κB signaling in wild type old mice (2 years old), *Ercc1*$^{-/\Delta}$ mice (3 months old) and *Ercc1*$^{-/-}$ mice (21 days old) and found that in kidney, muscle, pancreas, and liver tissue, there was a significant upregulation of NF-κB [78]. When NF-κB signaling was reduced, either by use of pharmacologic inhibitors or by genetically depleting p65, there was delayed onset of aging-associated symptoms, namely sarcopenia, kyphosis, urinary incontinence, osteoporosis and ocular impairment [78]. Histologically, there was a reduction of liver steatosis, glomerulosclerosis and renal protein cast formation as well as a reduction of the

neurodegeneration marker glial fibrillary acidic protein, all of which are typically increased in aging tissues [78, 321-323]. Furthermore, the cytokine IL-6 was shown to be significantly upregulated at the mRNA level in bone marrow stromal cells from *Ercc1*$^{-/\Delta}$ mice compared to BMSC derived from WT old mice [324]. Also, IL-6 is elevated in serum of *Ercc1*$^{-/\Delta}$ mice compared to age-matched WT animals [324]. This observed serum IL-6 upregulation is abrogated in *Ercc1*$^{-/\Delta}$ mice with deficient NF-κB signaling, either via pharmacological inhibition or genetic mutation (p65 deficiency) [324].

Non-coding RNAs, particularly miR-146a/b, have been identified as post-transcriptional regulators of inflammatory pathways dysregulated in aging and senescence. MiR-146a/b is upregulated by NF-kB signaling and targets TNF receptor-associated factor 6 (TRAF6) and interleukin-1 receptor-associated kinase 1 (IRAK1), both of which are involved in upregulation of NF-kB [159]. MiR-146a/b is therefore involved in a NF-kB negative feedback loop, allowing for fine-tuned modulation of NF-kB activation. Having previously identified senescence-associated microRNAs in the XFE Progeroid Syndrome and the *Ercc1*-deficient mouse modeling this disease, we hypothesize that these downregulated miRNAs (miR-128a, miR-449, miR-455*) may target downstream components of the NF-kB signaling pathway, particularly those involved in the SASP response, all of which are upregulated in senescence. Our results show that miR-128 expression is inversely correlated with IL-6 mRNA expression in livers and kidneys of Ercc1 progeroid syndrome mice and WT old mice and that modulating expression of miR-128 in fibroblasts leads to changes in expression of IL-6 mRNA and miR-146a, two major components of the SASP.

3.2 MATERIALS AND METHODS

3.2.1 Cell Culture and Transfections

Wild-type (WT) isogenic mouse embryonic fibroblasts (MEFs) derived from 13.5-day embryos with a 50:50 C57Bl/6:FVB/n background were used for transfections. Cells were grown in 50:50 F-10 media (Gibco, Grand Island, NY, USA) and Dulbecco's modified Eagle's medium (DMEM) (Lonza, Walkersville, MD, USA) and supplemented with 10% fetal bovine serum, 1% penicillin/streptomycin and 2% Non-essential amino acids, at 37 °C in the presence of 20% O_2 and 5% CO_2. NIH3T3 murine fibroblasts were grown in DMEM supplemented with 10% calf serum, 1% penicillin/streptomycin and 2% L-glutamine, and were grown at 37 °C in the presence of 20% O2 and 5% CO_2.

For transfections, 4 x 10^4 WT MEFs or 2 x 10^4 NIH3T3 cells were seeded in 6-well plates 24 hours prior to transfection in antibiotic-free media. The next day, cells were transfected with 50 nM pre-miR-128 or 50 nM anti-miR-128 (Applied Biosystems, Foster City, CA, USA). Transfections were performed using RNAiMAX (Invitrogen, Carlsbad, CA, USA) and Opti-MEM (Gibco). A FAM-labeled negative control pre-miR (Applied Biosystems) was used as a negative control to measure transfection efficiency. Cells were harvested 72 hours following transfection.

3.2.2 RNA Isolation

RNA was extracted using the Ultraspec RNA Isolation System (Biotecx, Houston, TX, USA), following manufacturer's instructions. Following isolation, RNA quantity was measured using a Nanodrop (Thermo Fisher Scientific Inc., Waltham, MA, USA).

3.2.3 MicroRNA Quantification by Quantitative Real Time RT-PCR

QRT-PCR analysis was performed on total RNA to confirm miRNA overexpression or knock-down using a two-step individual Mature Taqman® MicroRNA Assays kit (Applied Biosystems) and the Real-Time Thermocycler iQ5 (Bio-Rad, Hercules, CA, USA). All qRT-PCR assays were performed according to manufacturer's instructions and miRNA expression levels were normalized to snoRNA135. For all experiments, two independent cell lines were used and all assays were performed in triplicate. Relative expression was calculated using the $2^{-\Delta\Delta CT}$ method [220]. Welch's unpaired *t* test with 95% confidence intervals was performed for statistical analysis of all qRT-PCR experiments using Prism software (GraphPad Software, Inc., La Jolla, CA, USA).

Interleukin-6 (IL-6), p16 and Bax expression in primary MEFs, NIH3T3 cells, mouse livers and kidneys was quantified via qRT-PCR using the iScript One-Step RT-PCR Kit with SYBR Green (BioRad) in accordance with the manufacturer's instructions. Bax mRNA was amplified using the forward primer sequence 5'-GAGACACCTGAGCTGACCTT-3' and the reverse primer sequence 5'-CCATATTGCTGTCCAGTTCATC-3', amplifying a 103 bp region. The annealing temperature for Bax qRT-PCR was 60°C. IL-6 mRNA was amplified using the

forward primer sequence 5'-CCGGAGAGGAGACTTCACAG-3' and the reverse primer 5'-TCCACGATTTCCCAGAGAAC -3', amplifying a 102 bp region. The annealing temperature for the IL-6 qRT-PCR was 55°C. P16 mRNA was amplified using the forward primer sequence 5'-AACTCGAGGAGAGCCATCTG-3' and the reverse primer 5'-GGGGTACGACCGAAA GAGTT-3'. The annealing temperature for p16 qRT-PCR was 50°C. Bax, p16 and IL-6 mRNA levels were normalized to the glyceraldehyde-3-phosphate dehydrogenase (GAPDH) gene, using the forward primer 5'-AACTTTGGCATTGTGGAAGG-3' and the reverse primer 5'-GGA TGCAGGGATGATGTTCT-3', amplifying a 132-bp region. DNase I-treated total RNA (1 µg) was used for each reaction, and all the reactions were performed in triplicate. Relative IL-6 mRNA expression was calculated using $2^{-\Delta\Delta CT}$ values [220]. Welch's unpaired t test with 95% confidence intervals was performed for statistical analysis of all post-transfection qRT-PCR experiments. A one-way ANOVA with a Dunnett's multiple comparison test was performed on IL-6 and Bax qRT-PCRs of liver and kidney tissues. All statistical analyses were performed using Prism software (GraphPad Software, Inc., La Jolla, CA, USA).

3.3 RESULTS

3.3.1 Progeroid *Ercc1*$^{-/\Delta}$ and WT old mice tissues are associated with increased IL-6 mRNA expression

One microRNA has the potential to target many genes, which makes identifying gene targets for miRNAs challenging [134]. The many *in silico* miRNA target prediction programs rely on conservation of seed sequence binding sites in mRNA 3'-UTR as well as on thermodynamic principles. The context of the binding site, such as location within the 3'UTR and neighboring sequences, can also impart certain sites with more effective mRNA targeting [325, 326]. Focusing on the three miRNAs that were downregulated in both liver and kidney tissues of *Ercc1*$^{-/\Delta}$ progeroid and WT old mice relative to young mice, miR-128, miR-449 and miR-455*, we identified components of the senescence-associated secretory phenotype that contain potential binding sites for these three miRNAs in their 3'-UTRs (Table 9). We focused on IL-6, one of the key cytokines produced in the senescence-associated secretory phenotype (SASP). We found an increase in IL-6 mRNA in WT old mice livers (Figure 11A) and in *Ercc1*$^{-/\Delta}$ kidneys (Figure 11B) compared to WT young mouse tissues. Although both of these tissues have been shown to have increased cellular senescence markers by other groups, the differences observed in IL-6 mRNA expression of liver and kidney tissues may be due to different mechanisms of aging [124, 231]. Liver and kidney tissues of WT old mice and *Ercc1*$^{-/\Delta}$ mice demonstrate significant miR-128 downregulation via qRT-PCR analysis (Figures 9C and 10C). Using data

from the miRNA target database TargetScan, we found that the murine IL-6 3'-UTR contains one binding site for miR-128 (Figure 12), and was therefore considered a possible target of this miRNA for further study [232]. The human IL-6 3'-UTR does not contain a miR-128 binding site.

We first confirmed that the Bcl-2-associated X protein (Bax), a previously identified target of miR-128, is upregulated in livers (Figure 13A) and kidneys (Figure 13B) from *Ercc1*$^{-/\Delta}$ and WT old mice [235]. Previous studies overexpressing miR-128 in human embryonic kidney cells and lung-derived cells induces apoptosis, cell cycle changes and increased ROS production [235]. These studies demonstrated a reduction of Bax at both mRNA and protein levels [235]. Confirming Bax upregulation in liver and kidney tissues showed that downregulation of miR-128 in tissues has functional consequences *in vivo* by upregulating known miR-128 targets.

Table 9: Identification of miRNAs that target murine SASP components
Senescence-associated miRNAs identified in our study that target murine SASP components [232, 327]

SASP Factor	**3'UTR binding site**
IL-6	miR-128
KC/GROα/CXCL1	miR-128
Tnfrsf1b	miR-128, miR-449a
IL-1b	miR-128
MCP1/CCL2	miR-128
IGFBP-3	miR-449a
Eotaxin/CCL11	miR-128
VEGFa	miR-449a
VEGFb	miR-128
VEGFc	miR-128
CCL1	miR-449a
CCL27a	miR-128
IL-1a	miR-128

Figure 11: Ercc1-deficient mouse liver and kidney tissues demonstrate increased IL-6 mRNA expression

IL-6 qRT-PCR analysis was performed on tissues of WT young (20 weeks), *Ercc1*$^{-/\Delta}$ (20 weeks), and WT old mice (30 months). **(A)** Livers. **(B)** Kidneys. IL-6 was upregulated in *Ercc1*$^{-/\Delta}$ progeroid mice and WT old mice compared to WT young mice. No RT, no reverse transcriptase added. Three mouse livers were used in each experiment. The mean of three experimental replicates for each sample is graphed as relative to WT young samples, which were normalized to a value of 1. The standard deviation is plotted as error bars. *P*-values were calculated using one-way ANOVA with a post hoc Dunnett's multiple comparison test, with WT young as the control sample: * ($p < .05$) and ** ($p < .01$).

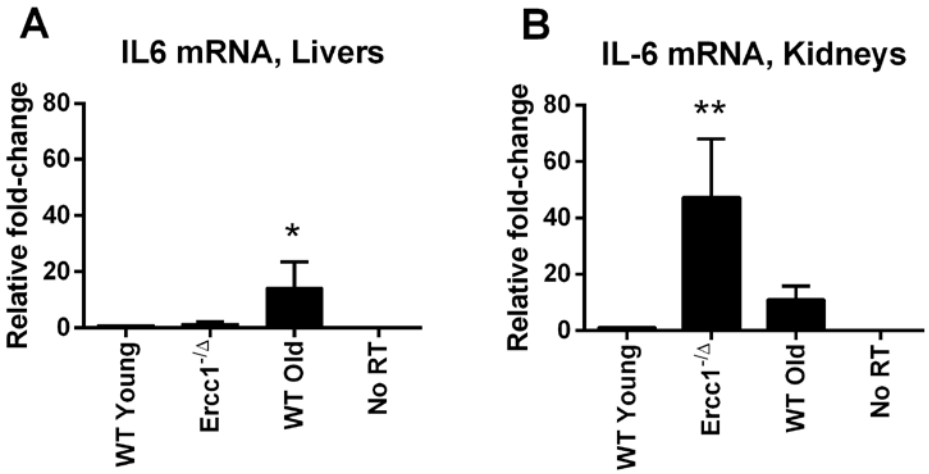

Figure 12: IL-6 3'UTR demonstrates one miR-128 binding site.

The miR-128 binding site contains perfect complementarity in the seed sequence (nucleotides 2 – 8, in red). Sequence obtained from TargetScan 6.2 [232].

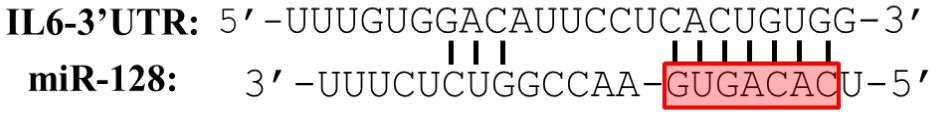

Figure 13: Bax, a confirmed target of miR-128, is upregulated in Ercc1-deficient mouse livers and kidneys.

Bax mRNA, a previously confirmed target of miR-128 [235], was upregulated in livers and kidneys from *Ercc1*$^{-/\Delta}$ progeroid and WT old mice compared to WT young mice. QRT-PCR analysis was performed on **(A)** livers and **(B)** kidneys of WT young (20 weeks), *Ercc1*$^{-/\Delta}$ (20 weeks), and WT old mice (30 months). No RT, no reverse transcriptase added. Three mouse livers and kidneys were used in each experiment. The mean of three experimental replicates for each sample is graphed as relative to WT young samples, which were normalized to a value of 1. The standard deviation is plotted as error bars. *P*-values were calculated using one-way ANOVA with a post hoc Dunnett's multiple comparison test, with WT young as the control sample: * ($p < .05$).

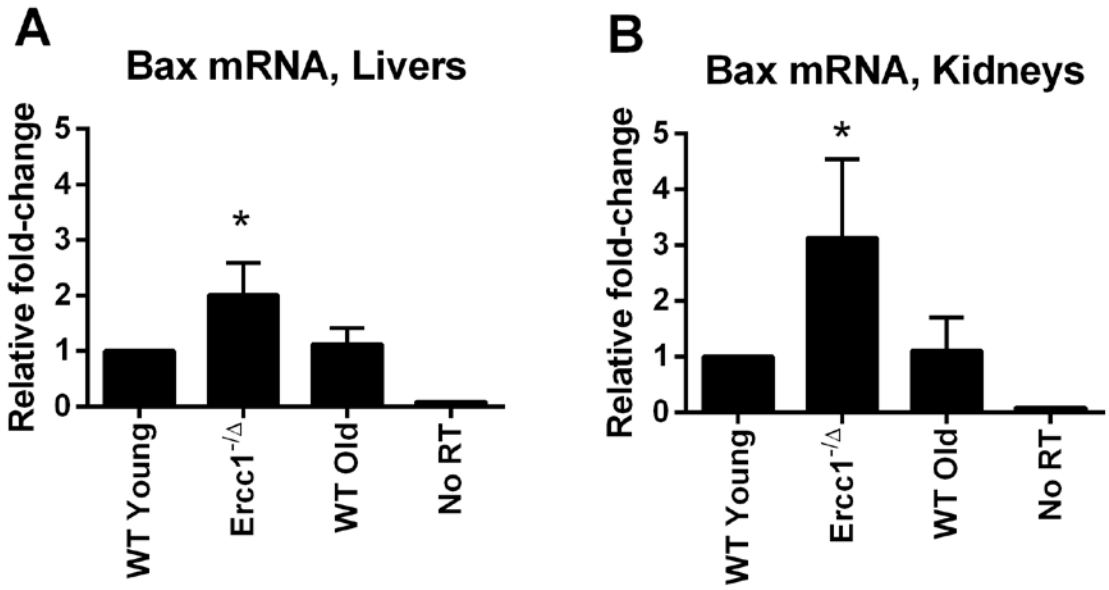

3.3.2 MiR-128 knock-down in NIH3T3 cells results in increased IL-6 mRNA

We next performed functional studies with miRNA inhibitors (anti-miRs) for miR-128 in NIH3T3 fibroblasts. NIH3T3 mouse embryonic fibroblast cell lines were used because knock-down of miR-128 in WT MEFs proved difficult to quantify via qRT-PCR analysis (data not shown). Transfecting NIH3T3 fibroblasts with 50 nM of non-targeting Cy3 anti-miR and subsequently performing flow cytometry showed that the transfection efficiency was approximately 90% (data not shown). Next, we transfected NIH3T3 cells with 50 nM of either non-targeting FAM labeled anti-miR or 50 nM of anti-miR-128. Seventy-two hours post-transfection, RNA was isolated and miR-128 knock-down was quantified via qRT-PCR. MiR-128 expression was reduced by approximately 80% (Figure 14A). In the cells with miR-128 knock-down, IL-6 mRNA was significantly upregulated by over 30% (Figure 14B).

Figure 14: MiR-128 is significantly knocked-down in NIH3T3 fibroblasts and results in upregulation of IL-6 mRNA.

(A) MiR-128 was confirmed to be significantly knocked-down by transfecting 50 nM anti-miR-128 into NIH3T3 fibroblasts for 72 hours. **(B)** IL-6 mRNA expression was significantly upregulated in cells that had reduced miR-128 expression. No RT, no reverse transcriptase added. The mean of three experimental replicates for each sample is graphed as relative to FAM 50 nM transfection, which was normalized to a value of 1. The standard deviation is plotted as error bars. *P*-values were calculated comparing samples to FAM 50 nM using Welch's t-tests and are indicated by * ($p < .05$) and *** ($p < .001$).

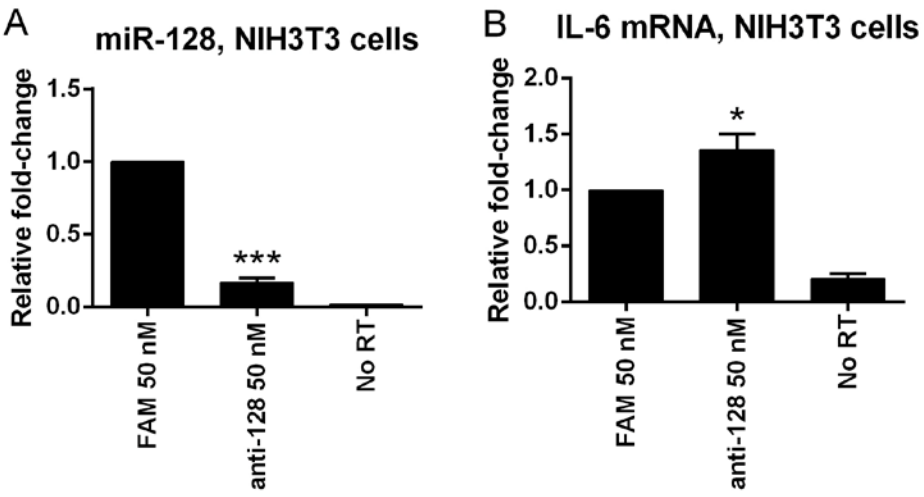

3.3.3 MiR-128 knock-down in NIH3T3 cells results in increased miR-146a and p16 mRNA expression

Due to the consistent upregulation of IL-6 following miR-128 knock-down, we next tested whether the levels of a miRNA component of SASP, miR-146a, are also increased. MiR-146a demonstrates robust expression in senescent fibroblast and endothelial cells, and its expression increases approximately 12 days following treatment with DNA damaging agents, oxidative stress or oncogene expression [75, 81]. Interestingly, increased secretion of SASP components is observed within 4 days following DNA damage, indicating that miR-146a upregulation requires a robust SASP response to be established first [71, 288].

MiR-146a expression was quantified via qRT-PCR 72 hours following miR-128 knock-down (Figure 15). MiR-146a was significantly upregulated in NIH3T3 cells with miR-128 knock-down, further indicating a connection between upregulation of SASP components, namely IL-6, and upregulation of miR-146a promoter expression. P16, a key component that is significantly upregulated in cellular senescence, was also upregulated after miR-128 knock-down, further suggesting that reduced levels of miR-128 may promote cellular senescence (Figure 16). Notably, in our studies, we did not see increased staining of senescence-associated beta-galactosidase within the 72 hour time frame that we examined (data not shown). However a limitation to our studies is that we did not examine cellular changes beyond 72 hours post-transfection.

Figure 15: MiR-128 knock-down in murine fibroblasts results in upregulation of miR-146a

QRT-PCR analysis of miR-146a was performed in NIH3T3 fibroblasts with transient miR-128 knock-down. No RT, no reverse transcriptase added. The mean of three experimental replicates for each sample is graphed as relative to FAM 50 nM transfection, which was normalized to a value of 1. The standard deviation is plotted as error bars. *P*-values were calculated comparing samples to FAM 50 nM transfection using Welch's t-tests and are indicated by * ($p < .05$).

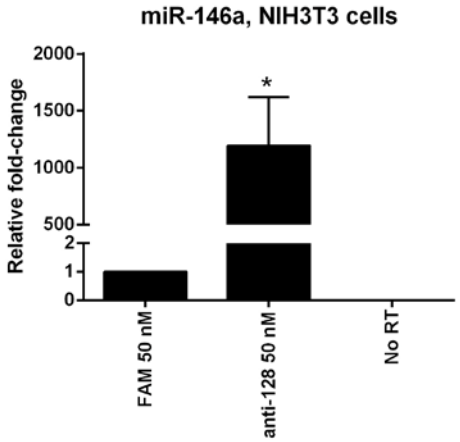

Figure 16: MiR-128 knock-down increases p16, a marker of cellular senescence.

QRT-PCR analysis of p16 was performed in NIH3T3 fibroblasts with transient miR-128 knock-down. No RT, no reverse transcriptase added. The mean of three experimental replicates for each sample is graphed as relative to FAM 50 nM transfection, which was normalized to a value of 1. The standard deviation is plotted as error bars.

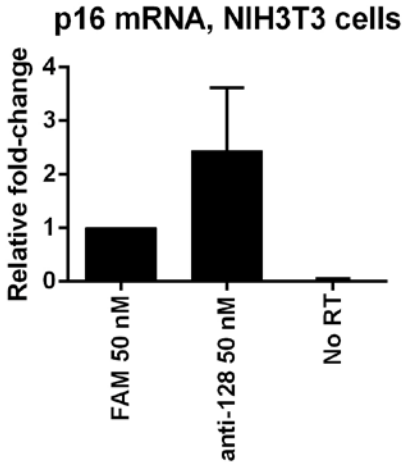

3.3.4 MiR-128 over-expression in WT MEFs results in reduced IL-6 and miR-146a expression

We next over-expressed miR-128 in WT MEFs (Passage 7) that were grown in 20% O_2, to examine whether changes in IL-6 mRNA expression were directly mediated by miR-128. Seventy-two hours post-transfection with miR-128 precursor (pre-miR-128), we harvested MEFs and isolated RNA. MiR-128 was confirmed to be significantly overexpressed via qRT-PCR (Figure 17A) and IL-6 mRNA was found to be downregulated (Figure 17B). Interestingly, miR-146a levels were also significantly downregulated upon miR-128 over-expression as demonstrated by qRT-PCR (Figure 17C).

Figure 17: MiR-128 over-expression in WT MEFs reduces expression of IL-6 mRNA and miR-146a.

QRT-PCR analysis of miR-128, IL-6 and miR-146a was performed in WT P7 MEFs with transient miR-128 over-expression. No RT, no reverse transcriptase added. The mean of three experimental replicates for each sample is graphed as relative to WT young samples, which were normalized to a value of 1. The standard deviation is plotted as error bars. *P*-values were calculated comparing samples to FAM 50 nM using Welch's t-tests and are indicated by * ($p < .05$) and # ($p < .0001$).

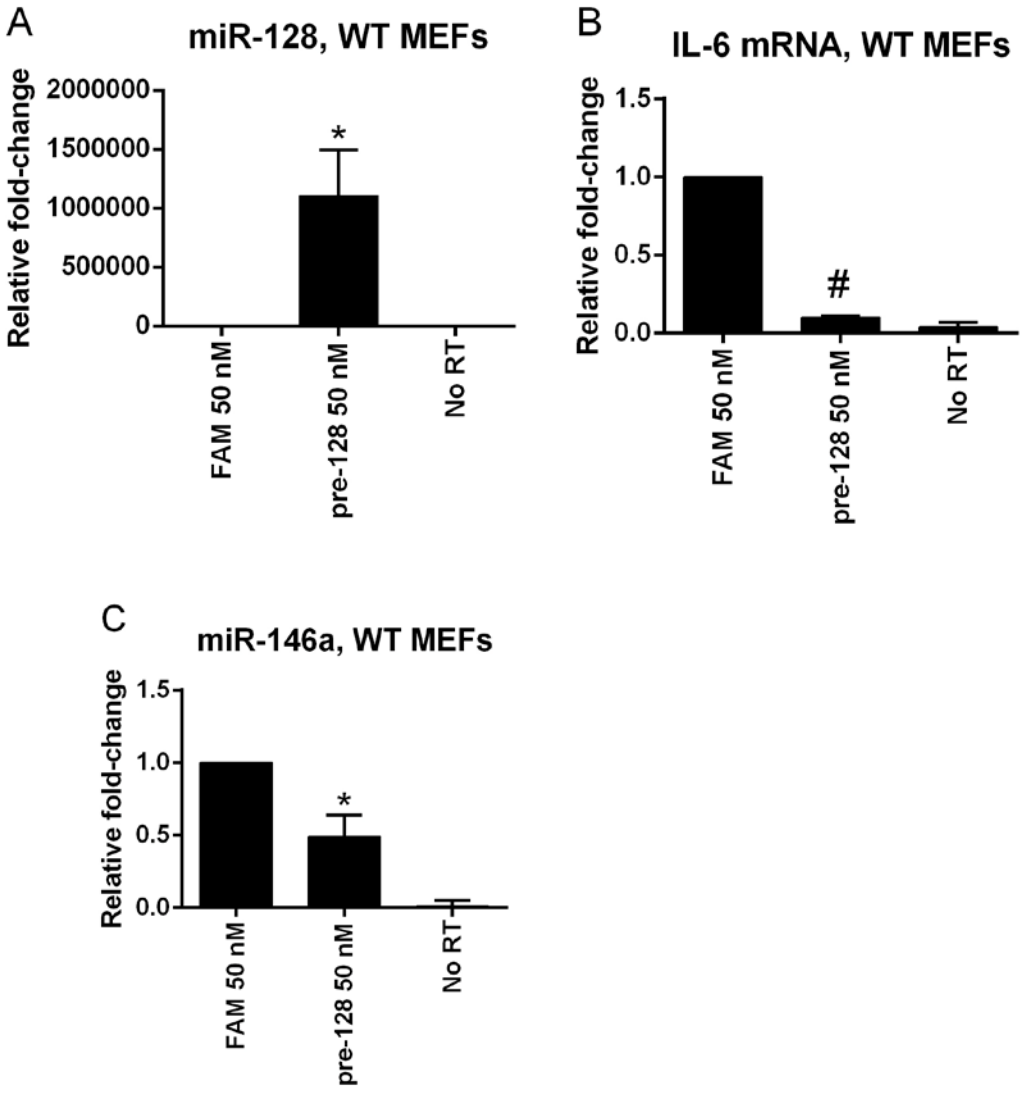

3.4 DISCUSSION

We have shown that miR-128 is a senescence-associated microRNA that has the capacity to modulate several SASP components: IL-6 and miR-146a as well as the senescence-associated marker p16. The regulation that miR-128 may have IL-6 has not yet been confirmed to be directly through interactions with the IL-6 3'-UTR, but this can be shown with luciferase-based assays to see if there is direct binding of miR-128 to the IL-6 3'-UTR. Interestingly, liver tissues of wild type young, wild type old and progeroid *Ercc1*$^{-/\Delta}$ mice demonstrated that IL-6 mRNA expression was highest in WT old mice (Figure 11A), while IL-6 mRNA expression was highest in kidneys from *Ercc1*$^{-/\Delta}$ mice (Figure 11B). This result is likely due to inherent differences in the biology of aging for liver and kidney tissues. A recent paper analyzed accumulation of a particular type of DNA damage, 8,5'-cyclopurine-2'-deoxynucleosides (cPu) in liver and kidney of *Ercc1*-deficient mice and compared them to age-matched WT mice tissues [218]. The authors showed that there is an overall two-fold higher amount of cPu lesions in liver tissues compared to kidney tissues of *Ercc1*$^{-/\Delta}$ mice [218]. Furthermore, the authors also showed that while *Ercc1*$^{-/\Delta}$ mouse livers developed significantly more cPu lesions compared to WT aged mice livers, *Ercc1*$^{-/\Delta}$ mouse kidneys develop approximately the same amount of cPu lesions as WT aged mouse kidneys [218]. This biological difference in DNA damage burden in liver and kidney tissues could also result in differences in IL-6/STAT3 pathway activation, leading to differences in IL-6 transcription[328].

MiR-128 is a conserved microRNA among mammals and is encoded by two genes, miR-128-1 and miR-128-2. The murine miR-128-1 transcript is encoded in an exon in the R3H domain containing 1 (R3hdm1) gene on chromosome 1and the miR-128-2 transcript is encoded in an exon in the gene cyclic AMP-regulated phosphoprotein, 21 (Arpp21) on chromosome 9 [329]. Both of these precursor transcripts are processed into the same mature miRNA, miR-128 [329]. Like many microRNAs, miR-128 appears to have different functions depending on the cell type. MiR-128 expression is upregulated in endometrial cancers, but was shown to be downregulated in glioblastomas [330, 331]. A recent study identified two components of the Polycomb Repressor Complex (PRC) in glioma stem cells, B lymphoma Mo-MLV insertion region 1 (BMI1) and suppressor of zeste 12 (SUZ12), as targets of miR-128. PRC components are commonly upregulated in glioblastoma multiforme, and concomitant miR-128 suppression is also observed [332]. The diversity of function of miR-128 is further suggested by a recent finding that miR-128 is one of the most commonly identified miRNAs derived from exosomes from human plasma [333]. Uptake of these miRNA-containing exosomes by diverse target tissues can expose cell populations with varying transcriptomes to the effects of miR-128 targeting, resulting in different functional outcomes.

Argonaute 2 immunoprecipitation studies in hepatic stellate cells demonstrated a high degree of interaction between miR-128 and chemokine and chemokine receptor mRNAs, indicating a role for miR-128 in regulating inflammatory responses [334]. Our work has demonstrated another link between miR-128 and inflammatory pathways. *Ercc1*$^{-/\Delta}$ progeroid and WT old mice livers and kidneys, which demonstrate reduced miR-128 expression, have increased expression of Bax (Figure 13), a confirmed miR-128 target, and IL-6 (Figure 11), another predicted miR-128 target.

MiR-128 knock-down in NIH-3T3 fibroblasts resulted in increased IL-6 expression (Figure 14B) as well as increases in a marker of cellular senescence, p16 (Figure 16). Also, a miRNA involved in regulating the senescence-associated secretory phenotype (SASP), miR-146a, was upregulated in cells with significant miR-128 knock-down (Figure 15). Over-expression studies were performed in WT P7 MEFs, due to technical difficulties in quantifying miR-128 knock-down in these primary cells (data not shown). Robust over-expression of miR-128 (Figure 17A) resulted in significant IL-6 knock-down (Figure 17B) and concomitant miR-146a knock-down (Figure 17C).

The data presented in this study suggests that miR-128 targets IL-6 *in vivo* in mouse liver and kidney tissues and in mouse fibroblast cell lines. Interestingly, the human IL-6 3'-UTR does not contain a canonical binding site for miR-128, however, it is possible that a different human microRNA could serve a similar function to that of miR-128 in regulating the expression of IL-6, a critical cytokine mediator of senescence-associated inflammatory responses. Future studies could also examine whether miR-128 targets IL-6 mRNA via non-canonical miRNA targeting mechanisms, such as targeting the coding region or 5'UTR of a target mRNA transcript [335, 336]. This data could lead to a better understanding of the complex manner in which the SASP is regulated, further elucidating the role of inflammation in cellular senescence. MiR-128 knock-down in senescent or aged tissues could be a regulatory mechanism influencing the establishment of SASP and exerting its effects on the cellular microenvironment.

4.0 SUMMARY, CONCLUSION AND FUTURE DIRECTIONS

4.1 GENERAL SUMMARY AND CONCLUSIONS

MicroRNAs dysregulation has been observed in aging and in regulating key pathways that are involved in senescence [157, 188, 337, 338]. While many recent papers have examined miRNA dysregulation in naturally aged humans and mice, there is utility in studying progeroid, or rapid aging, models to identify miRNA dysregulation that occurs in common with progeroid and normal aging. Previous studies have examined the Hutchinson-Guilford Progeroid Syndrome (HGPS) and Werner Syndrome, to identify aging-associated pathways that are regulated by miRNAs [176, 177]. The XFE Progeroid Syndrome and *Ercc1*-deficient mouse models are also useful tools to study the effects of endogenous DNA damage on aging and cellular senescence [122, 123, 213, 214].

Our studies are the first to characterize miRNA expression in the *Ercc1*-deficient mouse model of progeria. We have identified miRNAs dysregulated in $Ercc1^{-/-}$ MEFs at early and late passage and compared them to WT MEFs at early and late passage in varying oxidative stress growth conditions. This study shows that there is indeed a dysregulation of miRNAs in WT MEFs and $Ercc1^{-/-}$ MEFs, and that some of these dysregulated miRNAs are similarly dysregulated in conditions of increased endogenous DNA damage as well as in cases of increased oxidative stress. A significant subset of miRNAs identified from our MEF microarray were similarly downregulated in livers and kidneys of WT old mice as well as progeroid $Ercc1^{-/\Delta}$ mice compared to WT young counterparts (Figure 8, Figure 9). This similar dysregulation is especially interesting because many miRNAs are known to have different expression patterns in different tissues, so these similarities strongly suggest that there is a common upstream

mechanism in fibroblasts, liver and kidney tissues that is responsible for downregulation of these particular miRNAs.

We have also shown in these studies a possible function for one of the downregulated miRNAs: miR-128. This miRNA has been previously implicated in regulating inflammatory processes, and we have found a role for this miRNA in targeting the pro-inflammatory IL-6 [334]. MiR-128 and IL-6 expression were inversely correlated in our studies, and we believe that this effect is mediated by miR-128 directly binding to a target site in the 3'-UTR of the IL-6 mRNA. MiR-128 knock-down and overexpression also modulates the expression of two senescence-associated markers, p16 and miR-146a.

4.2 FUTURE DIRECTIONS

The data presented in this study is a promising first step in identifying miRNAs that are dysregulated in aging and in further charactering the role(s) they may play in modulating known aging and senescence pathways. The current study focused primarily on the role of miR-128, however, future studies can look at the two other miRNAs that were commonly downregulated in senescent fibroblasts, aged livers and kidneys, miR-449 and miR-455*.

Additional studies are necessary to further confirm the role of miR-128 in targeting the IL-6 3'UTR, namely studies with the IL-6 3'-UTR cloned into a luciferase plasmid, to test whether transient over-expression of miR-128 results in a reduction of luciferase expression. Another luciferase reporter study that should also be done is to mutate the mRNA:miRNA binding site in the 3'-UTR which should abolish the effect of miR-128 on luciferase expression. These studies are expected to show that miR-128 indeed targets IL-6 and this binding is dependent on the seed sequence binding site in the IL-6 3'-UTR. Also, a western blot of IL-6 in fibroblasts with increased or reduced expression of miR-128 will further support that miR-128 targets IL-6.

In addition to identifying IL-6 as a novel target of miR-128, other SASP components have miR-128 binding sites in their 3'-UTR regions (Table 9). As of now, none of the genes listed in this table have been validated as miR-128 targets; however, future studies examining whether miR-128 directly modulates expression of these mRNAs would further substantiate the findings that miR-128 appears to be a modulator of many key inflammatory processes, which a

recent paper suggested was a possibility with Argonaute-2 precipitation studies using miR-128 [334]. Identification of other SASP components being targeted by miR-128 would give new evidence for miR-128 as a modulator of SASP expression in senescence. Subsequent studies can examine whether this down-regulation of miR-128 and upregulation of IL-6 is seen in other modes of inducing senescence, such as oncogene-induced senescence, replicative senescence and stress-induced senescence (treatment with hydrogen peroxide or generalized epigenetic modifiers such as HDAC inhibitor compounds).

Additionally, we would like to perform further functional studies using over-expression and knock-down of miR-128 in fibroblast cell lines and liver-derived primary cells to see whether miR-128 regulates apoptosis, cell cycling or cell proliferation, to determine whether miR-128 is a driver of senescence or is merely downregulated as a result of senescence. Also, while we have shown that miR-128 modulates the expression of two senescence markers, p16 and miR-146a, there is no gold standard marker of senescence, and other studies will need to be done to concretely show that miR-128 knock-down is able to increase cellular senescence. Some of these experiments would include, senescence-associated beta-galactosidase staining, lipofuscin staining, proliferation assays, BrdU proliferation studies to show reduced cell cycling, and apoptosis assays to confirm that any changes observed in miR-128 knock-down cells is not due to increased apoptosis.

To further characterize the regulation of miR-128 in aging and senescence, future studies can also examine the miR-128 promoter region to look for binding sites of known transcription factors that are regulated in aging, such as NF-kB [339]. Also, studies can examine the methylation and chromatin state of the miR-128 promoters, since recent studies have shown that there are significant global changes in the methylome with aging [340]. Treatment with the drug

inhibitors of DNA methylation and inhibitors of histone acetyltransferases and methyltransferases should provide insight into the mechanisms by which miR-128 may be epigenetically modified in aging and senescence [341].

APPENDIX A

MICRORNAS LISTED IN AGILENT MOUSE MICROARRAY

A.1 MICRORNAS LISTED IN MOUSE MICROARRAY

mcmv-miR-m01-1	mghv-miR-M1-6	mmu-miR-1186	mmu-miR-133a
mcmv-miR-m01-2	mghv-miR-M1-7-3p	mmu-miR-1187	mmu-miR-133a*
mcmv-miR-m01-2*	mghv-miR-M1-7-5p	mmu-miR-1188	mmu-miR-133b
mcmv-miR-m01-3	mghv-miR-M1-8	mmu-miR-1190	mmu-miR-134
mcmv-miR-m01-3*	mghv-miR-M1-9	mmu-miR-1191	mmu-miR-135a
mcmv-miR-m01-4	mmu-let-7a	mmu-miR-1192	mmu-miR-135a*
mcmv-miR-m01-4*	mmu-let-7a*	mmu-miR-1193	mmu-miR-135b
mcmv-miR-m107-1-3p	mmu-let-7b	mmu-miR-1194	mmu-miR-136
mcmv-miR-m107-1-5p	mmu-let-7b*	mmu-miR-1195	mmu-miR-136*
mcmv-miR-m108-1	mmu-let-7c	mmu-miR-1196	mmu-miR-137
mcmv-miR-m108-1*	mmu-let-7c-1*	mmu-miR-1197	mmu-miR-138
mcmv-miR-m108-2-3p	mmu-let-7d	mmu-miR-1198	mmu-miR-138*
mcmv-miR-m108-2-5p.1	mmu-let-7d*	mmu-miR-1199	mmu-miR-138*
mcmv-miR-m108-2-5p.2	mmu-let-7e	mmu-miR-122	mmu-miR-139-3p
mcmv-miR-m21-1	mmu-let-7f	mmu-miR-1224	mmu-miR-139-5p
mcmv-miR-m22-1	mmu-let-7f*	mmu-miR-124	mmu-miR-140
mcmv-miR-M23-1-3p	mmu-let-7g	mmu-miR-124*	mmu-miR-140*
mcmv-miR-M23-1-5p	mmu-let-7g*	mmu-miR-125a-3p	mmu-miR-141
mcmv-miR-M23-2	mmu-let-7i	mmu-miR-125a-5p	mmu-miR-141*
mcmv-miR-M23-2*	mmu-let-7i*	mmu-miR-125b*	mmu-miR-142-3p
mcmv-miR-M44-1	mmu-miR-1	mmu-miR-125b-3p	mmu-miR-142-5p
mcmv-miR-M55-1	mmu-miR-100	mmu-miR-125b-5p	mmu-miR-143
mcmv-miR-m59-1	mmu-miR-101a	mmu-miR-126-3p	mmu-miR-144
mcmv-miR-m59-2	mmu-miR-101a*	mmu-miR-126-5p	mmu-miR-145
mcmv-miR-M87-1	mmu-miR-101b	mmu-miR-127	mmu-miR-145*
mcmv-miR-m88-1	mmu-miR-103	mmu-miR-127*	mmu-miR-146a
mcmv-miR-m88-1*	mmu-miR-105	mmu-miR-128	mmu-miR-146b
mcmv-miR-M95-1-3p	mmu-miR-106b	mmu-miR-129-3p	mmu-miR-146b*
mcmv-miR-M95-1-5p	mmu-miR-106b*	mmu-miR-129-5p	mmu-miR-147
mghv-miR-M1-1	mmu-miR-107	mmu-miR-1-2-as	mmu-miR-148a
mghv-miR-M1-2	mmu-miR-10a	mmu-miR-130a	mmu-miR-148a*
mghv-miR-M1-3	mmu-miR-10a*	mmu-miR-130b	mmu-miR-148b
mghv-miR-M1-4	mmu-miR-10b	mmu-miR-130b*	mmu-miR-149
mghv-miR-M1-5	mmu-miR-10b*	mmu-miR-132	mmu-miR-150

mmu-miR-150*	mmu-miR-1894-3p	mmu-miR-199a-5p	mmu-miR-216a
mmu-miR-151-3p	mmu-miR-1894-5p	mmu-miR-199b*	mmu-miR-216b
mmu-miR-151-5p	mmu-miR-1895	mmu-miR-19a	mmu-miR-217
mmu-miR-152	mmu-miR-1896	mmu-miR-19a*	mmu-miR-218
mmu-miR-153	mmu-miR-1897-3p	mmu-miR-19b	mmu-miR-218-1*
mmu-miR-154	mmu-miR-1897-5p	mmu-miR-200a	mmu-miR-218-2*
mmu-miR-154*	mmu-miR-1898	mmu-miR-200a*	mmu-miR-219
mmu-miR-155	mmu-miR-1899	mmu-miR-200b	mmu-miR-22
mmu-miR-15a	mmu-miR-18a	mmu-miR-200b*	mmu-miR-22*
mmu-miR-15a*	mmu-miR-18a*	mmu-miR-200c	mmu-miR-220
mmu-miR-15b	mmu-miR-18b	mmu-miR-200c*	mmu-miR-221
mmu-miR-15b*	mmu-miR-190	mmu-miR-201	mmu-miR-222
mmu-miR-16	mmu-miR-1900	mmu-miR-202-3p	mmu-miR-223
mmu-miR-16*	mmu-miR-1901	mmu-miR-202-5p	mmu-miR-224
mmu-miR-17	mmu-miR-1902	mmu-miR-203	mmu-miR-23a
mmu-miR-17*	mmu-miR-1903	mmu-miR-203*	mmu-miR-23b
mmu-miR-181a	mmu-miR-1904	mmu-miR-204	mmu-miR-24
mmu-miR-181a-1*	mmu-miR-1905	mmu-miR-205	mmu-miR-24-1*
mmu-miR-181a-2*	mmu-miR-1906	mmu-miR-206	mmu-miR-24-2*
mmu-miR-181b	mmu-miR-1907	mmu-miR-207	mmu-miR-25
mmu-miR-181c	mmu-miR-190b	mmu-miR-208a	mmu-miR-26a
mmu-miR-181d	mmu-miR-191	mmu-miR-208b	mmu-miR-26b
mmu-miR-182	mmu-miR-191*	mmu-miR-20a	mmu-miR-26b*
mmu-miR-183	mmu-miR-192	mmu-miR-20a*	mmu-miR-27a
mmu-miR-183*	mmu-miR-193	mmu-miR-20b	mmu-miR-27a*
mmu-miR-184	mmu-miR-193*	mmu-miR-20b*	mmu-miR-27b
mmu-miR-185	mmu-miR-193b	mmu-miR-21	mmu-miR-27b*
mmu-miR-186	mmu-miR-194	mmu-miR-21*	mmu-miR-28
mmu-miR-186*	mmu-miR-195	mmu-miR-210	mmu-miR-28*
mmu-miR-187	mmu-miR-196a	mmu-miR-211	mmu-miR-290-3p
mmu-miR-188-3p	mmu-miR-196a*	mmu-miR-212	mmu-miR-290-5p
mmu-miR-188-5p	mmu-miR-196b	mmu-miR-214	mmu-miR-291a-3p
mmu-miR-1892	mmu-miR-197	mmu-miR-214*	mmu-miR-291a-5p
mmu-miR-1893	mmu-miR-199a-3p	mmu-miR-215	mmu-miR-291b-3p

mmu-miR-291b-5p	mmu-miR-30a	mmu-miR-337-3p	mmu-miR-375
mmu-miR-292-3p	mmu-miR-30a*	mmu-miR-337-5p	mmu-miR-376a
mmu-miR-292-5p	mmu-miR-30b	mmu-miR-338-3p	mmu-miR-376a*
mmu-miR-293	mmu-miR-30b*	mmu-miR-338-5p	mmu-miR-376b
mmu-miR-293*	mmu-miR-30c	mmu-miR-339-3p	mmu-miR-376b*
mmu-miR-294	mmu-miR-30c-1*	mmu-miR-339-5p	mmu-miR-376c
mmu-miR-294*	mmu-miR-30c-2*	mmu-miR-340-3p	mmu-miR-376c*
mmu-miR-295	mmu-miR-30d	mmu-miR-340-5p	mmu-miR-377
mmu-miR-295*	mmu-miR-30e	mmu-miR-341	mmu-miR-378
mmu-miR-296-3p	mmu-miR-30e*	mmu-miR-342-3p	mmu-miR-378*
mmu-miR-296-5p	mmu-miR-31	mmu-miR-342-5p	mmu-miR-379
mmu-miR-297a*	mmu-miR-31*	mmu-miR-343	mmu-miR-380-3p
mmu-miR-297b-5p	mmu-miR-32	mmu-miR-344	mmu-miR-380-5p
mmu-miR-297c	mmu-miR-320	mmu-miR-345-3p	mmu-miR-381
mmu-miR-298	mmu-miR-322	mmu-miR-345-5p	mmu-miR-382
mmu-miR-299	mmu-miR-322*	mmu-miR-346	mmu-miR-382*
mmu-miR-299*	mmu-miR-323-3p	mmu-miR-34a	mmu-miR-383
mmu-miR-29a	mmu-miR-323-5p	mmu-miR-34b-3p	mmu-miR-384-3p
mmu-miR-29a*	mmu-miR-324-3p	mmu-miR-34b-5p	mmu-miR-384-5p
mmu-miR-29b	mmu-miR-324-5p	mmu-miR-34c	mmu-miR-409-3p
mmu-miR-29b*	mmu-miR-325	mmu-miR-34c*	mmu-miR-409-5p
mmu-miR-29c	mmu-miR-325*	mmu-miR-350	mmu-miR-410
mmu-miR-29c*	mmu-miR-326	mmu-miR-351	mmu-miR-411
mmu-miR-300	mmu-miR-327	mmu-miR-361	mmu-miR-411*
mmu-miR-300*	mmu-miR-328	mmu-miR-362-3p	mmu-miR-412
mmu-miR-301a	mmu-miR-329	mmu-miR-362-5p	mmu-miR-421
mmu-miR-301b	mmu-miR-33	mmu-miR-363	mmu-miR-423-3p
mmu-miR-302a	mmu-miR-33*	mmu-miR-365	mmu-miR-423-5p
mmu-miR-302a*	mmu-miR-330	mmu-miR-367	mmu-miR-425
mmu-miR-302b	mmu-miR-330*	mmu-miR-369-3p	mmu-miR-425*
mmu-miR-302b*	mmu-miR-331-3p	mmu-miR-369-5p	mmu-miR-429
mmu-miR-302c	mmu-miR-331-5p	mmu-miR-370	mmu-miR-431
mmu-miR-302c*	mmu-miR-335-3p	mmu-miR-374	mmu-miR-431*
mmu-miR-302d	mmu-miR-335-5p	mmu-miR-374*	mmu-miR-433

mmu-miR-433*	mmu-miR-466j	mmu-miR-497	mmu-miR-615-3p
mmu-miR-434-3p	mmu-miR-466k	mmu-miR-499	mmu-miR-615-5p
mmu-miR-434-5p	mmu-miR-466l	mmu-miR-500	mmu-miR-652
mmu-miR-448	mmu-miR-467a	mmu-miR-501-3p	mmu-miR-653
mmu-miR-449a	mmu-miR-467a*	mmu-miR-501-5p	mmu-miR-654-3p
mmu-miR-449b	mmu-miR-467b	mmu-miR-503	mmu-miR-654-5p
mmu-miR-449c	mmu-miR-467b*	mmu-miR-503*	mmu-miR-665
mmu-miR-450a-3p	mmu-miR-467c	mmu-miR-504	mmu-miR-666-3p
mmu-miR-450a-5p	mmu-miR-467d	mmu-miR-505	mmu-miR-666-5p
mmu-miR-450b-3p	mmu-miR-467e	mmu-miR-509-3p	mmu-miR-667
mmu-miR-450b-5p	mmu-miR-467e*	mmu-miR-509-5p	mmu-miR-668
mmu-miR-451	mmu-miR-467f	mmu-miR-511	mmu-miR-669a
mmu-miR-452	mmu-miR-467g	mmu-miR-532-3p	mmu-miR-669b
mmu-miR-453	mmu-miR-468	mmu-miR-532-5p	mmu-miR-669e
mmu-miR-455	mmu-miR-469	mmu-miR-539	mmu-miR-669f
mmu-miR-455*	mmu-miR-470	mmu-miR-540-3p	mmu-miR-669g
mmu-miR-463	mmu-miR-470*	mmu-miR-540-5p	mmu-miR-669h-3p
mmu-miR-463*	mmu-miR-471	mmu-miR-541	mmu-miR-669h-5p
mmu-miR-464	mmu-miR-483	mmu-miR-542-3p	mmu-miR-669i
mmu-miR-465a-3p	mmu-miR-483*	mmu-miR-542-5p	mmu-miR-669j
mmu-miR-465a-5p	mmu-miR-484	mmu-miR-543	mmu-miR-669k
mmu-miR-465b-5p	mmu-miR-485	mmu-miR-544	mmu-miR-669l
mmu-miR-465c-5p	mmu-miR-485*	mmu-miR-546	mmu-miR-669n
mmu-miR-466a-3p	mmu-miR-486	mmu-miR-547	mmu-miR-670
mmu-miR-466a-5p	mmu-miR-487b	mmu-miR-551b	mmu-miR-671-3p
mmu-miR-466b-5p	mmu-miR-488	mmu-miR-568	mmu-miR-671-5p
mmu-miR-466c-5p	mmu-miR-488*	mmu-miR-574-3p	mmu-miR-672
mmu-miR-466d-3p	mmu-miR-489	mmu-miR-574-5p	mmu-miR-673-3p
mmu-miR-466d-5p	mmu-miR-490	mmu-miR-582-3p	mmu-miR-673-5p
mmu-miR-466f-3p	mmu-miR-491	mmu-miR-582-5p	mmu-miR-674
mmu-miR-466f-5p	mmu-miR-493	mmu-miR-590-3p	mmu-miR-674*
mmu-miR-466g	mmu-miR-494	mmu-miR-590-5p	mmu-miR-675-3p
mmu-miR-466h	mmu-miR-495	mmu-miR-592	mmu-miR-675-5p
mmu-miR-466i	mmu-miR-496	mmu-miR-598	mmu-miR-676

mmu-miR-676*	mmu-miR-708*	mmu-miR-7b	mmu-miR-96
mmu-miR-677	mmu-miR-709	mmu-miR-802	mmu-miR-98
mmu-miR-678	mmu-miR-710	mmu-miR-804	mmu-miR-99a
mmu-miR-679	mmu-miR-711	mmu-miR-805	mmu-miR-99b
mmu-miR-680	mmu-miR-712	mmu-miR-871	mmu-miR-99b*
mmu-miR-681	mmu-miR-712*	mmu-miR-872	dmr_285
mmu-miR-682	mmu-miR-713	mmu-miR-872*	dmr_3
mmu-miR-683	mmu-miR-714	mmu-miR-873	dmr_308
mmu-miR-684	mmu-miR-715	mmu-miR-874	dmr_316
mmu-miR-685	mmu-miR-717	mmu-miR-875-3p	dmr_31a
mmu-miR-686	mmu-miR-718	mmu-miR-875-5p	dmr_6
mmu-miR-687	mmu-miR-719	mmu-miR-876-3p	hur_1
mmu-miR-688	mmu-miR-720	mmu-miR-876-5p	hur_2
mmu-miR-689	mmu-miR-721	mmu-miR-877	hur_4
mmu-miR-690	mmu-miR-741	mmu-miR-877*	hur_5
mmu-miR-691	mmu-miR-742	mmu-miR-878-3p	hur_6
mmu-miR-692	mmu-miR-742*	mmu-miR-878-5p	mr_1
mmu-miR-693-3p	mmu-miR-743a	mmu-miR-879	
mmu-miR-693-5p	mmu-miR-743b-3p	mmu-miR-879*	
mmu-miR-694	mmu-miR-743b-5p	mmu-miR-880	
mmu-miR-695	mmu-miR-744	mmu-miR-881	
mmu-miR-696	mmu-miR-744*	mmu-miR-881*	
mmu-miR-697	mmu-miR-758	mmu-miR-882	
mmu-miR-698	mmu-miR-759	mmu-miR-883a-3p	
mmu-miR-699_v12.0	mmu-miR-760	mmu-miR-883a-5p	
mmu-miR-700	mmu-miR-761	mmu-miR-883b-3p	
mmu-miR-701	mmu-miR-762	mmu-miR-883b-5p	
mmu-miR-702	mmu-miR-763	mmu-miR-9	
mmu-miR-703	mmu-miR-764-3p	mmu-miR-9*	
mmu-miR-704	mmu-miR-764-5p	mmu-miR-92a	
mmu-miR-705	mmu-miR-770-3p	mmu-miR-92a*	
mmu-miR-706	mmu-miR-770-5p	mmu-miR-92b	
mmu-miR-707	mmu-miR-7a	mmu-miR-93	
mmu-miR-708	mmu-miR-7a*	mmu-miR-93*	

BIBLIOGRAPHY

1. *United Nations: World Population Prospects: The 2010 Revision, Volume 1: Comprehensive Tables.* 2011.

2. Kinsella, K. and W. He, *An Aging World: 2008*, in *International Population Reports*. 2009, U.S. Census Bureau: Washington, D.C. p. 191.

3. *Older Americans 2012: Key Indicators of Well-Being*. 2012, Federal Interagency Forum on Aging-Related Statistics: Washington, DC.

4. Salive, M.E., *Multimorbidity in Older Adults.* Epidemiol Rev, 2013.

5. Baraibar, M.A., et al., *Protein oxidative damage at the crossroads of cellular senescence, aging, and age-related diseases.* Oxid Med Cell Longev, 2012. **2012**: p. 919832.

6. Baraibar, M.A. and B. Friguet, *Oxidative proteome modifications target specific cellular pathways during oxidative stress, cellular senescence and aging.* Exp Gerontol, 2012.

7. Brack, A.S., et al., *Increased Wnt signaling during aging alters muscle stem cell fate and increases fibrosis.* Science, 2007. **317**(5839): p. 807-10.

8. Green, D.R., L. Galluzzi, and G. Kroemer, *Mitochondria and the autophagy-inflammation-cell death axis in organismal aging.* Science, 2011. **333**(6046): p. 1109-12.

9. Chen, D., et al., *Longevity determined by developmental arrest genes in Caenorhabditis elegans.* Aging Cell, 2007. **6**(4): p. 525-33.

10. Leontieva, O.V., G.M. Paszkiewicz, and M.V. Blagosklonny, *Mechanistic or mammalian target of rapamycin (mTOR) may determine robustness in young male mice at the cost of accelerated aging.* Aging (Albany NY), 2012. **4**(12): p. 899-916.

11. Grivennikova, V.G. and A.D. Vinogradov, *Generation of superoxide by the mitochondrial Complex I.* Biochim Biophys Acta, 2006. **1757**(5-6): p. 553-61.

12. Henle, E.S. and S. Linn, *Formation, prevention, and repair of DNA damage by iron/hydrogen peroxide.* J Biol Chem, 1997. **272**(31): p. 19095-8.

13. Wei, Y.H., *Oxidative stress and mitochondrial DNA mutations in human aging.* Proc Soc Exp Biol Med, 1998. **217**(1): p. 53-63.

14. Shen, H.M., C.N. Ong, and C.Y. Shi, *Involvement of reactive oxygen species in aflatoxin B1-induced cell injury in cultured rat hepatocytes.* Toxicology, 1995. **99**(1-2): p. 115-23.

15. Ryter, S.W. and A.M. Choi, *Heme oxygenase-1: redox regulation of a stress protein in lung and cell culture models.* Antioxid Redox Signal, 2005. **7**(1-2): p. 80-91.

16. Ichimiya, S., et al., *Murine thioredoxin peroxidase delays neuronal apoptosis and is expressed in areas of the brain most susceptible to hypoxic and ischemic injury.* DNA Cell Biol, 1997. **16**(3): p. 311-21.

17. Elchuri, S., et al., *CuZnSOD deficiency leads to persistent and widespread oxidative damage and hepatocarcinogenesis later in life.* Oncogene, 2005. **24**(3): p. 367-80.

18. Yang, W. and S. Hekimi, *A mitochondrial superoxide signal triggers increased longevity in Caenorhabditis elegans.* PLoS Biol, 2010. **8**(12): p. e1000556.

19. Van Raamsdonk, J.M. and S. Hekimi, *Deletion of the mitochondrial superoxide dismutase sod-2 extends lifespan in Caenorhabditis elegans.* PLoS Genet, 2009. **5**(2): p. e1000361.

20. Zarse, K., et al., *Impaired insulin/IGF1 signaling extends life span by promoting mitochondrial L-proline catabolism to induce a transient ROS signal.* Cell Metab, 2012. **15**(4): p. 451-65.

21. Campisi, J., *Replicative senescence: an old lives' tale?* Cell, 1996. **84**(4): p. 497-500.

22. Campisi, J., *Aging, cellular senescence, and cancer.* Annu Rev Physiol, 2013. **75**: p. 685-705.

23. Sitte, N., et al., *Lipofuscin accumulation in proliferating fibroblasts in vitro: an indicator of oxidative stress.* Exp Gerontol, 2001. **36**(3): p. 475-86.

24. Dimri, G.P., et al., *A biomarker that identifies senescent human cells in culture and in aging skin in vivo.* Proc Natl Acad Sci U S A, 1995. **92**(20): p. 9363-7.

25. Zwerschke, W., et al., *Metabolic analysis of senescent human fibroblasts reveals a role for AMP in cellular senescence.* Biochem J, 2003. **376**(Pt 2): p. 403-11.

26. Di Micco, R., et al., *Interplay between oncogene-induced DNA damage response and heterochromatin in senescence and cancer.* Nat Cell Biol, 2011. **13**(3): p. 292-302.

27. Rodier, F., et al., *DNA-SCARS: distinct nuclear structures that sustain damage-induced senescence growth arrest and inflammatory cytokine secretion.* J Cell Sci, 2011. **124**(Pt 1): p. 68-81.

28. Zindy, F., et al., *Expression of the p16INK4a tumor suppressor versus other INK4 family members during mouse development and aging.* Oncogene, 1997. **15**(2): p. 203-11.

29. Krishnamurthy, J., et al., *Ink4a/Arf expression is a biomarker of aging.* J Clin Invest, 2004. **114**(9): p. 1299-307.

30. Kamminga, L.M., et al., *Impaired hematopoietic stem cell functioning after serial transplantation and during normal aging.* Stem Cells, 2005. **23**(1): p. 82-92.

31. Lopez-Otin, C., et al., *The hallmarks of aging.* Cell, 2013. **153**(6): p. 1194-217.

32. Lee, A.T., et al., *Comparative analysis of DNA mutations in lacI transgenic mice with age.* FASEB J, 1994. **8**(8): p. 545-50.

33. Dolle, M.E., et al., *Distinct spectra of somatic mutations accumulated with age in mouse heart and small intestine.* Proc Natl Acad Sci U S A, 2000. **97**(15): p. 8403-8.

34. Hayflick, L., *The Limited in Vitro Lifetime of Human Diploid Cell Strains.* Exp Cell Res, 1965. **37**: p. 614-36.

35. Harley, C.B., A.B. Futcher, and C.W. Greider, *Telomeres shorten during ageing of human fibroblasts.* Nature, 1990. **345**(6274): p. 458-60.

36. Di Leonardo, A., et al., *DNA damage triggers a prolonged p53-dependent G1 arrest and long-term induction of Cip1 in normal human fibroblasts.* Genes Dev, 1994. **8**(21): p. 2540-51.

37. Martens, U.M., et al., *Accumulation of short telomeres in human fibroblasts prior to replicative senescence.* Exp Cell Res, 2000. **256**(1): p. 291-9.

38. Abdallah, P., et al., *A two-step model for senescence triggered by a single critically short telomere.* Nat Cell Biol, 2009. **11**(8): p. 988-93.

39. Serrano, M., et al., *Oncogenic ras provokes premature cell senescence associated with accumulation of p53 and p16INK4a.* Cell, 1997. **88**(5): p. 593-602.

40. Narita, M., et al., *Rb-mediated heterochromatin formation and silencing of E2F target genes during cellular senescence.* Cell, 2003. **113**(6): p. 703-16.

41. Braig, M., et al., *Oncogene-induced senescence as an initial barrier in lymphoma development.* Nature, 2005. **436**(7051): p. 660-5.

42. Collado, M., et al., *Tumour biology: senescence in premalignant tumours.* Nature, 2005. **436**(7051): p. 642.

43. Shamma, A., et al., *Rb Regulates DNA damage response and cellular senescence through E2F-dependent suppression of N-ras isoprenylation.* Cancer Cell, 2009. **15**(4): p. 255-69.

44. Shay, J.W., O.M. Pereira-Smith, and W.E. Wright, *A role for both RB and p53 in the regulation of human cellular senescence.* Exp Cell Res, 1991. **196**(1): p. 33-9.

45. Hara, E., et al., *Cooperative effect of antisense-Rb and antisense-p53 oligomers on the extension of life span in human diploid fibroblasts, TIG-1.* Biochem Biophys Res Commun, 1991. **179**(1): p. 528-34.

46. Herbig, U., et al., *Telomere shortening triggers senescence of human cells through a pathway involving ATM, p53, and p21(CIP1), but not p16(INK4a).* Mol Cell, 2004. **14**(4): p. 501-13.

47. Karamurzin, Y., M.M. Leitao, Jr., and R.A. Soslow, *Clinicopathologic analysis of low-stage sporadic ovarian carcinomas: a reappraisal.* Am J Surg Pathol, 2013. **37**(3): p. 356-67.

48. Bellini, M.F., et al., *Alterations of the TP53 gene in gastric and esophageal carcinogenesis.* J Biomed Biotechnol, 2012. **2012**: p. 891961.

49. Liu, J., et al., *Alterations of TP53 are associated with a poor outcome for patients with hepatocellular carcinoma: evidence from a systematic review and meta-analysis.* Eur J Cancer, 2012. **48**(15): p. 2328-38.

50. Kubbutat, M.H., S.N. Jones, and K.H. Vousden, *Regulation of p53 stability by Mdm2.* Nature, 1997. **387**(6630): p. 299-303.

51. Fang, S., et al., *Mdm2 is a RING finger-dependent ubiquitin protein ligase for itself and p53.* J Biol Chem, 2000. **275**(12): p. 8945-51.

52. Banin, S., et al., *Enhanced phosphorylation of p53 by ATM in response to DNA damage.* Science, 1998. **281**(5383): p. 1674-7.

53. Craig, A.L., et al., *Novel phosphorylation sites of human tumour suppressor protein p53 at Ser20 and Thr18 that disrupt the binding of mdm2 (mouse double minute 2) protein are modified in human cancers.* Biochem J, 1999. **342 (Pt 1)**: p. 133-41.

54. Bae, I., et al., *Relationships between G1 arrest and stability of the p53 and p21Cip1/Waf1 proteins following gamma-irradiation of human lymphoma cells.* Cancer Res, 1995. **55**(11): p. 2387-93.

55. Xiong, Y., et al., *p21 is a universal inhibitor of cyclin kinases.* Nature, 1993. **366**(6456): p. 701-4.

56. Zuo, S., et al., *IGFBP-rP1 induces p21 expression through a p53-independent pathway, leading to cellular senescence of MCF-7 breast cancer cells.* J Cancer Res Clin Oncol, 2012. **138**(6): p. 1045-55.

57. Toyama, T., et al., *Ninjurin1 increases p21 expression and induces cellular senescence in human hepatoma cells.* J Hepatol, 2004. **41**(4): p. 637-43.

58. Ohtani, K., J. DeGregori, and J.R. Nevins, *Regulation of the cyclin E gene by transcription factor E2F1.* Proc Natl Acad Sci U S A, 1995. **92**(26): p. 12146-50.

59. Huet, X., et al., *Cyclin A expression is under negative transcriptional control during the cell cycle.* Mol Cell Biol, 1996. **16**(7): p. 3789-98.

60. DeGregori, J., T. Kowalik, and J.R. Nevins, *Cellular targets for activation by the E2F1 transcription factor include DNA synthesis- and G1/S-regulatory genes.* Mol Cell Biol, 1995. **15**(8): p. 4215-24.

61. Weintraub, S.J., C.A. Prater, and D.C. Dean, *Retinoblastoma protein switches the E2F site from positive to negative element.* Nature, 1992. **358**(6383): p. 259-61.

62. Nevins, J.R., *E2F: a link between the Rb tumor suppressor protein and viral oncoproteins.* Science, 1992. **258**(5081): p. 424-9.

63. Luo, R.X., A.A. Postigo, and D.C. Dean, *Rb interacts with histone deacetylase to repress transcription.* Cell, 1998. **92**(4): p. 463-73.

64. Rayess, H., M.B. Wang, and E.S. Srivatsan, *Cellular senescence and tumor suppressor gene p16.* Int J Cancer, 2012. **130**(8): p. 1715-25.

65. Krishnamurthy, J., et al., *p16INK4a induces an age-dependent decline in islet regenerative potential.* Nature, 2006. **443**(7110): p. 453-7.

66. Al-Mohanna, M.A., et al., *The tumor suppressor p16(INK4a) gene is a regulator of apoptosis induced by ultraviolet light and cisplatin.* Oncogene, 2004. **23**(1): p. 201-12.

67. Sherr, C.J., *Ink4-Arf Locus in Cancer and Aging.* Wiley Interdiscip Rev Dev Biol, 2012. **1**(5): p. 731-741.

68. Harbour, J.W., et al., *Cdk phosphorylation triggers sequential intramolecular interactions that progressively block Rb functions as cells move through G1.* Cell, 1999. **98**(6): p. 859-69.

69. Takahashi, A., et al., *Mitogenic signalling and the p16INK4a-Rb pathway cooperate to enforce irreversible cellular senescence.* Nat Cell Biol, 2006. **8**(11): p. 1291-7.

70. Li, Y., et al., *Transcriptional repression of the D-type cyclin-dependent kinase inhibitor p16 by the retinoblastoma susceptibility gene product pRb.* Cancer Res, 1994. **54**(23): p. 6078-82.

71. Rodier, F., et al., *Persistent DNA damage signalling triggers senescence-associated inflammatory cytokine secretion.* Nat Cell Biol, 2009. **11**(8): p. 973-9.

72. Kuilman, T., et al., *Oncogene-induced senescence relayed by an interleukin-dependent inflammatory network.* Cell, 2008. **133**(6): p. 1019-31.

73. Coppe, J.P., et al., *Tumor suppressor and aging biomarker p16(INK4a) induces cellular senescence without the associated inflammatory secretory phenotype.* J Biol Chem, 2011. **286**(42): p. 36396-403.

74. Pazolli, E., et al., *Chromatin remodeling underlies the senescence-associated secretory phenotype of tumor stromal fibroblasts that supports cancer progression.* Cancer Res, 2012. **72**(9): p. 2251-61.

75. Bhaumik, D., et al., *MicroRNAs miR-146a/b negatively modulate the senescence-associated inflammatory mediators IL-6 and IL-8.* Aging (Albany NY), 2009. **1**(4): p. 402-11.

76. Orjalo, A.V., et al., *Cell surface-bound IL-1alpha is an upstream regulator of the senescence-associated IL-6/IL-8 cytokine network.* Proc Natl Acad Sci U S A, 2009. **106**(40): p. 17031-6.

77. Ohanna, M., et al., *Senescent cells develop a PARP-1 and nuclear factor-{kappa}B-associated secretome (PNAS).* Genes Dev, 2011. **25**(12): p. 1245-61.

78. Tilstra, J.S., et al., *NF-kappaB inhibition delays DNA damage-induced senescence and aging in mice.* J Clin Invest, 2012. **122**(7): p. 2601-12.

79. Wajapeyee, N., et al., *Oncogenic BRAF induces senescence and apoptosis through pathways mediated by the secreted protein IGFBP7.* Cell, 2008. **132**(3): p. 363-74.

80. Zdanov, S., et al., *Normal or stress-induced fibroblast senescence involves COX-2 activity.* Exp Cell Res, 2007. **313**(14): p. 3046-56.

81. Olivieri, F., et al., *MiR-146a as marker of senescence-associated pro-inflammatory status in cells involved in vascular remodelling.* Age (Dordr), 2012.

82. Salminen, A., et al., *Astrocytes in the aging brain express characteristics of senescence-associated secretory phenotype.* Eur J Neurosci, 2011. **34**(1): p. 3-11.

83. Burton, D.G., H. Matsubara, and K. Ikeda, *Pathophysiology of vascular calcification: Pivotal role of cellular senescence in vascular smooth muscle cells.* Exp Gerontol, 2010. **45**(11): p. 819-24.

84. Bitto, A., et al., *Stress-induced senescence in human and rodent astrocytes.* Exp Cell Res, 2010. **316**(17): p. 2961-8.

85. Lindahl, T. and D.E. Barnes, *Repair of endogenous DNA damage.* Cold Spring Harb Symp Quant Biol, 2000. **65**: p. 127-33.

86. Cheng, W.H., M. Muftuoglu, and V.A. Bohr, *Werner syndrome protein: functions in the response to DNA damage and replication stress in S-phase.* Exp Gerontol, 2007. **42**(9): p. 871-8.

87. Dong, Y.P., et al., *WRN functions in a RAD18-dependent damage avoidance pathway.* Biol Pharm Bull, 2007. **30**(6): p. 1080-3.

88. Bai, Y. and J.P. Murnane, *Telomere instability in a human tumor cell line expressing a dominant-negative WRN protein.* Hum Genet, 2003. **113**(4): p. 337-47.

89. Salk, D., *Can we learn about aging from a study of Werner's syndrome?* J Am Geriatr Soc, 1982. **30**(5): p. 334-9.

90. Eriksson, M., et al., *Recurrent de novo point mutations in lamin A cause Hutchinson-Gilford progeria syndrome.* Nature, 2003. **423**(6937): p. 293-8.

91. Scaffidi, P. and T. Misteli, *Lamin A-dependent nuclear defects in human aging.* Science, 2006. **312**(5776): p. 1059-63.

92. Liu, B., et al., *Genomic instability in laminopathy-based premature aging.* Nat Med, 2005. **11**(7): p. 780-5.

93. Mahen, R., et al., *A-type lamins maintain the positional stability of DNA damage repair foci in Mammalian nuclei.* PLoS One, 2013. **8**(5): p. e61893.

94. Baker, P.B., N. Baba, and C.P. Boesel, *Cardiovascular abnormalities in progeria. Case report and review of the literature.* Arch Pathol Lab Med, 1981. **105**(7): p. 384-6.

95. Gaillard, P.H. and R.D. Wood, *Activity of individual ERCC1 and XPF subunits in DNA nucleotide excision repair.* Nucleic Acids Res, 2001. **29**(4): p. 872-9.

96. Chipchase, M.D. and D.W. Melton, *The formation of UV-induced chromosome aberrations involves ERCC1 and XPF but not other nucleotide excision repair genes.* DNA Repair (Amst), 2002. **1**(4): p. 335-40.

97. Houtsmuller, A.B., et al., *Action of DNA repair endonuclease ERCC1/XPF in living cells.* Science, 1999. **284**(5416): p. 958-61.

98. Becker, M.M. and Z. Wang, *Origin of ultraviolet damage in DNA.* J Mol Biol, 1989. **210**(3): p. 429-38.

99. Nouspikel, T., *DNA repair in mammalian cells : Nucleotide excision repair: variations on versatility.* Cell Mol Life Sci, 2009. **66**(6): p. 994-1009.

100. Sugasawa, K., et al., *Xeroderma pigmentosum group C protein complex is the initiator of global genome nucleotide excision repair.* Mol Cell, 1998. **2**(2): p. 223-32.

101. Mone, M.J., et al., *Local UV-induced DNA damage in cell nuclei results in local transcription inhibition.* EMBO Rep, 2001. **2**(11): p. 1013-7.

102. Mellon, I., G. Spivak, and P.C. Hanawalt, *Selective removal of transcription-blocking DNA damage from the transcribed strand of the mammalian DHFR gene.* Cell, 1987. **51**(2): p. 241-9.

103. Bessho, T., et al., *Reconstitution of human excision nuclease with recombinant XPF-ERCC1 complex.* J Biol Chem, 1997. **272**(6): p. 3833-7.

104. Fousteri, M. and L.H. Mullenders, *Transcription-coupled nucleotide excision repair in mammalian cells: molecular mechanisms and biological effects.* Cell Res, 2008. **18**(1): p. 73-84.

105. Weeda, G., et al., *Disruption of mouse ERCC1 results in a novel repair syndrome with growth failure, nuclear abnormalities and senescence.* Curr Biol, 1997. **7**(6): p. 427-39.

106. Furuta, T., et al., *Transcription-coupled nucleotide excision repair as a determinant of cisplatin sensitivity of human cells.* Cancer Res, 2002. **62**(17): p. 4899-902.

107. Reed, W.B., et al., *Xeroderma pigmentosum. Clinical and laboratory investigation of its basic defect.* JAMA, 1969. **207**(11): p. 2073-9.

108. Kraemer, K.H., M.M. Lee, and J. Scotto, *Xeroderma pigmentosum. Cutaneous, ocular, and neurologic abnormalities in 830 published cases.* Arch Dermatol, 1987. **123**(2): p. 241-50.

109. Tang, J.Y., et al., *Xeroderma pigmentosum p48 gene enhances global genomic repair and suppresses UV-induced mutagenesis.* Mol Cell, 2000. **5**(4): p. 737-44.

110. Rapic Otrin, V., et al., *Relationship of the xeroderma pigmentosum group E DNA repair defect to the chromatin and DNA binding proteins UV-DDB and replication protein A.* Mol Cell Biol, 1998. **18**(6): p. 3182-90.

111. Kobayashi, T., et al., *Mutations in the XPD gene in xeroderma pigmentosum group D cell strains: confirmation of genotype-phenotype correlation.* Am J Med Genet, 2002. **110**(3): p. 248-52.

112. Falik-Zaccai, T.C., et al., *A novel XPD mutation in a compound heterozygote; the mutation in the second allele is present in three homozygous patients with mild sun sensitivity.* Environ Mol Mutagen, 2012. **53**(7): p. 505-14.

113. Laugel, V., *Cockayne syndrome: The expanding clinical and mutational spectrum.* Mech Ageing Dev, 2013. **134**(5-6): p. 161-70.

114. Bhagwat, N., et al., *XPF-ERCC1 participates in the Fanconi anemia pathway of cross-link repair.* Mol Cell Biol, 2009. **29**(24): p. 6427-37.

115. Niedernhofer, L.J., et al., *The structure-specific endonuclease Ercc1-Xpf is required to resolve DNA interstrand cross-link-induced double-strand breaks.* Mol Cell Biol, 2004. **24**(13): p. 5776-87.

116. Le May, N., et al., *NER factors are recruited to active promoters and facilitate chromatin modification for transcription in the absence of exogenous genotoxic attack.* Mol Cell, 2010. **38**(1): p. 54-66.

117. Le May, N., et al., *XPG and XPF endonucleases trigger chromatin looping and DNA demethylation for accurate expression of activated genes.* Mol Cell, 2012. **47**(4): p. 622-32.

118. Naim, V., et al., *ERCC1 and MUS81-EME1 promote sister chromatid separation by processing late replication intermediates at common fragile sites during mitosis.* Nat Cell Biol, 2013.

119. Niedernhofer, L.J., et al., *A new progeroid syndrome reveals that genotoxic stress suppresses the somatotroph axis.* Nature, 2006. **444**(7122): p. 1038-43.

120. McWhir, J., et al., *Mice with DNA repair gene (ERCC-1) deficiency have elevated levels of p53, liver nuclear abnormalities and die before weaning.* Nat Genet, 1993. **5**(3): p. 217-24.

121. Schumacher, B., et al., *Delayed and accelerated aging share common longevity assurance mechanisms.* PLoS Genet, 2008. **4**(8): p. e1000161.

122. Vo, N., et al., *Accelerated aging of intervertebral discs in a mouse model of progeria.* J Orthop Res, 2010. **28**(12): p. 1600-7.

123. Goss, J.R., et al., *Premature aging-related peripheral neuropathy in a mouse model of progeria.* Mech Ageing Dev, 2011. **132**(8-9): p. 437-42.

124. Gregg, S.Q., et al., *A mouse model of accelerated liver aging caused by a defect in DNA repair.* Hepatology, 2012. **55**(2): p. 609-21.

125. Lee, Y., et al., *MicroRNA genes are transcribed by RNA polymerase II.* EMBO J, 2004. **23**(20): p. 4051-60.

126. Gregory, R.I., et al., *The Microprocessor complex mediates the genesis of microRNAs.* Nature, 2004. **432**(7014): p. 235-40.

127. Kim, V.N., *MicroRNA precursors in motion: exportin-5 mediates their nuclear export.* Trends Cell Biol, 2004. **14**(4): p. 156-9.

128. Lund, E., et al., *Nuclear export of microRNA precursors.* Science, 2004. **303**(5654): p. 95-8.

129. Chendrimada, T.P., et al., *TRBP recruits the Dicer complex to Ago2 for microRNA processing and gene silencing.* Nature, 2005. **436**(7051): p. 740-4.

130. Bernstein, E., et al., *Role for a bidentate ribonuclease in the initiation step of RNA interference.* Nature, 2001. **409**(6818): p. 363-6.

131. Hammond, S.M., et al., *Argonaute2, a link between genetic and biochemical analyses of RNAi.* Science, 2001. **293**(5532): p. 1146-50.

132. Rivas, F.V., et al., *Purified Argonaute2 and an siRNA form recombinant human RISC.* Nat Struct Mol Biol, 2005. **12**(4): p. 340-9.

133. Kawamata, T., H. Seitz, and Y. Tomari, *Structural determinants of miRNAs for RISC loading and slicer-independent unwinding.* Nat Struct Mol Biol, 2009. **16**(9): p. 953-60.

134. Lim, L.P., et al., *Microarray analysis shows that some microRNAs downregulate large numbers of target mRNAs.* Nature, 2005. **433**(7027): p. 769-73.

135. Eulalio, A., E. Huntzinger, and E. Izaurralde, *Getting to the root of miRNA-mediated gene silencing.* Cell, 2008. **132**(1): p. 9-14.

136. Martinez, J., et al., *Single-stranded antisense siRNAs guide target RNA cleavage in RNAi.* Cell, 2002. **110**(5): p. 563-74.

137. Filipowicz, W., S.N. Bhattacharyya, and N. Sonenberg, *Mechanisms of post-transcriptional regulation by microRNAs: are the answers in sight?* Nat Rev Genet, 2008. **9**(2): p. 102-14.

138. Valeri, N., et al., *Modulation of mismatch repair and genomic stability by miR-155.* Proc Natl Acad Sci U S A, 2010. **107**(15): p. 6982-7.

139. Moskwa, P., et al., *miR-182-mediated downregulation of BRCA1 impacts DNA repair and sensitivity to PARP inhibitors.* Mol Cell, 2011. **41**(2): p. 210-20.

140. Krishnan, K., et al., *MicroRNA-182-5p targets a network of genes involved in DNA repair*. RNA, 2013. **19**(2): p. 230-42.

141. Pothof, J., et al., *MicroRNA-mediated gene silencing modulates the UV-induced DNA-damage response.* EMBO J, 2009. **28**(14): p. 2090-9.

142. Mailand, N., et al., *Rapid destruction of human Cdc25A in response to DNA damage.* Science, 2000. **288**(5470): p. 1425-9.

143. Rother, K., et al., *p53 downregulates expression of the G1/S cell cycle phosphatase Cdc25A.* Oncogene, 2007. **26**(13): p. 1949-53.

144. Zhang, X., et al., *The ATM kinase induces microRNA biogenesis in the DNA damage response.* Mol Cell, 2011. **41**(4): p. 371-83.

145. Kawai, S. and A. Amano, *BRCA1 regulates microRNA biogenesis via the DROSHA microprocessor complex.* J Cell Biol, 2012. **197**(2): p. 201-8.

146. Chang, S., et al., *Tumor suppressor BRCA1 epigenetically controls oncogenic microRNA-155.* Nat Med, 2011. **17**(10): p. 1275-82.

147. Sachdeva, M., et al., *p53 represses c-Myc through induction of the tumor suppressor miR-145.* Proc Natl Acad Sci U S A, 2009. **106**(9): p. 3207-12.

148. Yamakuchi, M., et al., *P53-induced microRNA-107 inhibits HIF-1 and tumor angiogenesis.* Proc Natl Acad Sci U S A, 2010. **107**(14): p. 6334-9.

149. Braun, C.J., et al., *p53-Responsive micrornas 192 and 215 are capable of inducing cell cycle arrest.* Cancer Res, 2008. **68**(24): p. 10094-104.

150. Yamakuchi, M., M. Ferlito, and C.J. Lowenstein, *miR-34a repression of SIRT1 regulates apoptosis.* Proc Natl Acad Sci U S A, 2008. **105**(36): p. 13421-6.

151. Luo, J., et al., *Negative control of p53 by Sir2alpha promotes cell survival under stress.* Cell, 2001. **107**(2): p. 137-48.

152. Chang, T.C., et al., *Transactivation of miR-34a by p53 broadly influences gene expression and promotes apoptosis.* Mol Cell, 2007. **26**(5): p. 745-52.

153. Bommer, G.T., et al., *p53-mediated activation of miRNA34 candidate tumor-suppressor genes.* Curr Biol, 2007. **17**(15): p. 1298-307.

154. d'Adda di Fagagna, F., et al., *A DNA damage checkpoint response in telomere-initiated senescence.* Nature, 2003. **426**(6963): p. 194-8.

155. Bischof, O. and A. Dejean, *SUMO is growing senescent.* Cell Cycle, 2007. **6**(6): p. 677-81.

156. Christoffersen, N.R., et al., *p53-independent upregulation of miR-34a during oncogene-induced senescence represses MYC.* Cell Death Differ, 2010. **17**(2): p. 236-45.

157. Mudhasani, R., et al., *Loss of miRNA biogenesis induces p19Arf-p53 signaling and senescence in primary cells.* J Cell Biol, 2008. **181**(7): p. 1055-63.

158. Gomez-Cabello, D., et al., *DGCR8-mediated disruption of miRNA biogenesis induces cellular senescence in primary fibroblasts.* Aging Cell, 2013.

159. Bhaumik, D., et al., *Expression of microRNA-146 suppresses NF-kappaB activity with reduction of metastatic potential in breast cancer cells.* Oncogene, 2008. **27**(42): p. 5643-7.

160. Taganov, K.D., et al., *NF-kappaB-dependent induction of microRNA miR-146, an inhibitor targeted to signaling proteins of innate immune responses.* Proc Natl Acad Sci U S A, 2006. **103**(33): p. 12481-6.

161. Sansone, P., et al., *IL-6 triggers malignant features in mammospheres from human ductal breast carcinoma and normal mammary gland.* J Clin Invest, 2007. **117**(12): p. 3988-4002.

162. Korkaya, H., et al., *Activation of an IL6 inflammatory loop mediates trastuzumab resistance in HER2+ breast cancer by expanding the cancer stem cell population.* Mol Cell, 2012. **47**(4): p. 570-84.

163. Lin, J.T., et al., *Colon cancer mesenchymal stem cells modulate the tumorigenicity of colon cancer through interleukin 6.* Exp Cell Res, 2013.

164. Dellago, H., et al., *High levels of oncomiR-21 contribute to the senescence-induced growth arrest in normal human cells and its knock-down increases the replicative lifespan.* Aging Cell, 2013. **12**(3): p. 446-58.

165. Ouellet, S., et al., *Transcriptional regulation of the cyclin-dependent kinase inhibitor 1A (p21) gene by NFI in proliferating human cells.* Nucleic Acids Res, 2006. **34**(22): p. 6472-87.

166. Lu, T.X., et al., *Targeted ablation of miR-21 decreases murine eosinophil progenitor cell growth.* PLoS One, 2013. **8**(3): p. e59397.

167. Wang, F., et al., *Antagonist of microRNA-21 improves balloon injury-induced rat iliac artery remodeling by regulating proliferation and apoptosis of adventitial fibroblasts and myofibroblasts.* J Cell Biochem, 2012. **113**(9): p. 2989-3001.

168. Loayza-Puch, F., et al., *Hypoxia and RAS-signaling pathways converge on, and cooperatively downregulate, the RECK tumor-suppressor protein through microRNAs.* Oncogene, 2010. **29**(18): p. 2638-48.

169. Lee, S., et al., *Histone deacetylase regulates high mobility group A2-targeting microRNAs in human cord blood-derived multipotent stem cell aging.* Cell Mol Life Sci, 2011. **68**(2): p. 325-36.

170. Zhu, S., et al., *MicroRNA-10A* and MicroRNA-21 modulate endothelial progenitor cell senescence via suppressing high-mobility group A2.* Circ Res, 2013. **112**(1): p. 152-64.

171. Ma, W.J., et al., *Cloning and characterization of HuR, a ubiquitously expressed Elav-like protein.* J Biol Chem, 1996. **271**(14): p. 8144-51.

172. Kundu, P., et al., *HuR protein attenuates miRNA-mediated repression by promoting miRISC dissociation from the target RNA.* Nucleic Acids Res, 2012. **40**(11): p. 5088-100.

173. Bhattacharyya, S.N., et al., *Relief of microRNA-mediated translational repression in human cells subjected to stress.* Cell, 2006. **125**(6): p. 1111-24.

174. Kawagishi, H., et al., *HuR maintains a replicative life span by repressing the ARF tumor suppressor.* Mol Cell Biol, 2013. **33**(10): p. 1886-900.

175. Marasa, B.S., et al., *MicroRNA profiling in human diploid fibroblasts uncovers miR-519 role in replicative senescence.* Aging (Albany NY), 2010. **2**(6): p. 333-43.

176. Ugalde, A.P., et al., *Aging and chronic DNA damage response activate a regulatory pathway involving miR-29 and p53.* EMBO J, 2011. **30**(11): p. 2219-32.

177. Dallaire, A., et al., *Down regulation of miR-124 in both Werner syndrome DNA helicase mutant mice and mutant Caenorhabditis elegans wrn-1 reveals the importance of this microRNA in accelerated aging.* Aging (Albany NY), 2012. **4**(9): p. 636-47.

178. Toledano, H., *The role of the heterochronic microRNA let-7 in the progression of aging.* Exp Gerontol, 2012.

179. Tzatsos, A., et al., *Lysine-specific demethylase 2B (KDM2B)-let-7-enhancer of zester homolog 2 (EZH2) pathway regulates cell cycle progression and senescence in primary cells.* J Biol Chem, 2011. **286**(38): p. 33061-9.

180. Saunders, L.R., et al., *miRNAs regulate SIRT1 expression during mouse embryonic stem cell differentiation and in adult mouse tissues.* Aging (Albany NY), 2010. **2**(7): p. 415-31.

181. Li, J., et al., *miR-10a restores human mesenchymal stem cell differentiation by repressing KLF4.* J Cell Physiol, 2013.

182. Xu, D., et al., *miR-22 represses cancer progression by inducing cellular senescence.* J Cell Biol, 2011. **193**(2): p. 409-24.

183. Jazbutyte, V., et al., *MicroRNA-22 increases senescence and activates cardiac fibroblasts in the aging heart.* Age (Dordr), 2013. **35**(3): p. 747-62.

184. Verduci, L., et al., *MicroRNA (miRNA)-mediated interaction between leukemia/lymphoma-related factor (LRF) and alternative splicing factor/splicing factor 2 (ASF/SF2) affects mouse embryonic fibroblast senescence and apoptosis.* J Biol Chem, 2010. **285**(50): p. 39551-63.

185. Takahashi, M., et al., *Reduction of type IV collagen by upregulated miR-29 in normal elderly mouse and klotho-deficient, senescence-model mouse.* PLoS One, 2012. **7**(11): p. e48974.

186. Martinez, I., et al., *miR-29 and miR-30 regulate B-Myb expression during cellular senescence.* Proc Natl Acad Sci U S A, 2011. **108**(2): p. 522-7.

187. Bai, X.Y., et al., *miR-335 and miR-34a Promote renal senescence by suppressing mitochondrial antioxidative enzymes.* J Am Soc Nephrol, 2011. **22**(7): p. 1252-61.

188. Greussing, R., et al., *Identification of microRNA-mRNA functional interactions in UVB-induced senescence of human diploid fibroblasts.* BMC Genomics, 2013. **14**(1): p. 224.

189. Hackl, M., et al., *miR-17, miR-19b, miR-20a, and miR-106a are down-regulated in human aging.* Aging Cell, 2010. **9**(2): p. 291-6.

190. Volinia, S., et al., *A microRNA expression signature of human solid tumors defines cancer gene targets.* Proc Natl Acad Sci U S A, 2006. **103**(7): p. 2257-61.

191. Rippe, C., et al., *MicroRNA changes in human arterial endothelial cells with senescence: relation to apoptosis, eNOS and inflammation.* Exp Gerontol, 2012. **47**(1): p. 45-51.

192. Li, G., et al., *Modulation of inflammatory markers by miR-146a during replicative senescence in trabecular meshwork cells.* Invest Ophthalmol Vis Sci, 2010. **51**(6): p. 2976-85.

193. Mancini, M., et al., *MicroRNA-152 and -181a participate in human dermal fibroblasts senescence acting on cell adhesion and remodeling of the extra-cellular matrix.* Aging (Albany NY), 2012. **4**(11): p. 843-53.

194. Martinez-Nunez, R.T., et al., *MicroRNA-155 modulates the pathogen binding ability of dendritic cells (DCs) by down-regulation of DC-specific intercellular adhesion molecule-3 grabbing non-integrin (DC-SIGN).* J Biol Chem, 2009. **284**(24): p. 16334-42.

195. Song, J., et al., *MiR-155 negatively regulates c-Jun expression at the post-transcriptional level in human dermal fibroblasts in vitro: implications in UVA irradiation-induced photoaging.* Cell Physiol Biochem, 2012. **29**(3-4): p. 331-40.

196. Dorsett, Y., et al., *MicroRNA-155 suppresses activation-induced cytidine deaminase-mediated Myc-Igh translocation.* Immunity, 2008. **28**(5): p. 630-8.

197. Basso, K., et al., *BCL6 positively regulates AID and germinal center gene expression via repression of miR-155.* J Exp Med, 2012. **209**(13): p. 2455-65.

198. Li, G., et al., *Decline in miR-181a expression with age impairs T cell receptor sensitivity by increasing DUSP6 activity.* Nat Med, 2012. **18**(10): p. 1518-24.

199. Lena, A.M., et al., *MicroRNA-191 triggers keratinocytes senescence by SATB1 and CDK6 downregulation.* Biochem Biophys Res Commun, 2012. **423**(3): p. 509-14.

200. Magenta, A., et al., *miR-200c is upregulated by oxidative stress and induces endothelial cell apoptosis and senescence via ZEB1 inhibition.* Cell Death Differ, 2011. **18**(10): p. 1628-39.

201. Noguchi, S., et al., *Anti-oncogenic microRNA-203 induces senescence by targeting E2F3 protein in human melanoma cells.* J Biol Chem, 2012. **287**(15): p. 11769-77.

202. Dar, A.A., et al., *miRNA-205 suppresses melanoma cell proliferation and induces senescence via regulation of E2F1 protein.* J Biol Chem, 2011. **286**(19): p. 16606-14.

203. Menghini, R., et al., *MicroRNA 217 modulates endothelial cell senescence via silent information regulator 1.* Circulation, 2009. **120**(15): p. 1524-32.

204. Pitto, L., et al., *miR-290 acts as a physiological effector of senescence in mouse embryo fibroblasts.* Physiol Genomics, 2009. **39**(3): p. 210-8.

205. Jong, H.L., et al., *MicroRNA 299-3p modulates replicative senescence in endothelial cells.* Physiol Genomics, 2013. **45**(7): p. 256-67.

206. Yang, M.Y., et al., *Induction of cellular senescence by doxorubicin is associated with upregulated miR-375 and induction of autophagy in K562 cells.* PLoS One, 2012. **7**(5): p. e37205.

207. Kim, Y.J., et al., *miR-486-5p induces replicative senescence of human adipose tissue-derived mesenchymal stem cells and its expression is controlled by high glucose.* Stem Cells Dev, 2012. **21**(10): p. 1749-60.

208. Ohdaira, H., et al., *MicroRNA-494 suppresses cell proliferation and induces senescence in A549 lung cancer cells.* Cell Prolif, 2012. **45**(1): p. 32-8.

209. Poliseno, L., et al., *The proto-oncogene LRF is under post-transcriptional control of MiR-20a: implications for senescence.* PLoS One, 2008. **3**(7): p. e2542.

210. Frankel, L.B., et al., *Programmed cell death 4 (PDCD4) is an important functional target of the microRNA miR-21 in breast cancer cells.* J Biol Chem, 2008. **283**(2): p. 1026-33.

211. Wang, Y., et al., *Tumor-suppressive effects of miR-29c on gliomas.* Neuroreport, 2013.

212. Bae, H.J., et al., *MicroRNA-29c functions as a tumor suppressor by direct targeting oncogenic SIRT1 in hepatocellular carcinoma.* Oncogene, 2013.

213. Lawrence, N.J., et al., *A neurological phenotype in mice with DNA repair gene Ercc1 deficiency.* DNA Repair (Amst), 2008. **7**(2): p. 281-91.

214. Dollé, M.E.T., et al., *Broad segmental progeroid changes in short-lived Ercc1 -/ Δ7 mice*. 2011. 2011.

215. Borgesius, N.Z., et al., *Accelerated age-related cognitive decline and neurodegeneration, caused by deficient DNA repair.* J Neurosci, 2011. **31**(35): p. 12543-53.

216. Moggs, J.G., et al., *Analysis of incision sites produced by human cell extracts and purified proteins during nucleotide excision repair of a 1,3-intrastrand d(GpTpG)-cisplatin adduct.* J Biol Chem, 1996. **271**(12): p. 7177-86.

217. Ahmad, A., et al., *ERCC1-XPF endonuclease facilitates DNA double-strand break repair.* Mol Cell Biol, 2008. **28**(16): p. 5082-92.

218. Wang, J., et al., *The oxidative DNA lesions 8,5'-cyclopurines accumulate with aging in a tissue-specific manner.* Aging Cell, 2012. **11**(4): p. 714-6.

219. Parrinello, S., et al., *Oxygen sensitivity severely limits the replicative lifespan of murine fibroblasts.* Nat Cell Biol, 2003. **5**(8): p. 741-7.

220. Livak, K.J. and T.D. Schmittgen, *Analysis of relative gene expression data using real-time quantitative PCR and the 2(-Delta Delta C(T)) Method.* Methods, 2001. **25**(4): p. 402-8.

221. Griffiths-Jones, S., *The microRNA Registry.* Nucleic Acids Research, 2004. **32**(suppl 1): p. D109-D111.

222. Griffiths-Jones, S., et al., *miRBase: microRNA sequences, targets and gene nomenclature.* Nucleic Acids Research, 2006. **34**(suppl 1): p. D140-D144.

223. Griffiths-Jones, S., et al., *miRBase: tools for microRNA genomics.* Nucleic Acids Research, 2008. **36**(suppl 1): p. D154-D158.

224. Kozomara, A. and S. Griffiths-Jones, *miRBase: integrating microRNA annotation and deep-sequencing data.* Nucleic Acids Research, 2011. **39**(suppl 1): p. D152-D157.

225. Wynne, H., et al., *The influence of age, liver size and enantiomer concentrations on warfarin requirements.* Br J Clin Pharmacol, 1995. **40**(3): p. 203-7.

226. Wakabayashi, H., et al., *Evaluation of the effect of age on functioning hepatocyte mass and liver blood flow using liver scintigraphy in preoperative estimations for surgical patients: comparison with CT volumetry.* J Surg Res, 2002. **106**(2): p. 246-53.

227. Fry, M., et al., *Delayed and reduced cell replication and diminishing levels of DNA polymerase-alpha in regenerating liver of aging mice.* J Cell Physiol, 1984. **118**(3): p. 225-32.

228. Chipchase, M.D., M. O'Neill, and D.W. Melton, *Characterization of premature liver polyploidy in DNA repair (Ercc1)-deficient mice.* Hepatology, 2003. **38**(4): p. 958-66.

229. Kuk, J.L., et al., *Age-related changes in total and regional fat distribution.* Ageing Res Rev, 2009. **8**(4): p. 339-48.

230. Lavasani, M., et al., *Muscle-derived stem/progenitor cell dysfunction limits healthspan and lifespan in a murine progeria model.* Nat Commun, 2012. **3**: p. 608.

231. Selfridge, J., et al., *Correction of liver dysfunction in DNA repair-deficient mice with an ERCC1 transgene.* Nucleic Acids Res, 2001. **29**(22): p. 4541-50.

232. Friedman, R.C., et al., *Most mammalian mRNAs are conserved targets of microRNAs.* Genome Res, 2009. **19**(1): p. 92-105.

233. Gabriely, G., et al., *Human glioma growth is controlled by microRNA-10b.* Cancer Res, 2011. **71**(10): p. 3563-72.

234. Zhu, Y., et al., *Reduced miR-128 in breast tumor-initiating cells induces chemotherapeutic resistance via Bmi-1 and ABCC5.* Clin Cancer Res, 2011. **17**(22): p. 7105-15.

235. Adlakha, Y.K. and N. Saini, *MicroRNA-128 downregulates Bax and induces apoptosis in human embryonic kidney cells.* Cell Mol Life Sci, 2011. **68**(8): p. 1415-28.

236. Donzelli, S., et al., *MicroRNA-128-2 targets the transcriptional repressor E2F5 enhancing mutant p53 gain of function.* Cell Death Differ, 2012. **19**(6): p. 1038-48.

237. Guidi, M., et al., *Overexpression of miR-128 specifically inhibits the truncated isoform of NTRK3 and upregulates BCL2 in SH-SY5Y neuroblastoma cells.* BMC Mol Biol, 2010. **11**: p. 95.

238. Shi, Z.M., et al., *MiR-128 inhibits tumor growth and angiogenesis by targeting p70S6K1*. PLoS One, 2012. **7**(3): p. e32709.

239. Lize, M., A. Klimke, and M. Dobbelstein, *MicroRNA-449 in cell fate determination.* Cell Cycle, 2011. **10**(17): p. 2874-82.

240. Yadav, S., et al., *miR-497 and miR-302b regulate ethanol-induced neuronal cell death through BCL2 protein and cyclin D2.* J Biol Chem, 2011. **286**(43): p. 37347-57.

241. Guo, S.T., et al., *MicroRNA-497 targets insulin-like growth factor 1 receptor and has a tumour suppressive role in human colorectal cancer*. Oncogene, 2013. **32**(15): p. 1910-20.

242. Zheng, D., A. Radziszewska, and P. Woo, *MicroRNA 497 modulates interleukin 1 signalling via the MAPK/ERK pathway*. FEBS Lett, 2012. **586**(23): p. 4165-72.

243. Haga, C.L. and D.G. Phinney, *MicroRNAs in the imprinted DLK1-DIO3 region repress the epithelial-to-mesenchymal transition by targeting the TWIST1 protein signaling network.* J Biol Chem, 2012. **287**(51): p. 42695-707.

244. Papaioannou, M.D., et al., *Loss of Dicer in Sertoli cells has a major impact on the testicular proteome of mice.* Mol Cell Proteomics, 2011. **10**(4): p. M900587MCP200.

245. Papagiannakopoulos, T., et al., *Pro-neural miR-128 is a glioma tumor suppressor that targets mitogenic kinases*. Oncogene, 2011.

246. Noonan, E.J., et al., *miR-449a causes Rb-dependent cell cycle arrest and senescence in prostate cancer cells.* Oncotarget, 2010. **1**(5): p. 349-58.

247. Bou Kheir, T., et al., *miR-449 inhibits cell proliferation and is down-regulated in gastric cancer*. Mol Cancer, 2011. **10**: p. 29.

248. Leontieva, O.V., et al., *Hyper-mitogenic drive coexists with mitotic incompetence in senescent cells.* Cell Cycle, 2012. **11**(24): p. 4642-9.

249. Lucibello, F.C., et al., *Deregulation of cyclins D1 and E and suppression of cdk2 and cdk4 in senescent human fibroblasts.* J Cell Sci, 1993. **105 (Pt 1)**: p. 123-33.

250. Ramamoorthy, A., et al., *In silico and in vitro identification of microRNAs that regulate hepatic nuclear factor 4alpha expression.* Drug Metab Dispos, 2012. **40**(4): p. 726-33.

251. Hatziapostolou, M., et al., *An HNF4alpha-miRNA inflammatory feedback circuit regulates hepatocellular oncogenesis.* Cell, 2011. **147**(6): p. 1233-47.

252. Mori, M.A., et al., *Role of microRNA processing in adipose tissue in stress defense and longevity.* Cell Metab, 2012. **16**(3): p. 336-47.

253. Fried, L.P., et al., *Frailty in older adults: evidence for a phenotype.* J Gerontol A Biol Sci Med Sci, 2001. **56**(3): p. M146-56.

254. Ershler, W.B. and E.T. Keller, *Age-associated increased interleukin-6 gene expression, late-life diseases, and frailty.* Annu Rev Med, 2000. **51**: p. 245-70.

255. Jiang, J., E.M. Fisher, and D.M. Murasko, *CD8 T cell responses to influenza virus infection in aged mice.* Ageing Res Rev, 2011. **10**(4): p. 422-7.

256. Howard, W.A., K.L. Gibson, and D.K. Dunn-Walters, *Antibody quality in old age.* Rejuvenation Res, 2006. **9**(1): p. 117-25.

257. Hara, H., et al., *Age-associated changes in proliferative and differentiative response of human B cells and production of T cell-derived factors regulating B cell functions.* Mech Ageing Dev, 1987. **38**(3): p. 245-58.

258. Tarazona, R., et al., *Basic biology and clinical impact of immunosenescence.* Exp Gerontol, 2002. **37**(2-3): p. 183-9.

259. Alvarez, E., et al., *Age-related changes in membrane lipid composition, fluidity and respiratory burst in rat peritoneal neutrophils.* Clin Exp Immunol, 2001. **124**(1): p. 95-102.

260. Panda, A., et al., *Age-associated decrease in TLR function in primary human dendritic cells predicts influenza vaccine response.* J Immunol, 2010. **184**(5): p. 2518-27.

261. Kissin, E., et al., *Age-related decline in murine macrophage production of nitric oxide.* J Infect Dis, 1997. **175**(4): p. 1004-7.

262. Naylor, K., et al., *The influence of age on T cell generation and TCR diversity.* J Immunol, 2005. **174**(11): p. 7446-52.

263. Effros, R.B., et al., *Decline in CD28+ T cells in centenarians and in long-term T cell cultures: a possible cause for both in vivo and in vitro immunosenescence.* Exp Gerontol, 1994. **29**(6): p. 601-9.

264. Siegrist, C.A. and R. Aspinall, *B-cell responses to vaccination at the extremes of age.* Nat Rev Immunol, 2009. **9**(3): p. 185-94.

265. Goto, M., *Inflammaging (inflammation + aging): A driving force for human aging based on an evolutionarily antagonistic pleiotropy theory?* Biosci Trends, 2008. **2**(6): p. 218-30.

266. Blasko, I., et al., *How chronic inflammation can affect the brain and support the development of Alzheimer's disease in old age: the role of microglia and astrocytes.* Aging Cell, 2004. **3**(4): p. 169-76.

267. Libby, P., *Inflammation and cardiovascular disease mechanisms.* Am J Clin Nutr, 2006. **83**(2): p. 456S-460S.

268. Lio, D., et al., *Gender-specific association between -1082 IL-10 promoter polymorphism and longevity.* Genes Immun, 2002. **3**(1): p. 30-3.

269. Forsythe, L.K., J.M. Wallace, and M.B. Livingstone, *Obesity and inflammation: the effects of weight loss.* Nutr Res Rev, 2008. **21**(2): p. 117-33.

270. Maggio, M., et al., *Correlation between testosterone and the inflammatory marker soluble interleukin-6 receptor in older men.* J Clin Endocrinol Metab, 2006. **91**(1): p. 345-7.

271. Franceschi, C., et al., *The immunology of exceptional individuals: the lesson of centenarians.* Immunol Today, 1995. **16**(1): p. 12-6.

272. Derhovanessian, E., et al., *Hallmark features of immunosenescence are absent in familial longevity.* J Immunol, 2010. **185**(8): p. 4618-24.

273. Jenny, N.S., et al., *Long-term assessment of inflammation and healthy aging in late life: the Cardiovascular Health Study All Stars.* J Gerontol A Biol Sci Med Sci, 2012. **67**(9): p. 970-6.

274. Seino, Y., et al., *Interleukin 6 gene transcripts are expressed in human atherosclerotic lesions.* Cytokine, 1994. **6**(1): p. 87-91.

275. Scheidt-Nave, C., et al., *Serum interleukin 6 is a major predictor of bone loss in women specific to the first decade past menopause.* J Clin Endocrinol Metab, 2001. **86**(5): p. 2032-42.

276. Barr, T.A., et al., *B cell depletion therapy ameliorates autoimmune disease through ablation of IL-6-producing B cells.* J Exp Med, 2012. **209**(5): p. 1001-10.

277. Mohamed-Ali, V., et al., *Subcutaneous adipose tissue releases interleukin-6, but not tumor necrosis factor-alpha, in vivo.* J Clin Endocrinol Metab, 1997. **82**(12): p. 4196-200.

278. Seshadri, S., et al., *MAIL regulates human monocyte IL-6 production.* J Immunol, 2009. **183**(8): p. 5358-68.

279. Rochester, C.L., et al., *Eosinophil-fibroblast interactions. Granule major basic protein interacts with IL-1 and transforming growth factor-beta in the stimulation of lung fibroblast IL-6-type cytokine production.* J Immunol, 1996. **156**(11): p. 4449-56.

280. Northemann, W., et al., *Production of interleukin 6 by hepatoma cells.* Mol Biol Med, 1990. **7**(3): p. 273-85.

281. Podor, T.J., et al., *Human endothelial cells produce IL-6. Lack of responses to exogenous IL-6.* Ann N Y Acad Sci, 1989. **557**: p. 374-85; discussion 386-7.

282. Senn, J.J., et al., *Interleukin-6 induces cellular insulin resistance in hepatocytes.* Diabetes, 2002. **51**(12): p. 3391-9.

283. Kern, P.A., et al., *Adipose tissue tumor necrosis factor and interleukin-6 expression in human obesity and insulin resistance.* Am J Physiol Endocrinol Metab, 2001. **280**(5): p. E745-51.

284. Fey, G.H., et al., *Regulation of rat liver acute phase genes by interleukin-6 and production of hepatocyte stimulating factors by rat hepatoma cells.* Ann N Y Acad Sci, 1989. **557**: p. 317-29; discussion 329-31.

285. Oguro, T., et al., *Humanised antihuman IL-6R antibody with interferon inhibits renal cell carcinoma cell growth in vitro and in vivo through suppressed SOCS3 expression.* Eur J Cancer, 2013. **49**(7): p. 1715-24.

286. Klein, B., et al., *Paracrine rather than autocrine regulation of myeloma-cell growth and differentiation by interleukin-6.* Blood, 1989. **73**(2): p. 517-26.

287. Montero-Julian, F.A., *The soluble IL-6 receptors: serum levels and biological function.* Cell Mol Biol (Noisy-le-grand), 2001. **47**(4): p. 583-97.

288. Coppe, J.P., et al., *Senescence-associated secretory phenotypes reveal cell-nonautonomous functions of oncogenic RAS and the p53 tumor suppressor.* PLoS Biol, 2008. **6**(12): p. 2853-68.

289. Lu, S.Y., et al., *Ripe areca nut extract induces G1 phase arrests and senescence-associated phenotypes in normal human oral keratinocyte.* Carcinogenesis, 2006. **27**(6): p. 1273-84.

290. Sarkar, D., et al., *Human polynucleotide phosphorylase (hPNPaseold-35): a potential link between aging and inflammation.* Cancer Res, 2004. **64**(20): p. 7473-8.

291. Sen, R. and D. Baltimore, *Multiple nuclear factors interact with the immunoglobulin enhancer sequences.* Cell, 1986. **46**(5): p. 705-16.

292. Ghosh, S., M.J. May, and E.B. Kopp, *NF-kappa B and Rel proteins: evolutionarily conserved mediators of immune responses.* Annu Rev Immunol, 1998. **16**: p. 225-60.

293. Correa, R.G., et al., *Characterization of NF-kappa B/I kappa B proteins in zebra fish and their involvement in notochord development.* Mol Cell Biol, 2004. **24**(12): p. 5257-68.

294. Beg, A.A., et al., *Embryonic lethality and liver degeneration in mice lacking the RelA component of NF-kappa B.* Nature, 1995. **376**(6536): p. 167-70.

295. Seitz, C.S., et al., *Alterations in NF-kappaB function in transgenic epithelial tissue demonstrate a growth inhibitory role for NF-kappaB.* Proc Natl Acad Sci U S A, 1998. **95**(5): p. 2307-12.

296. Hayden, M.S. and S. Ghosh, *Signaling to NF-kappaB.* Genes Dev, 2004. **18**(18): p. 2195-224.

297. Beg, A.A., et al., *Tumor necrosis factor and interleukin-1 lead to phosphorylation and loss of I kappa B alpha: a mechanism for NF-kappa B activation.* Mol Cell Biol, 1993. **13**(6): p. 3301-10.

298. Hacker, H. and M. Karin, *Regulation and function of IKK and IKK-related kinases.* Sci STKE, 2006. **2006**(357): p. re13.

299. Henkel, T., et al., *Rapid proteolysis of I kappa B-alpha is necessary for activation of transcription factor NF-kappa B.* Nature, 1993. **365**(6442): p. 182-5.

300. Libermann, T.A. and D. Baltimore, *Activation of interleukin-6 gene expression through the NF-kappa B transcription factor.* Mol Cell Biol, 1990. **10**(5): p. 2327-34.

301. Zhang, D., et al., *The effect of interleukin-1 on C-reactive protein expression in Hep3B cells is exerted at the transcriptional level.* Biochem J, 1995. **310 (Pt 1)**: p. 143-8.

302. Yamamoto, K., et al., *Transcriptional roles of nuclear factor kappa B and nuclear factor-interleukin-6 in the tumor necrosis factor alpha-dependent induction of cyclooxygenase-2 in MC3T3-E1 cells.* J Biol Chem, 1995. **270**(52): p. 31315-20.

303. Schroeder, T.H., et al., *CFTR is a pattern recognition molecule that extracts Pseudomonas aeruginosa LPS from the outer membrane into epithelial cells and activates NF-kappa B translocation.* Proc Natl Acad Sci U S A, 2002. **99**(10): p. 6907-12.

304. Osborn, L., S. Kunkel, and G.J. Nabel, *Tumor necrosis factor alpha and interleukin 1 stimulate the human immunodeficiency virus enhancer by activation of the nuclear factor kappa B.* Proc Natl Acad Sci U S A, 1989. **86**(7): p. 2336-40.

305. Bouwmeester, T., et al., *A physical and functional map of the human TNF-alpha/NF-kappa B signal transduction pathway.* Nat Cell Biol, 2004. **6**(2): p. 97-105.

306. Brach, M.A., et al., *Ionizing radiation induces expression and binding activity of the nuclear factor kappa B.* J Clin Invest, 1991. **88**(2): p. 691-5.

307. Bernard, D., et al., *Involvement of Rel/nuclear factor-kappaB transcription factors in keratinocyte senescence.* Cancer Res, 2004. **64**(2): p. 472-81.

308. Cai, D., et al., *IKKbeta/NF-kappaB activation causes severe muscle wasting in mice.* Cell, 2004. **119**(2): p. 285-98.

309. Argiles, J.M., et al., *Molecular mechanisms involved in muscle wasting in cancer and ageing: cachexia versus sarcopenia.* Int J Biochem Cell Biol, 2005. **37**(5): p. 1084-104.

310. Janssens, S., et al., *PIDD mediates NF-kappaB activation in response to DNA damage.* Cell, 2005. **123**(6): p. 1079-92.

311. Habraken, Y. and J. Piette, *NF-kappaB activation by double-strand breaks.* Biochem Pharmacol, 2006. **72**(9): p. 1132-41.

312. Wu, Z.H., et al., *Molecular linkage between the kinase ATM and NF-kappaB signaling in response to genotoxic stimuli.* Science, 2006. **311**(5764): p. 1141-6.

313. Schreck, R., K. Albermann, and P.A. Baeuerle, *Nuclear factor kappa B: an oxidative stress-responsive transcription factor of eukaryotic cells (a review).* Free Radic Res Commun, 1992. **17**(4): p. 221-37.

314. Tanaka, K., et al., *Prevention of the ultraviolet B-mediated skin photoaging by a nuclear factor kappaB inhibitor, parthenolide.* J Pharmacol Exp Ther, 2005. **315**(2): p. 624-30.

315. Chien, Y., et al., *Control of the senescence-associated secretory phenotype by NF-kappaB promotes senescence and enhances chemosensitivity.* Genes Dev, 2011. **25**(20): p. 2125-36.

316. Helenius, M., et al., *Characterization of aging-associated up-regulation of constitutive nuclear factor-kappa B binding activity.* Antioxid Redox Signal, 2001. **3**(1): p. 147-56.

317. de Magalhaes, J.P., J. Curado, and G.M. Church, *Meta-analysis of age-related gene expression profiles identifies common signatures of aging.* Bioinformatics, 2009. **25**(7): p. 875-81.

318. Yeung, F., et al., *Modulation of NF-kappaB-dependent transcription and cell survival by the SIRT1 deacetylase.* EMBO J, 2004. **23**(12): p. 2369-80.

319. Kawahara, T.L., et al., *SIRT6 links histone H3 lysine 9 deacetylation to NF-kappaB-dependent gene expression and organismal life span.* Cell, 2009. **136**(1): p. 62-74.

320. Lin, L., J.D. Hron, and S.L. Peng, *Regulation of NF-kappaB, Th activation, and autoinflammation by the forkhead transcription factor Foxo3a.* Immunity, 2004. **21**(2): p. 203-13.

321. Farrell, G.C. and C.Z. Larter, *Nonalcoholic fatty liver disease: from steatosis to cirrhosis.* Hepatology, 2006. **43**(2 Suppl 1): p. S99-S112.

322. Remuzzi, A., et al., *Effect of angiotensin II antagonism on the regression of kidney disease in the rat.* Kidney Int, 2002. **62**(3): p. 885-94.

323. Nichols, N.R., et al., *GFAP mRNA increases with age in rat and human brain.* Neurobiol Aging, 1993. **14**(5): p. 421-9.

324. Chen, Q., et al., *DNA damage drives accelerated bone aging via an NF-kappaB-dependent mechanism.* J Bone Miner Res, 2013. **28**(5): p. 1214-28.

325. Grimson, A., et al., *MicroRNA targeting specificity in mammals: determinants beyond seed pairing.* Mol Cell, 2007. **27**(1): p. 91-105.

326. Garcia, D.M., et al., *Weak seed-pairing stability and high target-site abundance decrease the proficiency of lsy-6 and other microRNAs.* Nat Struct Mol Biol, 2011. **18**(10): p. 1139-46.

327. Coppe, J.P., et al., *A human-like senescence-associated secretory phenotype is conserved in mouse cells dependent on physiological oxygen.* PLoS One, 2010. **5**(2): p. e9188.

328. Yun, U.J., et al., *DNA damage induces the IL-6/STAT3 signaling pathway, which has anti-senescence and growth-promoting functions in human tumors.* Cancer Lett, 2012. **323**(2): p. 155-60.

329. Chiang, H.R., et al., *Mammalian microRNAs: experimental evaluation of novel and previously annotated genes.* Genes Dev, 2010. **24**(10): p. 992-1009.

330. Myatt, S.S., et al., *Definition of microRNAs that repress expression of the tumor suppressor gene FOXO1 in endometrial cancer.* Cancer Res, 2010. **70**(1): p. 367-77.

331. Ciafre, S.A., et al., *Extensive modulation of a set of microRNAs in primary glioblastoma.* Biochem Biophys Res Commun, 2005. **334**(4): p. 1351-8.

332. Godlewski, J., et al., *Targeting of the Bmi-1 oncogene/stem cell renewal factor by microRNA-128 inhibits glioma proliferation and self-renewal.* Cancer Res, 2008. **68**(22): p. 9125-30.

333. Huang, X., et al., *Characterization of human plasma-derived exosomal RNAs by deep sequencing.* BMC Genomics, 2013. **14**: p. 319.

334. Noetel, A., et al., *Next generation sequencing of the Ago2 interacting transcriptome identified chemokine family members as novel targets of neuronal microRNAs in hepatic stellate cells.* J Hepatol, 2013. **58**(2): p. 335-41.

335. Loeb, G.B., et al., *Transcriptome-wide miR-155 binding map reveals widespread noncanonical microRNA targeting.* Mol Cell, 2012. **48**(5): p. 760-70.

336. Liu, C., et al., *CLIP-based prediction of mammalian microRNA binding sites.* Nucleic Acids Res, 2013.

337. Wang, C., et al., *DNA damage response and cellular senescence in tissues of aging mice.* Aging Cell, 2009. **8**(3): p. 311-23.

338. Bates, D.J., et al., *MicroRNA regulation in Ames dwarf mouse liver may contribute to delayed aging.* Aging Cell, 2010. **9**(1): p. 1-18.

339. Donato, A.J., et al., *Aging is associated with greater nuclear NF kappa B, reduced I kappa B alpha, and increased expression of proinflammatory cytokines in vascular endothelial cells of healthy humans.* Aging Cell, 2008. **7**(6): p. 805-12.

340. Johansson, A., S. Enroth, and U. Gyllensten, *Continuous Aging of the Human DNA Methylome Throughout the Human Lifespan.* PLoS One, 2013. **8**(6): p. e67378.

341. Christman, J.K., *5-Azacytidine and 5-aza-2'-deoxycytidine as inhibitors of DNA methylation: mechanistic studies and their implications for cancer therapy.* Oncogene, 2002. **21**(35): p. 5483-95.